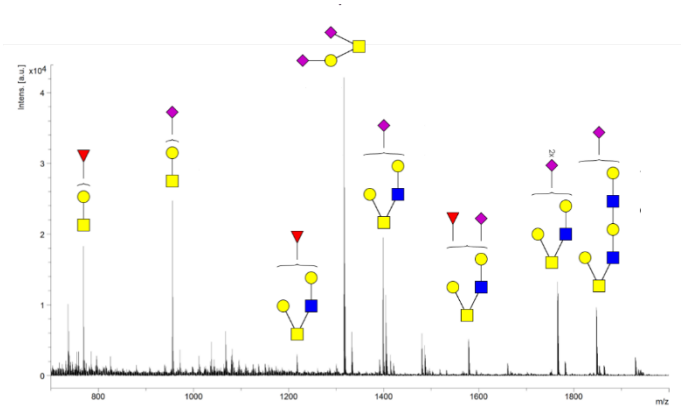

Bladder cancer glycome and glycoproteome microenvironmental regulation: the role of oxygen and glucose

Marta Filipa Relvas dos Santos
Mestrado em Bioquímica
Faculdade de Ciências e Instituto de Ciências Biomédicas Abel Salazar
Universidade do Porto
2018

Orientador
José Alexandre Ferreira, Investigador auxiliar, IPO-Porto

Coorientador
André M. N. Silva, Investigador externo, FCUP

Coorientador
Lúcio Lara Santos, Coordenador do Grupo de Patologia e Terapêutica Experimental, IPO-Porto
Professor afiliado, ICBAS

IPOPORTO

INSTITUTO DE CIÊNCIAS BIOMÉDICAS ABEL SALAZAR
UNIVERSIDADE DO PORTO

U.PORTO

FACULDADE DE CIÊNCIAS
UNIVERSIDADE DO PORTO

Todas as correções determinadas pelo júri, e só essas, foram efetuadas.
O Presidente do Júri,

Porto, _____/_____/_____

Contribution in the concept and accomplishment of the following research work during the year of development of Master degree's Thesis:

Scientific Papers

I. Azevedo R, Gaiteiro C, Peixoto A, **Relvas-Santos M**, Lima L, Santos LL, Ferreira JA. CD44 glycoprotein in cancer: a molecular conundrum hampering clinical applications. Clin Proteomics. 2018; 15:22.

II. Azevedo R, Soares J, Gaiteiro C, Peixoto A, Lima L, Ferreira D, **Relvas-Santos M**, Fernandes E, Tavares A, Cotton S, Daniel-da-Silva AL, Santos LL, Vitorino R, Amado F, Ferreira JA. Glycan affinity magnetic nanoplatforms for urinary glycobiomarkers discovery in bladder cancer. Talanta. 2018; 184:347-55.

Poster

I. Peixoto A, Fernandes E, Gaiteiro C, Lima L, Azevedo R, Soares J, Cotton S, Parreira B, Neves M, **Relvas-Santos M**, Amaro T, Tavares A, Teixeira F, Palmeira C, Rangel M, Silva AM, Reis CA, Santos LL, Oliveira MJ, Ferreira JA. Hypoxia enhances the malignant nature of bladder cancer cells and concomitantly antagonizes protein O-glycosylation. Conference: ICS 2018: 29th International Carbohydrate Symposium

Oral communications

I. Peixoto A, Fernandes E, Gaiteiro C, Lima L, Azevedo R, Soares J, Cotton S, Parreira B, Neves M, **Relvas-Santos M**, Amaro T, Tavares A, Teixeira F, Palmeira C, Rangel M, Silva AM, Reis CA, Santos LL, Oliveira MJ, Ferreira JA. Hypoxia enhances the malignant nature of bladder cancer cells and concomitantly antagonizes protein O-glycosylation extension. Conference: ICS 2018: 29th International Carbohydrate Symposium

II. Azevedo R, Gaiteiro C, Soares J, Peixoto A, **Relvas-Santos M**, Ferreira D, Lima L, Santos LL, Ferreira JA. CD44-glycoprofilling: Estabilishing the molecular basis for targeted therapeutics in bladder cancer. Conference: ICS 2018: 29th International Carbohydrate Symposium

Agradecimentos

Na conclusão deste trabalho, gratidão parece-me a palavra certa para exprimir o que sinto. Estou imensamente grata aos meus orientadores por há cerca de ano e meio terem acreditado e apostado em mim. Obrigada por esta oportunidade incrível, por poder aprender tanto todos os dias. Obrigada por toda a ajuda, dedicação, incentivo e amizade.

Ao Doutor José Alexandre Ferreira o meu profundo obrigada pela confiança e pela forma sábia como me ajuda a contruir o meu percurso e a moldar-me como cientista que aspiro um dia ser. É um privilégio poder aprender e fazer Ciência consigo.

Ao Doutor André Silva o meu muito obrigada pela partilha de conhecimento e pela discussão valiosa de abordagens experimentais. Também ele constitui parte muito importante neste percurso e alguém com quem aprendo sempre muito.

Um agradecimento especial ao Professor Doutor Lúcio Lara Santos por me ter permitido integrar tão fantástico grupo.

Ao Grupo de Patologia e Terapêutica Experimental: Andreia, Cristiana, Dylan, Elisabete, Janine, Manuel, Rita, Rui, Sofia e Doutor Luís Lima. Obrigada pela amizade e pela enorme interajuda. O que cresci, aprendi e evoluí, também muito o devo a vocês.

Não posso deixar também de agradecer a todos aqueles que na FCUP e no CEMUP de alguma forma contribuíram para que este projeto decorresse ao melhor ritmo.

Aos meus amigos, em particular à Rita e ao Miguel, é muito bom partilhar convosco mais uma etapa.

À minha família, pelas pessoas maravilhosas que são, por todo o apoio que me dão sempre,… Muito obrigada!

Sumário

O tratamento de cancro da bexiga, principalmente dos estadios mais avançados, permanece um desafio, devido à significativa heterogeneidade molecular. Frequentemente, o glicoproteoma da membrana plasmática sofre remodelação, o que contribui para a progressão e disseminação da doença. Além disso, o facto do padrão glicoproteómico ser dependente do contexto em que está inserido pode fornecer informação molecular bastante específica para intervenção dirigida. Alterações na *O*-glicosilação, uma importante modificação pós-traducional das proteínas à superfície celular, constitui um dos principais eventos moleculares que levam à alteração do glicoproteoma em cancro da bexiga. Contudo, a complexa estrutura dos glicanos e a sua natureza dinâmica, associados à falta de protocolos de glicoproteómica padronizados, têm atrasado o conhecimento compreensivo do glicoma e do glicoproteoma, tendo em vista possíveis biomarcadores para intervenção clínica. Por outro lado, a informação sobre o impacto do microambiente na glicosilação é escassa e, por isso também dificulta estudos funcionais e terapêuticas dirigidas. Assim, este trabalho dedicou-se a padronizar um protocolo para investigação de glicobiomarcadores. De seguida, concentrou-se em explorar as mudanças no glicoma que possam ocorrer em resposta à hipóxia e à privação de glucose, as quais constituem importantes caraterísticas microambientais dos tumores sólidos, devido à ineficiente vasculatura promovida pelo crescimento tumoral rápido e não controlado.

De forma a responder a estes objetivos, este trabalho começa por propor um protocolo apoiado na bioinformática para análise glicómica e glicoproteómica. Resumidamente, três modelos celulares de cancro da bexiga (5637 derivado de grau II, T24 e HT1376 derivados de grau III) foram sujeitos a caraterização *O*-glicómica, através do método *Cellular O-glycome Reporter/Amplification* (CORA) e espetrometria de massa (MALDI-TOF-MS e nanoLC-ESI-MS). Estas linhas celulares apresentaram como estruturas dominantes as formas sialiladas do antigénio T, bem como mostraram similaridade a nível do proteoma e do *O-glicoma*, apesar das suas diferenças moleculares e histológicas. Esta informação permitiu desenhar estratégias adequadas de enriquecimento glicoproteico, o que foi feito através de cromatografia de afinidade com *Peanut agglutinin* (PNA). A identificação das glicoproteínas foi conseguida através duma estratégia proteómica de *bottom up*, usando nanoLC-ESI-MS/MS, dados cuidados de ontologia génica para proteínas da membrana plasmática e de previsão de locais de glicosilação, usando o NetOGlyc. As proteínas identificadas foram então integradas com

dados de transcritómica e imunohistoquímica, usando as bases de dados *Oncomine* e o *Human Protein Atlas*. Esta abordagem permitiu gerar uma libraria composta por relevantes glicoproteínas, que justificam posteriores estudos clínicos. Além do contributo para um maior conhecimento da glicobiologia do cancro da bexiga, este protocolo pode fomentar novas aplicações clínicas baseadas em glicobiomaracadores.

A segunda parte deste trabalho implementou estes avanços analíticos na análise da influência da diminuição de oxigénio e da privação de glucose no *O*-glicoma. Apesar de explorativo, este trabalho destacou a similaridade e consistência dos padrões de *O*-glicosilação de todas as linhas celulares em hipóxia, na privação de glucose e quando sujeitas ao efeito sinérgico de ambos os fatores. Resumidamente, a hipóxia teve pouco impacto no *O*-glicoma, enquanto a privação de glucose originou um impressionante remodelamento. Esta alteração do *O*-glicoma é caraterizada pela significante diminuição da biossíntese de *O*-glicanos, pela paragem total da extensão dos glicanos além do core 1, pela troca da fucosilação do core 1 pela sialilação e pela sobreexpressão do sialyl Tn, um glicano bastante associado ao cancro da bexiga. A combinação da hipóxia à privação de glucose, o que frequentemente ocorre *in vivo*, exacerbou estes eventos. Para conhecimento futuro, este é o primeiro estudo abrangente e compreensivo da plasticidade do *O*-glicoma, face a estes estímulos microambientais. Além disso, estes resultados, apoiados pela plataforma analítica desenvolvida na primeira parte deste trabalho, ajudam a guiar futuros estudos de glicoproteómica funcional, bem com na descoberta de glicobiomarcadores, especialmente contra os nichos de hipóxia, constituídos por células mais malignas.

Palavras-chave: antigénios T sialilados, cancro da bexiga, glicoproteínas, glicosilação, hipóxia, *O*-glicanos, privação de glucose

Abstract

Bladder cancer management, especially at advanced stages, remains challenging due to significant molecular heterogeneity. In particular, cancer cells often experience plasma membrane glycoproteome remodelling that contributes to disease progression and dissemination. Moreover, the context-dependent nature of the glycoproteome may provide highly cancer-specific signatures for targeted intervention. Changes in *O*-glycosylation, a main post-translation modification of cell surface proteins, are amongst the main molecular events driving alteration in the bladder cancer glycoproteome. However, glycans complex structure, non-templated and dynamic nature associated to the lack of standardized glycoproteomics protocols has delayed a comprehensive interrogation of the glycome and glycoproteome for cancer biomarkers capable of aiding clinical intervention. On the other hand, there is little information on the impact of the cancer microenvironment on glycosylation, which has hampered functional studies and targeted therapeutics. As such, this work has devoted to standardizing a workflow to aid glycobiomarker research. It then focused on exploring this knowledge to disclose changes in the glycome in response to hypoxia and glucose deprivation, two salient microenvironmental features of solid tumours due to inefficient vasculature and sustained tumour growth.

Responding to these objectives, this work starts by proposing a bioinformatics-assisted protocol for glycomics and glycoproteomics analysis. Briefly, three of the most studied bladder cancer cell models (5637 from grade II, T24 and HT176 from grade III) were subjected to *O*-glycome characterization by Cellular *O*-glycome Reporter/Amplification (CORA) and Mass Spectrometry (MALDI-TOF/TOF-MS and nanoLC-ESI-MS). These cell lines showed some degree of proteome and *O*-glycome similarity, with sialylated T antigens as dominant glycan species, despite marked molecular and histological differences. This information was latter used to design adequate glycoprotein enrichment strategies by peanut agglutinin (PNA) affinity chromatography. Glycoprotein identification was achieved by bottom-up nanoLC-ESI-MS/MS proteomics and data was curated by gene ontology for plasma membrane proteins and glycosites prediction using NetOGlyc. Identified glycoproteins were comprehensively integrated with transcriptomics and immunohistochemistry data using Oncomine and the Human Protein Atlas databases. This generated a library of potentially relevant glycoproteins that now warrants clinical validation. We anticipate that this

workflow may aid bladder cancer glycobiology interrogation and ultimately foster novel clinical applications based on glycobiomakers.

The second part of this work explored these analytical advances to disclose the influence of oxygen shortage and glucose deprivation in the *O*-glycome. Despite explorative, it highlighted very similar and consistent patterns for all cell lines in hypoxia, glucose deprivation and under the combination of both factors. Briefly, hypoxia had little impact on the O-glycome. Conversely, glucose deprivation originated a striking glycome remodelling characterized by a significant decrease in *O*-glycans biosynthesis, complete stop of glycan extension beyond core 1, a shift from fucosylation towards sialylation of core 1 glycans and an overexpression of bladder cancer-associated glycan sialyl-Tn. Such events were reinforced when glucose deprivation was associated with hypoxia, as frequently occurs *in vivo*. To our knowledge, it is the first comprehensive view on *O*-glycome plasticity facing these microenvironmental stimuli. Moreover, these findings, supported by the analytical platform developed in the first part of the work, will help guiding functional glycoproteomics and glycobiomarkers discovery, especially against hypoxic niches known to harbour more malignant cells.

Keywords: bladder cancer, glucose deprivation, glycoproteins, glycosylation, hypoxia, *O*-glycans, sialylated T antigens

Index of contents

Index of figures

Chapter I

Chapter II

Chapter III

Index of tables

Appendix

Abbreviations

Asn Asparagine
BC Bladder cancer
BCG bacillus Calmette-Guérin
Bn-GalNAc benzyl-α-D-GalNAc or benzyl 2-acetamido2-deoxy-α-D-galactopyranoside
CID Collision-induced dissociation
CORA Cellular *O*-glycome Reporter Amplification
DMSO Dimethyl sulfoxide
dST di-Sialyl T
DTT Dithiothreitol
ECD Electron capture dissociation
EDTA Ethylenediamine tetraacetic acid
EGTA Ethylene glycol-bis(β-aminoethyl ether)-N,N,N′,N′-tetraacetic acid
ER Endoplasmic reticulum
ESI Electrospray ionization
FBS Fetal bovine serum
FGFR3 Fibroblast Growth Receptor Factor 3
Fuc Fucose
G6PD Glucose-6-phosphate dehydrogenase
GA Golgi apparatus
Gal Galactose
GalNAc *N*-acetylgalactosamine
GC Gemcitabine/cisplatin
GlcNAc *N*-acetylglucosamine
GLUT Glucose transporter
GnT GlcNAc transferase
GO Gene ontology
HBP Hexosamine biosynthetic pathway
HCD High-energy collision dissociation
HEPES 4-(2-hydroxyethyl)-1-piperazineethanesulfonic acid
HIFs Hypoxia-inducible factors
HK Hexokinase
HRAS Harvey rat sarcoma viral oncogene homolog
ICORA Isotope-Cellular *O*-glycome Reporter Amplification

ITGB1 Integrin beta-1

Le$^{a/x}$ Lewis a/x

MALDI Matrix-assisted laser desorption/ionization

MIBC Muscle invasive bladder cancer

MS/MS Tandem mass spectrometry

nanoLC nano-liquid chromatography

Neu5Ac *N*-acetylneuraminic acid

NMIBC Non-muscle invasive bladder cancer

OGA *O*-GlcNAcase

OGT *O*-GlcNAc transferase

PDH Pyruvate dehydrogenase

PDK Pyruvate dehydrogenase kinase

PHDs Prolyl hydroxylase domain enzymes

PNA Peanut Agglutinin

PNGase F Peptide-*N*-Glycosidase F

ppGalNAcT polypeptide GalNAc-transferases

PPP Pentose phosphate pathway

PTM Post-translational modification

RB Retinoblastoma

RTKs Receptor tyrosine kinases

S3T Sialyl-3-T

S6T Sialyl-6-T

SDS Sodium dodecyl sulfate

SDS-PAGE Sodium dodecyl sulfate–polyacrylamide gel electrophoresis

Ser Serine

SLe$^{a/x}$ Sialyl Lewis a/x

ST Sialyl T

ST3Gal α2-3 sialyltransferase

ST6GalNAc α2-6 sialyltransferase

STn Sialyl Tn

STRAP Software Tool for Researching Annotations of Proteins

STRING Search Tool for the Retrieval of Interacting Genes/Proteins

TBS Tris-buffered saline

TCA Tricarboxylic acid cycle

TFA Trifluoroacetic acid

Thr Threonine

TOF Time-of-flight

TUR Tumour resection

UDP-GlcNAc UDP-*N*-Acetylglucosamine

UPR Unfolded protein response

Chapter I | Introduction

1. Bladder cancer

1.1. Epidemiology and risk factors

Bladder cancer (BC) is the seventh most diagnosed cancer in the male population, dropping to tenth when both sexes are considered (1, 2). Furthermore, BC is the deadliest tumour of the urinary system, with approximately 429,000 new cases diagnosed and 1650,00 deaths estimated worldwide in 2012 (1-3).

There are multiple risk factors identified for BC, which are responsible for variations in incidence and pathophysiology (4). For instance, carcinogenic compounds present in cigarettes, such as aromatic amines, make of tobacco smoking and fume inhalation the main risk factor, being responsible by 50% of diagnosed cases (4-6). Inherited genetic factors represent additional risk by influencing individual susceptibility to external factors, mainly to tobacco smoke. Furthermore, occupational exposure to aromatic amines, polycyclic aromatic hydrocarbons and chlorinated hydrocarbons in industries linked to petroleum, coal, paint and metal, represents an additional risk for BC, despite rising safety measures (4, 5). In line with this, inadvertent consumption of chlorinated and arsenic-contaminated drinking water continues to be a major cause of BC. Other risks factors related to dietary habits as coffee consumption remain controversial (7). In addition, BC can arise from underlying medical conditions such as chronic urinary retention and upper tract dilation, contributing to higher exposure to carcinogens, as well as chronic inflammation or infection with *Schistosoma haematobium* (4, 5).

1.2. Pathophysiology and disease progression

Urothelial tumours frequently progress along with two molecular pathways, the more common leading to low-grade, multifocal, papillary, non-invasive carcinomas and the other being responsible for high-grade invasive carcinomas (8). The first is thought to arise from nodular hyperplasia and it is known to involve mutations in Fibroblast Growth Receptor Factor 3 (*FGFR3*), Harvey rat sarcoma viral oncogene homolog (*HRAS*), as well as phosphatidylinositol 3-kinase (*PI3KCA)* genes. On the other hand, non-papillary high-grade and invasive tumours should arise from carcinoma *in situ* or severe dysplasia, harbouring mutations on tumour suppressor genes *TP53*, *p16* and

retinoblastoma (*RB*) (8-10). Notwithstanding, although papillary tumours tend to recur, the vast majority does not evolve into high-grade and invasive tumours (11).

The vast majority of diagnosed BC cases are urothelial cell carcinomas, followed by carcinomas exhibiting squamous or glandular differentiation and other variants (12). Approximately 75% of newly diagnosed patients present superficial tumours (tumour *in situ* (Tis), Ta and T1), generally classified as non-muscle invasive bladder cancer (NMIBC). The standard management of these tumours comprises transurethral bladder tumour resection (TUR) and bacillus Calmette-Guérin (BCG) intravesical therapy (2, 13, 14). However, these therapeutic options fail to prevent recurrence and progression; thereby displaying poor disease-specific survival. The risk of progression of T1 tumours at 5 years is superior to 20% and, in case of confirmed progression to muscle invasive bladder cancer (MIBC, T2-T4), the cancer-specific survival drops to 35% after 4 years (Figure 1) (14).

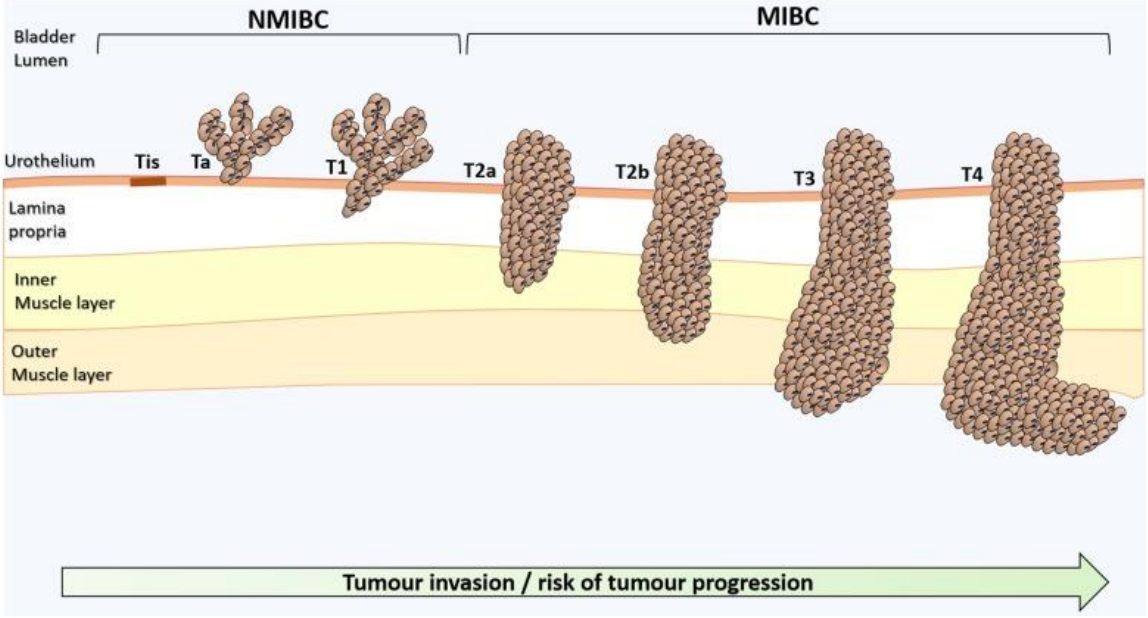

Figure 1 - Schematic representation of bladder cancer stage and grade (15). The stage of the primary tumour (T) is based on the extent of penetration or invasion into the bladder wall. Regarding tumour grading, bladder lesions can be classified as urothelial papilloma (a benign lesion), papillary urothelial neoplasm of low malignant potential (PUNLMP), low-grade papillary urothelial carcinoma and high grade papillary urothelial carcinoma. Of note, PUNLMP lesions do not have cytological features of malignancy and have a very low risk of progression. Nevertheless, they show high tendency to recur. Tis, Tumour in situ: ‘‘flat tumour’’; Ta, Non-invasive papillary carcinoma; T1, Tumour invades sub-epithelial connective tissue; T2, Tumour invades muscle; T2a, Tumour invades superficial muscle (inner half); T2b, Tumour invades deep muscle (outer half); T3, Tumour invades perivesical tissue; T4, Tumour invades any of the following: prostate, uterus, vagina, pelvic or abdominal wall (15).

1.3. Diagnosis and therapeutics of bladder cancer

The most common BC symptom is painless haematuria, which prompts cystoscopy examination, urine cytology and imaging of the upper urinary tract. The standard therapeutic approach on NMIBC is TUR, which removes all visible lesions while allowing a more precise diagnosis and staging (2). In addition, this surgical procedure is usually followed by adjuvant intravesical BCG immunotherapy, currently the most preventive treatment for NMIBC recurrence in non-immunocompromised patients. In case of BCG treatment failure (1/3 of cases) or in NMIBC patients with high risk of progression, radical cystectomy is the next logical step (2, 16). Radical cystectomy is also the standard treatment for localised MIBC (T2-T4), followed by pelvic lymph node dissection. A viable alternative involves debulking TUR and radiotherapy (13).

Metastatic patients with good renal function may be suitable for systemic chemotherapy with cisplatin-based combinations as methotrexate/vinblastine/adriamycin/cisplatin (MVAC) or Gemcitabine/cisplatin (GC) (14). The major difference between the above-mentioned combinations is toxicity. The lower toxicity of GC allied to an increase in cost effectiveness has resulted in it becoming the new standard regimen (17, 18). Carboplatin, an alkylating antineoplastic drug analogue of cisplatin, has been used in urinary and metastatic BC patients with impaired renal function due to its decreased nephrotoxicity compared to cisplatin (19). Even though chemotherapy is efficient against highly proliferative malignant cells that form the tumour bulk, the five-year overall survival does not exceed 25% and many patients die prematurely from adverse drug reactions, urging for effective and safe targeted therapeutics.

Tremendous efforts have been put in the development of biomarker panels for early diagnosis, follow-up, patient stratification, prognosis, treatment selection and development of targeted therapeutics (13). However, the highly heterogeneous molecular nature of bladder tumours has hampered true developments in this field (9) As such, BC remains mostly an “orphan disease” in terms of targeted therapeutics, leading to few improvements in patient’s overall survival over the last decade (10). Importantly, most of this molecular heterogeneity arises from microenvironmental features driving tumour cell adaptation to endogenous stress, such as nutrient deprivation resulting from sustained proliferative signalling and flawed neovascularization, as well as external challenges as chemotherapy. Facing these challenges, glycosylation changes capable of reflecting not only the tumour cells genomic, transcriptomic and metabolomic status but also its microenvironmental context

have major potential for clinical applications. Moreover, glycans and abnormally glycosylated molecules (e.g. proteins and lipids) hold tremendous value for non-invasive cancer detection, while membrane bound glycans may be used to selectively target tumour sites and specific cancer cells.

1.4. Characterization of glycoproteome envisaging novel biomarkers and targeted therapeutics

Despite tremendous research efforts, there is still a lack of useful biomarkers to determine prognosis, the most beneficial therapeutic regimen and, in particular, designing novel targeted therapeutics (20, 21). Membrane proteins offer significant potential for the development of targeted therapeutics by being exposed to extracellular ligands such as monoclonal antibodies. In this context, the most explored therapeutic targets in BC are receptor tyrosine kinases (RTKs), including epidermal growth factor receptor (EGFR; Cetuximab, Clinical Phase II), vascular endothelial growth factor receptor (VEGF; Bevacizumab, Clinical Phase II) and human epidermal growth factor receptor 2 (HER2; Trastuzumab, Clinical Phase II) (22). These proteins are essential for communication between cells and their environment and thereby for cell proliferation and growth; however, mutations of RTKs, which are often overexpressed in BC, significantly decrease the efficacy of current immunotherapies targeting these membrane receptors. Other identified potential targets involve signal transduction pathways and include, for example the protein mTOR and the signal transducer and activator of transcription 3 (STAT3) (23, 24). However, few clinical trials have been performed and with limited success. Moreover, many of these membrane glycoproteins are also expressed in many healthy human organs, lacking the necessary cancer-specificity and consequently resulting in relevant toxicity related with off-target effects (22).

Amongst the factors delaying effective targeted therapeutics is the significant molecular microheterogeneity presented by bladder tumours of apparently similar histology (25). This highlights the urgency in the identification of cancer-specific molecular signatures and the development of multi-targeted therapeutics. As such, particular emphasis should be put on screening the membrane proteome of bladder tumour cells for cancer-specific signatures. Moreover, more than 50% of membrane proteins are glycosylated (26) and BC cells are known to present particular glycosylation features (15). Therefore, the identification of cancer-specific glycosylation patterns and protein glycosites may allow narrowing down the specificity of already explored and new

cancer biomarkers. Finally, many biomarker discovery studies disregard the influence of key cancer-associated microenvironment features such as oxygen and nutrient deprivation, which drive key cancer hallmarks. As such, studies envisaging effective therapeutics should also focus on disclosing the impact of these events on the glycome and glycoproteome of cancer cells.

2. Glycosylation and cancer

2.1. General features and patterns of glycosylation

Glycosylation is the most common and structurally diverse post-translational modification (PTM) of membrane-bound and secreted proteins, as well as a common substitution in lipids and intracellular proteins. Accordingly, it has a key role in protein stability, folding, and trafficking, as well as in cell-cell adhesion, differentiation, migration, signalling, host-pathogen interaction and immune recognition (27-29).

This non-templated but highly regulated process is responsive to biological changes and results from the action of several glycosyltransferases, nucleotide sugar transporters and glycan-processing enzymes in the endoplasmic reticulum (ER) and Golgi apparatus (GA) (30, 31). It gives rise to two main classes of glycans found at the cell surface, namely *N*-glycans and *O*-glycans. Briefly, *N*-glycosylation starts with the covalent attachment of a 14-sugar glycan from the lipid precursor $Glc_3Man_9GlcNAc_2$-P-P-Dol to Asparagine (Asn) residues in Asn-X-Ser/Thr sequons (X denotes any amino acid except proline) of newly synthetized peptides (32, 33). The next processing steps comprise sugar moiety elongation and maturation at the GA to originate hybrid, complex and oligomannose type *N*-glycans through the action of glycosyltransferases and glycosidases. Branching of *N*-glycans results from the action of different GlcNAc transferases (GnT-III-VI), and additional elongation might occur through the addition of galactose, fucose, sialic acid or *N*-acetyllactosamine (LacNAc, Galβ1-4GlcNAc) sugars (34-36). Frequently, *N*-glycans exhibit Lewis blood group related antigens (Le^a, Le^x, Le^b, Le^y) or their sialylated forms, as well as ABO blood group antigens as terminal epitopes (15). As such, glycosylation increases the glycoproteome complexity not only by the vast carbohydrate repertoire but also by the possibility of several glycosidic linkages and isomer forms (37).

Previously *N*-glycosylated glycoproteins are subsequently *O*-glycosylated through the action of polypeptide GalNAc-transferases (ppGalNAcT) which α-link GalNAc moieties to serine (Ser) or threonine (Thr) residues, forming the simplest *O*-glycan Tn antigen. Subsequently, the attachment of Gal to Tn by C1GALT-1 (T synthase) originates the core 1 T antigen in a chaperone COSMC-dependent manner (38, 39). *O*-glycan extension beyond the Tn or T antigens can be blocked by sialyltransferases, giving rise to sialyl-Tn (STn), sialyl-T (ST) or di-sialyl-T (dST) antigens. Of note, α2-6 sialyltransferase ST6GalNAc I shows preferred affinity to the Tn antigen, also acting

upon T and sialyl-3-T (S3T) antigen, while ST6GalNAc II acts preferentially on T antigen (40, 41). α2-3 sialyltransferases (ST3Gal), namely ST3Gal I and ST3Gal IV, are also involved in sialylation of T antigen, originating the S3T antigen (39, 41). Furthermore, the synthesis of di-sialylated T antigen involves the conversion of T antigen into ST antigen, by core 1 α2-3 sialyltransferases (ST3Gal I and IV), followed by addition of another sialic acid via ST6GalNAc I, III or IV (41, 42). *O*-GalNAc glycans can be extended to form core 1 to 4, which are the most common in humans. Namely, Core 2 is formed by the addition of GlcNAc β1-6 branch to core 1, in a reaction catalysed by core 2 β1-6 *N*-acetylglucosaminyltransferases 1 or 3 (C2GnT-1/3). Moreover, core 3 is formed by core 3 β1-3 *N*-acetylglucosaminyltransferase 6 (C3GnT-6) which adds a GlcNAc moiety to the Tn antigen. This structure can be converted into core 4 by core 2/4 β1-6 *N*-acetylglucosaminyltransferase 2 (C2GnT-2) addition of another GlcNAc residue (Figure 3) (39, 43).

In addition to the structural modification of extracellular and cell membrane proteins, intracellular proteins can also be glycosylated, with serious implication to protein function. Glycosylation of intracellular proteins results from the attachment of a N-acetylglucosamine moiety (β-linked GlcNAc) to a Ser or Thr amino acid residue and presents significant differences to other forms of protein glycosylation (44). Namely, it occurs in the cytoplasmic and nuclear compartments, the GlcNAc residue is generally not elongated or modified to generate complex structures and it is a highly dynamic and reversible modification (45) . The dynamic cycling of *O*-GlcNAcylation is catalysed by two ubiquitously expressed and highly conserved enzymes: uridine diphospho-N-acetylglucosamine:polypeptide β-N-acetylglucosaminyltransferase (*O*-GlcNAc transferase, OGT), which adds GlcNAc to the hydroxyl side chain of Ser and Thr, and N-acetyl-β-D-glucosaminidase (*O*-GlcNAcase, OGA), the enzyme that removes *O*-GlcNAc (46). This post-translational modification has regulatory functions akin to phosphorylation, modulating protein conformation, stability, and reversible multimeric protein assembly (47). Moreover, it functions as a nutrient sensor, providing a biochemical switch to enable the cell to adapt to glucose level alterations and hormonal cues, while regulating a myriad of cellular processes like cellular adhesion, DNA transcription, translation, nuclear transport, and cytoskeletal assembly (48, 49). Interestingly, different isoforms of OGT and OGA vary in length and subcellular localization, suggesting that they target distinct subsets of the proteome (50).

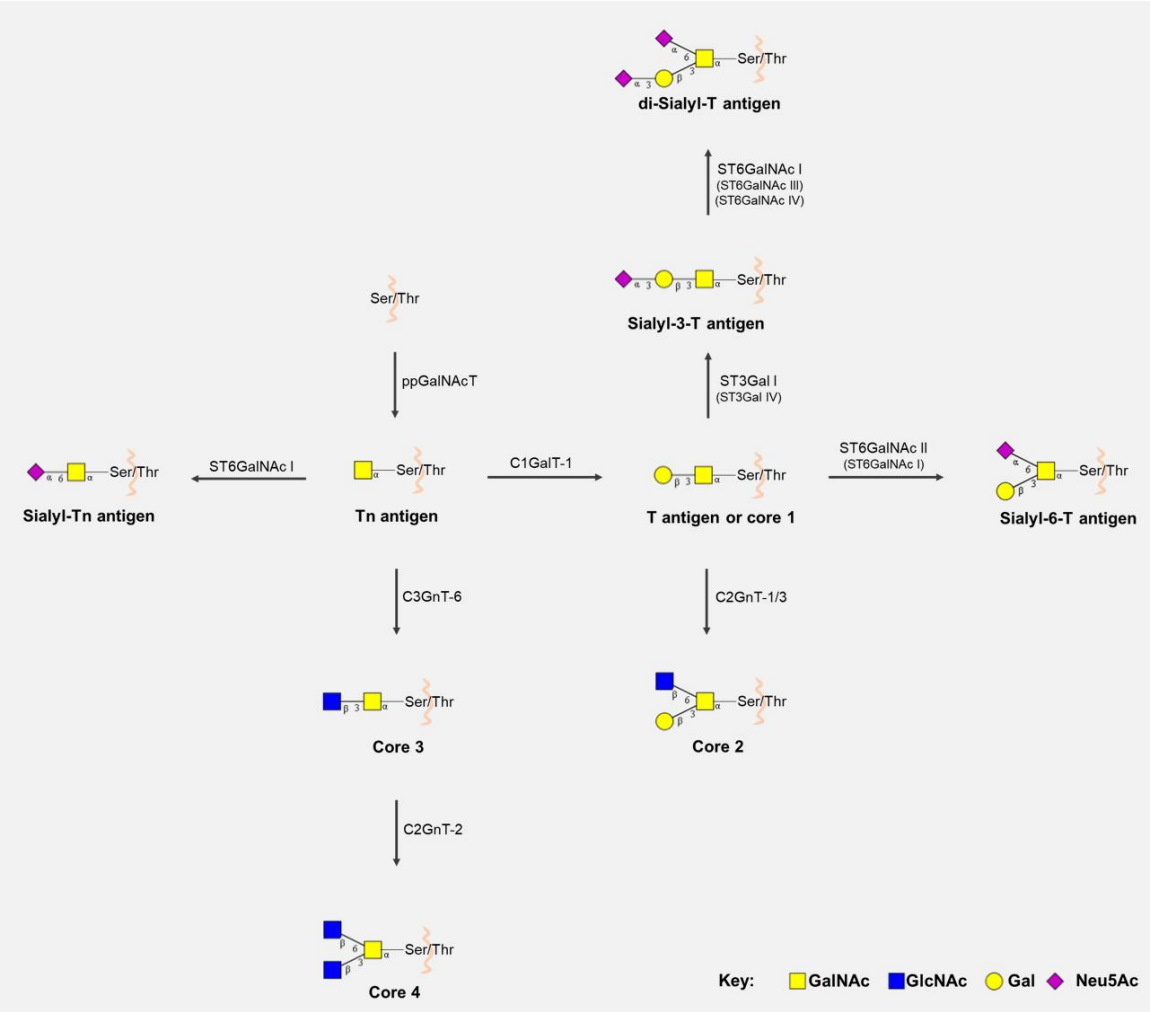

Figure 2 - Biosynthesis of core 1 to 4 and sialylated short-chain *O*-GalNAc glycans.

2.2. Protein Glycosylation in bladder cancer

The last four decades of glycobiology research have disclosed the existence of profound alterations in glycosylation patterns of proteins, lipids and proteoglycans associated with the neoplastic transformation of the bladder (15). Generally, the most frequently described cancer-related glycosylation modifications include the synthesis of highly branched and heavily sialylated glycans, the premature termination of biosynthesis, resulting in the expression of short-chain forms, and the expression *de-novo* of glycosidic antigens of foetal type. Herein, protein-associated alterations will be highlighted.

Alterations in N-glycans branching resulting from impaired GnTs expression have been evaluated in the context of BC, being associated with higher disease stage and grade, shorter disease-free survival and recurrence (51). Interestingly, antagonistic effects GnT-III and GnT-V enzymatic activity, producing *N*-glycans bisection and branching respectively, could be applied to risk stratification in BC, highlighting the importance of GnT-V/III evaluation (52, 53).

Amongst the most common cancer-associated structural features are alterations of terminal glycan epitopes. In fact, the first reported glycosylation alteration in BC was the loss of ABO(H) blood group determinants in advanced stage carcinomas of secretor individuals, as well as changes in Lewis antigens patterns (54). The ABO(H) blood group system refers to terminal oligosaccharides epitopes carried by glycoproteins and glycolipids in hematopoietic and epithelial cells. Their synthesis is controlled by specific glycosyltransferases codified by *ABO(H)*, *Se*, *H*, *Le* and *X* blood group genes (55). These antigens are present in normal urothelium, but not on some low-grade and early-stage papillary urothelial carcinomas (56). Moreover, loss of these epitopes in initially expressing tumours is associated with local recurrence, progression to invasion, metastization and shorter recurrence-free survival (57). In summary, alterations in ABO(H) genes and epitopes expression accompanying bladder malignant transformation and disease dissemination are well established surrogate markers of poor prognosis.

The ABO(H) determinants have biosynthetic and structural similarities with Lewis antigens a and x (Le^a, Le^x), which are highly expressed in invasive bladder tumour compared to healthy urothelium (58). Moreover, Lewis antigens expression was associated with higher tumour grade and shorter recurrence-free survival (58, 59). Their sialylated counterparts SLe^a and SLe^x are the molecular ligands of E- and P-selectins in endothelial cells, actively contributing to early and late stages of the metastatic cascade. First, these sialylated antigens promote anchoring of malignant cells to the activated endothelium, allowing active extravasation into the bloodstream and anchoring of these cells to distant locations (60). As such, overexpression of these glycosidic ligands is associated with the invasive and metastatic potential of primary bladder tumours as well as correlated with decreased survival (61). Importantly, serum overexpression of SLe^a (CA19-9 serological marker) was associated with higher stage, grade and invasion, while tissue loss/reduction of SLe^a expression was associated with higher atypia grade (62, 63). These observations support the need for a comprehensive interrogation of BC cells “sialome” towards understanding tumour progression and dissemination.

Increased expression of complex core-fucosylated *N*-glycans usually follows the hypersialylation observed in advanced bladder tumours (51). Importantly, changes in BC fucosylation patterns seem to be associated with invasion and progression to metastization in cancer cell lines (61, 64), suggesting that these changes could provide novel strategies for cancer therapy.

Perhaps the most studied glycosylation modification in BC lies in the premature stop of *O*-glycosylation extension, giving rise to the overexpression of Tn, T, ST, and STn short-chain *O*-GalNAc glycans. Frequently, these events are associated to an underlying disorganisation of secretory pathway organelles, mutations on *Cosmc*, a gene encoding the molecular chaperone of T-synthase (65), and absence or altered expression and/or activity of glycosyltransferases (66). The subsequent sections will specially focus on this particular class of *O*-GalNAc glycans.

2.3. Expression of short-chain *O*-glycans in bladder cancer: the disclosed role of the Sialyl-Tn antigen

As previously described, short-chain *O*-glycans (Tn, T, STn, ST, dST) are the result of a premature stop in *O*-glycosylation of plasma-membrane and secreted proteins, being expressed in advanced stage bladder tumours (42, 67). Moreover, the fact that these simple glycans are absent, significantly under-expressed or restricted to some cell types in healthy tissues, makes them ideal diagnostic and therapeutic targets for BC therapy (68).

Interestingly, the Tn and T antigens are poorly expressed in bladder tumours in comparison to their sialylated counterparts STn and ST antigens. More importantly, neutral glycoforms are mostly found in high-grade tumours, irrespective of the degree of invasion (69). Several reports have associated the presence of T antigens with higher grade, stage and poor prognosis in BC (69, 70), suggesting that these antigens may be surrogate markers of profound cellular alterations. Moreover, the expression of T antigen is significantly associated with higher risk for subsequent recurrences with deep muscle invasion and metastatic involvement of regional lymph nodes (70). Contrasting with neutral short-chain *O*-glycans, ST antigens, including mono- and/or di-sialyl-T, are widely detected in bladder tumours irrespective of their grade and degree of invasion (67). Particularly, in opposition to the ubiquitous nature of sialyl-6-T (S6T), the S3T antigen was mostly found in high-grade NMIBC (67). Nevertheless, many high-grade tumours co-express both T sialylated forms. These observations support previous associations

between the overexpression of both sialyl-T and ST3Gal-I, the sialyltransferase responsible for T antigen *O*-3 sialylation, in high-grade tumours (71). Moreover, similar to S6T, the S3T antigen was also not detected in the healthy urothelium, reinforcing the cancer-associated nature of these antigens (67). Glycoproteomic analyses of advanced bladder tumours based on enzymatic treatments, *Vicia villosa* lectin-affinity chromatography enrichment and nanoLC-ESI-MS/MS analysis resulted in the identification of several key cancer-associated glycoproteins carrying altered glycosylation, namely MUC16, CD44, and integrins (67).

In turn, the expression of STn in BC has been largely associated with the overexpression of ST6GalNAc I (68). Specifically, the STn antigen is absent in the healthy urothelium, while being present in more than 70% of high-grade NMIBC and MIBC, denoting a cancer specific nature (68). This post-translational modification of cell surface proteins is mostly expressed in non-proliferative tumour areas, known for their high resistance to cytostatic agents currently used to improve the overall survival of advanced stage BC patients (68). Recently, a novel STn-dependent mechanism for chemotherapeutic resistance of gastric cancer cells to cisplatin has been described, in which STn protects cancer cells against chemotherapeutic-induced cell death by decreasing the interaction of cell surface glycan receptors with galectin-3 and increasing its intracellular accumulation (72). Nevertheless, the relationship between chemoresistance and STn overexpression remains to be fully explored in BC. Furthermore, STn expression is significantly higher in MIBC when compared to NMIBC, denoting its association with muscle invasion and poor prognosis (73). Studies *in vitro* have further demonstrated that this antigen plays an important role in BC cell migration and invasion through mechanisms so far unexplored (68, 74). Recent glycoproteomics studies of BC cell models highlighted that STn was mainly present in integrins and cadherins, further reinforcing a possible role for this glycan in adhesion, cell motility and invasion (74). Moreover, glycoproteomic analysis of advanced-stage bladder tumours has disclosed MUC16 STn^+-glycoforms, characteristic of ovarian cancers, in a subset of tumours facing the worst prognosis (67). These findings suggest that abnormal MUC16 glycoforms hold potential as surrogate biomarkers of poor prognosis and unique molecular signatures for designing highly specific targeted therapeutics. Also, recent work from our group has demonstrated the presence of STn in MIBC, lymph nodes, circulating tumour cells and in distant metastasis, strengthening the notion that STn expression may influence cancer cell motility and metastization (75, 76). Furthermore, STn-expressing BC cells have shown the ability to induce a tolerogenic microenvironment by impairing dendritic cells maturation, allowing cancer cells to evade

innate and adaptive immune system responses (77). Interestingly, the tolerogenic effect of short-chain *O*-glycans has also been correlated with bladder tumour metastasis through a mechanism in which MUC1 carrying core 2 *O*-glycans functions as a molecular shield against NK cells attack, thereby promoting metastization (78). In addition, STn expression in BC tissues has been used in combination with other surrogate markers of tumour aggressiveness envisaging patient stratification regarding disease stage and therapeutic benefit. Specifically, expression of STn and S6T, a sialylated form of T antigen, are independent predictive markers of BCG treatment response and were found useful in the identification of patients who could benefit more from this immunotherapy (79). Moreover, STn was found to be a marker of poor prognosis in BC and, in combination with PI3K/Akt/mTOR pathway evaluation, holds potential to improve disease stage stratification (73).

3. Microenvironment-induced *O*-glycome alterations

3.1. Hypoxia: an hallmark of tumour progression

Hypoxia is characterized by a reduction in oxygen tension available to a cell, being characteristic to less vascularized regions of the bone marrow, locales of intense inflammation or necrosis, as well as solid tumours. While oxygen levels of most mammalians tissues vary between 2 and 9%, hypoxia is usually defined as ≤ 2% O_2 and severe hypoxia (or anoxia) is defined as ≤ 0.02% O_2 (80). In solid tumours, hypoxia usually arises from sustained proliferative signalling of tumours cells as well as flawed neoangiogenesis (81). Depending on regional and temporal status of blood flow through leaky vessels, hypoxia can vary from moderate to severe, acute to chronic, and intermittent to persistent. Moreover, both acute and chronic hypoxia co-exist within a tumour, resulting in differential gradients of oxygen consumption and contributing to intra-tumour heterogeneity (82).

The master regulators driving adaptation to O_2 deprivation are the hypoxia-inducible factors (HIFs), heterodimeric transcription factors comprising an α and β subunits. In mammals, there are three isoforms of the HIF-α subunit (HIF-1α, HIF-2α, and HIF-3α). While HIF-1α is ubiquitously expressed, HIF-2α and HIF-3α are tissue-specific (83). Moreover, heterodimers containing HIF-1α or HIF-2α seem to have overlapping but distinct specificities regarding both physiological inducers, target genes and transcriptional co-factors (84). Interestingly, HIF-3α seems to function primarily as a transcriptional inhibitor of HIF-1α. In addition, contrasting with the O_2-dependent nature of the HIF-α subunits, HIF-1β is constitutively expressed and insensitive to changes in O_2 levels (85-87).

Regarding the mechanisms of hypoxia sensing, HIF-1α is the major player driving adaptation during acute phases of oxygen shortage (88, 89). Briefly, under normoxia, prolyl hydroxylase domain enzymes (PHDs) hydroxylate two specific proline residues within the O_2-dependent degradation (ODD) domain of the α subunit of HIF-1α. Subsequently, the von Hippel-Lindau (VHL) tumour suppressor E3 ligase complex polyubiquitinates HIF-α and targets it for degradation by the 26S proteasome (84, 90). Concomitantly, factor inhibiting HIF-1 (FIH-1) mediated modification of HIF-1α blocks co-factor binding; thereby inhibiting HIF-1α transcriptional activity (91). Under low O_2

tension, HIFs are no longer modified by PHDs, but instead dimerize with ARNT/HIF-1β through HLH and PAS domain interactions, translocate to the nucleus, and recruit co-activators such as CBP/p300. HIF heterodimers bind and recognize hypoxia-response elements (HREs), with the consensus sequence G/ACGTG, within the promoter regions of target genes and drive adaptive gene transcription (92). Through the transcriptional remodelling promoted by HIF, hypoxia selects increasingly aggressive clones endowed with virtually all hallmark capabilities of cancer cells. Namely, by inducing the transcription of mitogenic factors, hypoxia maintains sustained proliferative signalling of tumour cells in a HIF-1α-dependent manner (93). Moreover, HIF-1α can drive antiapoptotic changes, as increase in Bcl-2 and Mcl-1 levels, Bcl-xL induction, and decrease in pro-apoptotic Bid, Bax, and Bak levels, thereby allowing tumour cells to scape programmed cell death (94). In addition, HIF-1α drives a major metabolic adaptation to nutrient shortage, controlling all glucose-dependent biosynthetic pathways, namely glycolysis, hexosamine biosynthetic pathway (HBP), pentose phosphate pathway (PPP), or glycogen synthesis (95). Also, it has been shown that hypoxia selects clones expressing mutant p53, a classical growth suppressor, facilitating the clonal expansion of cells that have a dominant-negative effect on the wild-type cells, thus evading apoptosis (96). The presence of intratumoral hypoxia also promotes genetic instability of tumour cells, leading to altered transcription and translation of several DNA damage response and repair genes, resulting in the inhibition of recombination-mediated repair of DNA double-strand breaks. Moreover, hypoxia increases the rate of mutation, microsatellite and chromosomal instability, driving genetic instability and malignant progression (97). Concomitantly, hypoxia also influences c-Myc activation which is known to transactivate the *telomerase reverse transcriptase (TERT)* gene, thereby enabling the replicative immortality of tumour cells (98). Tumour hypoxia also promotes vessel growth by upregulating multiple pro-angiogenic pathways that mediate key aspects of endothelial, stromal, and vascular support cell biology, mostly in a HIF-1α-dependent manner (99). Recent studies also show that hypoxia influences additional aspects of angiogenesis, including vessel patterning, maturation, and function (99). Furthermore, hypoxia influences early and late stages of metastasis, mostly in a HIF-dependent manner. Within the primary tumour HIF-dependent gene expression promotes an immunosuppressive microenvironment, neovascularization, epithelial-to-mesenchymal transition (EMT), and regulates glycosylation in adhesion molecules towards more motile and invasive phenotypes. At a distance, hypoxia contributes to the production of secreted factors and exosomes involved in premetastatic niche formation and regulates metabolic and survival pathways that allow cells to adapt to the

microenvironment of distant tissues while maintaining more aggressive clones (100). Hypoxia also drives cancer-associated inflammation by promoting granulocytes and monocytes/macrophages of the myeloid lineage infiltration and activation *in vivo* in a HIF-1α-dependent manner (101). Recent findings from our research group showed that hypoxia also regulates cell surface glycosylation towards a simpler phenotype characterized by sialylated short-chain *O*-glycans. In this context, given the self-like character of these antigens and the immunosupresive role of hypersialylation one can argue that cells might become increasingly less immunogenic, thereby contributing to immune scape.

Overall, these findings reflect the key role of hypoxia in all hallmarks of cancer, highlighting the potential clinical benefit of targeting these particularly aggressive subpopulations of tumour cells.

3.2. Hypoxia drives metabolic switch and altered glycosylation

Hypoxic stress within a tumour leads to a shift from aerobic oxidative phosphorylation to anaerobic glycolysis, with high rates of glucose and glutamine uptake (the Warburg effect) (102, 103). In this context, adaptation to hypoxia and cellular energetic reprograming occurs mostly in a HIF-1α-dependent manner, being frequently accompanied by cell dedifferentiation and acquisition of mesenchymal characteristics (104). Briefly, to compensate the reduction of intracellular ATP levels under hypoxic conditions, HIF-1α upregulates the expression of glucose transporters-1 and 3 (GLUT1, GLUT3), allowing the intracellular uptake of glucose (105). Of note, overexpression of GLUT1/3 is correlated with poor survival in most solid tumours, suggesting that its expression status is a vital prognostic indicator and promising therapeutic target in solid tumours (106-108). Once in the hypoxic cell, glucose is rapidly phosphorylated to glucose-6-phosphate (Glc-6-P), mostly by hexokinase-2 (HK2) and HK1 to a lesser extent, both HIF-1α targets (109). Subsequently, Glc-6-P enters one of several possible biosynthetic pathways, namely glycolysis, HBP, PPP, or glycogen synthesis, all of which substantially regulated by HIF-1α. Particularly, HIF- 1α channels glucose into glycolysis by upregulating the expression of glycolytic enzymes (110). Furthermore, to ensure continuous cycles of glycolysis, HIF-1α enables the removal of pyruvate, the end product of the pathway, as well as NAD^+ recycling by upregulating lactate dehydrogenases (LDH), which catalyses the conversion of pyruvate and NADH to lactate and NAD^+ (110). Lactate is then removed from the cell by the HIF-inducible plasma membrane

monocarboxylate transporter 4 (MCT4) (111). Simultaneously, to decrease O_2 consumption and reactive oxygen species (ROS) generation, HIF-1α downregulates oxidative phosphorylation within the mitochondria by transactivating genes such as pyruvate dehydrogenase kinase 1 (PDK1), inhibiting pyruvate dehydrogenase (PDH) generation of CoA, CO_2, and NADH from pyruvate (112). Under a chronic state of HIF-1α activation, it can reduce the need for oxygen by limiting mitochondrial biogenesis (113), altering the activity of cytochrome c oxidase (COX-4/10), inducing miR-210 transcription, or by decreasing the expression of iron-sulfur cluster assembly proteins (ISCU) (114, 115); thereby disrupting the electron transport chain and the TCA cycle.

By regulating the flux through the HBP and PPP pathways, HIF-1α dramatically affects glycosylation, either by altering precursor production or by governing enzymatic activity. Specifically, HIF-1α has significant impact on the HBP by increasing both mRNA and expression of its rate-limiting enzyme glutamine-fructose-6-phosphate amidotransferase (GFAT) (116). However, this event is not reflected in the intracellular abundance of the glycosylation precursor UDP-*N*-Acetylglucosamine (UDP-GlcNAc), mostly because HIF-1α induces PDK transcription, thereby inhibiting PDH activity as previously described (117). This process not only inhibits the TCA cycle but also suppresses the addition of an acetyl group to glucosamine, leading to an overall reduction in UDP-GlcNAc production (112, 117). Moreover, during acute hypoxia, the production of ATP, GTP, UTP and CTP nucleotides through the PPP is decreased, compromising the addition of UDP to GlcNAc (117, 118). Another branch of the HBP, namely the CMP-NeuAc nucleotide sugar biosynthesis pathway, is activated under hypoxia through the epimerization of UDP-GlcNAc by UDP-GlcNAc 2-epimerase (GNE), ultimately enabling cell surface sialylation in a HIF-1α-dependent manner (117, 119). Interestingly, while hypoxia causes downregulation of PPP enzymes, such as the rate limiting Glucose-6-phosphate dehydrogenase (G6PD) and 6-phosphogluconate dehydrogenase (6PGD) in several cancers (120), glycosylation activates G6PD activity and increases glucose flux through the PPP, providing precursors for nucleotide and lipid biosynthesis, and reducing equivalents for antioxidant defence. Particularly, G6PD is dynamically modified with an *O*-GlcNAc sugar in response to hypoxia and blocking glycosylation of G6PD reduces cancer cell proliferation in vitro while impairing tumour growth *in vivo* (121). Besides regulating glycolytic enzymes, *O*-GlcNAcylation also regulates transcription factors as carbohydrate-responsive element-binding protein (ChREBP) and Sp1 to modulate metabolic reprogramming towards increased aerobic glycolysis and lipogenesis (122). *O*-GlcNAcylation also plays a key role in the stabilization of transcription factor c-MYC, that cooperates with other transcription factors

to regulate genes involved in cell proliferation, differentiation, apoptosis, and nucleotide metabolism, as well as with HIF-1α to regulate genes involved in glucose metabolism (123). Of note, it has been reported that elevated *O*-GlcNAcylation in cancer cells stabilizes HIF-1α in an indirect manner, thereby reinforcing the Warburg effect (124). c-MYC stabilisation by *O*-GlcNAcylation occurs at Thr^{58} residue by competing with phosphorylation at the same site. The subsequent increase in c-MYC levels contributes to a switch towards aerobic glycolysis and upregulation of glutaminase for anaplerotic resupply of tricarboxylic acid intermediates used in biosynthesis (122). Together, these findings suggest that hyper-*O*-GlcNAcylation may contribute to oncogenicity and cancer metabolic reprograming through glycolytic enzymes activity modulation and stabilization of oncogenic transcription factors. As such, *O*-glycosylation directly regulates the PPP to confer a selective growth advantage to tumour cells under hypoxia.

Hypoxia also regulates almost all enzymes involved in glycogen metabolism (125). Moreover, it is proposed that a decrease in oxygen tension leads to glycogenesis, preparing the cells for subsequent nutrient depletion, while glycogenolysis is promptly activated upon glucose deprivation (126). Given these insights, one can conclude that during tumorigenesis tumour cells suffer metabolic reprograming starting with increased glycolytic flux through simple processes such as glycolysis, while decreasing the rate of complex pathways like oxidative phosphorylation. As such, oxygen availability appears to determine which catabolic process glucose undertakes even if it is not the more productive. In addition to intracellular glucose metabolism modifications, glycosyltransferases and glycosidases modulation towards the expression of short-chain sialylated *O*-glycans, decreased 1,2-fucosylation of cell-surface glycans, and galectin overexpression are some consequences of the hypoxic tumour microenvironment (127). Moreover, increased expression of gangliosides carrying *N*-glycolyl sialic acids can also be significantly affected by hypoxia (127). For all these reasons, it is possible to realize that hypoxia strongly alters glycobiologic events within tumours, resulting in increased *O*-GlcNAcylation and sialylation; thereby leading to more aggressive phenotypes (127, 128).

Based on these insights, hypoxia is a major driving force of the energetic reprograming of cancer cells, largely affecting glycosylation in a HIF-1α-dependent manner. As such, both *O*-GlcNAc modifications and HIF-1α transcriptional activity emerge as key metabolic modulators, envisaging tumour survival and growth.

3.3. Hypoxic modulation of *O*-GalNAc glycans in bladder cancer

Since hypoxia is a salient feature of advanced stage tumours, our group has recently searched into how it influences BC cells glycophenotype, with emphasis on STn expression (74). Accordingly, hypoxia was shown to promote STn antigen overexpression and enhanced the migration and invasion of cells presenting more mesenchymal characteristics, in a HIF-1α-dependent manner. These effects were reversed by reoxygenation, demonstrating that oxygen affects *O*-glycan extension (74). Glycoproteomics studies highlighted that STn was mainly present in integrins and cadherins, suggesting a possible role for this glycan in adhesion, cell motility and invasion under hypoxia. The association between HIF-1α and STn overexpressions and tumour invasion was further confirmed in BC patient samples (74). In conclusion, STn overexpression may, in part, result from a HIF-1α mediated cell-survival strategy to adapt to the hypoxic challenge, favouring cell invasion. In addition, targeting STn-expressing glycoproteins may offer potential to treat tumour hypoxic niches harbouring more malignant cells.

A more in-depth screening for other cancer associated O-GalNAc short-chain glycoforms by western blot further revealed that BC cells did not express the Tn and the T antigens in any of the studied conditions. In agreement with these observations and as previously described, the Tn and T antigens are also rarely detected in bladder tumours, irrespectively of their stage (67, 73). However, an increase of sialyl-T (ST) under hypoxia was observed. Nevertheless, when compared to STn expression, the ST antigen was mostly present in high molecular weight glycoproteins, denoting a more restricted glycoproteome which warrants validation future studies. Elevations in the ST antigen have been reported in bladder tumours but their contribution to BC progression and dissemination still warrants clarification (71, 79). These results suggest that sialylation, in particular of the Tn antigen, may be amongst the key events driving the premature stop in *O*-glycosylation extension in a wide number of membrane glycoproteins.

3.4. Hexosamine biosynthesis pathway: linking glucose availability and tumoral aberrant glycosylation

As previously described, the HBP provides the UDP-GlcNAc, UDP-GalNAc and CMP-Neu5Ac substrates for *N*-, *O*-GalNAc, and *O*-GlcNAc glycosylation (Figure 4).

Moreover, the increased glucose flux through the HBP upon hyperglycaemia often culminates in the overexpression of glucose transporters, as GLUT1, as well as in increased levels of UDP-GlcNAc and UDP-GalNAc precursors and upregulation of biosynthetic GalNAc transferases as ppGalNAc-T6 (129) (130). Concomitantly, these events translate into aberrant levels of the Tn antigen, α2-3- and α2-6-sialylation, fucosylation as well in complex β1,6-branched *N*-linked glycans (131). Contrastingly, under glucose starvation, UDP-GlcNAc, UDP-Gal, UDP-Glc and GDP-Man levels are negatively affected, while GDP-Fuc and CMP-NeuAc levels do not suffer alterations due to their posterior biosynthesis (130). In addition, under glutamine abundance but not of glucose, UDP-GlcNAc levels also increase (132). This reflects the fact that glutamine is also a substrate of HBP modulating the production of UDP-GlcNAc (133). Moreover, UDP-GlcNAc levels can be rescued under glucose deprivation through the lysosomal degradation of monosaccharides (134). These events may provide an explanation to the enhancement of HBP flux and to the tolerance acquired by glycolytic tumour cells under glucose depletion (133, 135). Tumour cells that are unable to rescue these alternative pathways commonly undergo programmed cell death due to ER stress and unfolded protein response (UPR) activation due to the accumulation of unfolded poorly glycosylated proteins. In line with this, UDP-GlcNAc supplementation rescues HBP and inhibits UPR activation under glucose deprivation (136).

Given these insights, glucose starvation which follows O_2 shortage largely contributes to aberrant glycosylation of tumour cells, mostly by affecting the bioavailability of glycosylation precursors. Moreover, similarly to the hypoxic challenge, glucose starvation acts as a selective pressor for more aggressive clones capable of enduring metabolic reprograming. As such, glycosylation incorporates the response to the microenvironmental challenge of oxygen and glucose deprivation, opening an avenue to target these highly aggressive subpopulations.

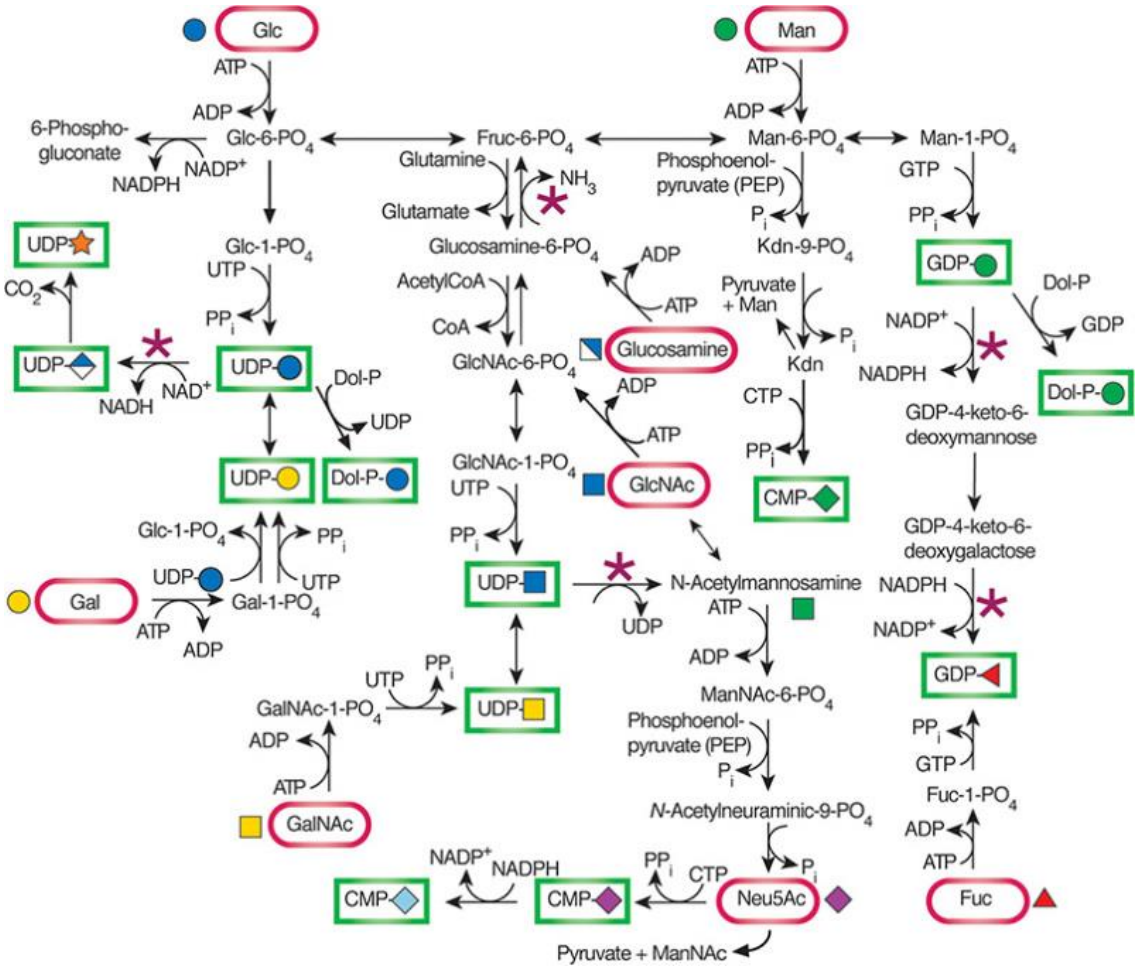

Figure 3 - Biosynthesis and interconversion of monosaccharides (137). Rectangles: donors; ovals: monosaccharides; asterisks: control points.

4. Glycoproteomics and Glycomics: Analytical overview and critical challenges

The cancer membrane glycoproteome bridges molecular features from the glycan and protein moieties, holding great potential for the identification of clinically relevant biomarkers (15). However, its characterization requires a prior knowledge of the repertoire of glycans that a cell or tissue exhibits under specific conditions, which depends not only on cellular molecular background but also on its microenvironment. In fact, glycomics is pivotal for guiding glycoproteomics, which focus on describing how the glycome appears on the cellular proteome. Glycoproteomics provides information on the nature and abundance of glycosylated proteins, as well as on the distribution and composition of glycosites for a given biological milieu. However, glycans are not direct gene products, but rather the results of a highly regulated process mediated by a wide array of glycosyltransferases, sialidases, chaperones and sugar donors along the protein secretory pathways (30, 31, 37). As such, neither the transcriptome nor the proteome can accurately predict the glycome and glycoproteome, making necessary to adapt conventional proteomics strategies to address both these aspects.

4.1. Glycomics

Glycoproteomics requires a prior knowledge of the cell glycome by mass spectrometry and other complementary techniques. Nevertheless, glycan analysis poses a significant analytical challenge due to its non-templated and structurally diverse nature, frequently characterized by the existence of isomeric/isobaric structures in the same sample (31, 138). Typical protocols initiate with the selective release of glycans from glycoproteins by either enzymatic of chemical methods. Generally, *N*-glycans are released by PnGaseF digestions whereas *O*-GalNAc glycans are released by reductive *β*-elimination (139). Subsequently, glycans may be directly analysed by mass spectrometry, which provides an overview on the main classes of glycans in the sample, or resolved by liquid chromatography into isomeric structures (140). *N*-glycans are also frequently derivatized by reductive amination using labels such as 2-AB (2-aminobenzamide) or 2-AA (2-aminobenzoic acid). Moreover, this enables its fluorescent detection and ultimately the establishment of mass-spectrometry independent analytical

platforms (141). Another widely explored derivatization method, explored for both *N*- and *O*-glycan analysis, involves the permethylation of glycans to stabilize labile sugars such as fucose and sialic acids, enabling detection by matrix-assisted laser desorption/ionization (MALDI) and softer ionization methods such as electrospray (ESI) (139). Moreover, all the above-mentioned derivatization methods render glycans more hydrophobic, thus facilitating separation by conventional C18 reverse phase LC columns, ionization and detection by mass spectrometry. Currently, underivatized glycan analysis has been gaining ground with the introduction of porous graphitized liquid chromatography columns that allow a good separation of isomeric structures. However, the standardization and generalization of these protocols has not yet been achieved. As such, permethylation is still by far the most used derivatization method for mass spectrometry analysis of glycans at the micromolar scale. In addition, several libraries exist for interpretation of permethylated glycans LC chromatograms. Moreover, product ion spectra are generally greatly informative by providing ions derived from both glycoside linkages and cross-ring fragmentations. Notwithstanding, the analysis of *O*-glycans still poses a significant challenge since it relies on chemical methods, namely *β*-elimination, that often degrades the protein backbone and significantly reduces the sensitivity of the analysis. This limitation has been recently addressed by a novel method based on CORA and, more recently, ICORA (Isotope-Cellular *O*-glycome Reporter Amplification), a semi-quantitative and qualitative tool for comparative *O*-glycomics (142, 143). CORA results in an ∼100–1,000-fold increase in sensitivity compared to *β*-elimination and identifies a more complex repertoire of *O*-glycans. In this new approach, cells are incubated with the previously peracetylated benzyl-α-D-GalNAc (benzyl 2-acetamido2-deoxy-α-D-galactopyranoside, Bn-GalNAc), a compound usually used in higher concentrations as inhibitor, mimicking the initial *O*-GalNAc-Ser/Thr. Peracetylation of Bn-GalNAc renders it more hydrophobic to enhance its cellular uptake where it is acted upon by deacetylases to constitute a substrate to glycosyltransferases. Subsequently, extended Bn-*O*-glycans are secreted into the extracellular medium, purified and permethylated before mass spectrometry analysis (143). In turn, ICORA uses a stable Benzyl-α-D-GalNAcAc$_3$ precursor presenting a deuterated benzyl group, allowing quantitative glycomics, since the isotope label precursor is 7 Da heavier than its hydraded counterpart (142).

4.2. Glycoproteomics

Membrane glycoproteins constitute a small portion of the proteome. A pre-enrichment of the sample for the glycans of interest, guided by a prior knowledge of the glycome, is often elected as the starting point to overcome this limitation. Samples may be pre-enriched for species of interest by physical methods, immunoprecipitation and affinity chromatography targeting specific glycans with antibodies or lectins, prior to analysis by mass spectrometry. The vast majority of studies subsequently apply conventional proteomics workflows for protein identification. In fact, the recent development of highly sensitive and accurate mass spectrometer analysers enables deep proteome mining, providing the identification and quantification of a vast array of proteins and peptides while simultaneously informing on their PTMs (144, 145). Currently, standard ionization techniques for protein and PTMs analysis involves MALDI (matrix-assisted laser desorption/ionization) and nES (nanoelectrospray ionization). Additionally, the employment of hybrid mass analysers, such as QqTOF (quadrupole time-of-flight), TOF/TOF (time-of-flight / time-of-flight), IT/Orbitrap (ion trap/orbitrap) and Q/Orbitrap (quadrupole/orbitrap), which allow rapid tandem mass spectrometry experiments (MS/MS) have contributed to increase confidence in protein identification and accurate mapping of PTM sites (146, 147).

Protein and PTMs identifications using mass spectrometry can be achieved by different strategies. The classical and most widely approach consists in a bottom-up analysis of peptides derived from the digestion of proteins with specific (148). Noteworthy, glycosylation often renders proteins less prone to proteases, limiting the success of these approaches. As such, many studies combine different broad spectra proteolytic enzymes in an attempt to increase protein coverage and the chances of glycopeptide identifications. Alternatively, the middle-down approach enables the analysis of large peptides resulting from soft proteolysis (149). Finally, top-down analysis focusses on the identification of intact protein mass by mass spectrometry followed by direct ion dissociation in the gas phase (150).

Relative and absolute quantification of proteins and PTMs has been classically achieved by 2-DE, before MS-based approaches emerged. The MS-based methods involve stable isotopic labelling and label-free workflows. Stable isotopic labelling currently refers to metabolic labelling of proteins in cell culture, such as SILAC (stable isotope labelling with amino acids in cell culture) or SILAM strategies (stable isotope labelling with amino acids in mammals). Otherwise, stable isotopic labelling can be made

post-metabolically, following several chemical derivatization strategies, such as iTRAQ (isobaric tags for relative and absolute quantification), TMT (tandem mass tag) and ICAT (isotope-coded affinity tag). However, with the increased resolution and sensitivity of modern mass spectrometer, label-free quantification methods have been gaining ground. These methods generally include the computational analysis of MS ion intensity, spectral counting, chromatogram peak area or targeted approaches, such as SRM (selected reaction monitoring) (145, 151, 152).

Tandem mass spectrometry, with different relevance of the fragmentation methods allows to obtain more structural information, namely of glycosylation sites. Collision-induced dissociation (CID), is by far the most commonly used and easily available ion fragmentation methodology. It is based on the collision of selected molecular ions with a neutral atom or molecule, leading to formation of protonated amide linkages, along with neutral loss of modification. Although capable of providing significant information on peptide sequence, CID does not provide ideal diagnostic sequence ion information for the identification of glycopeptides (153). Contrastingly, electron capture dissociation (ECD) induces preferential cleavage of peptide backbones at the N-C_α bond instead of at the amide linkage, being a better approach to glycosylated peptides. More recently, electron transfer dissociation (ETD) was developed, showing many similarities with ECD; however, it can be performed in ion trap mass spectrometers or even in QTOF type instruments. Lastly, high-energy collision dissociation (HCD) was implemented essentially to orbitrap platforms. This fragmentation technique is similar to CID, but fragmentations are carried at higher collision energies ensuring higher peptide sequence coverage and an improvement in the diagnosis of glycopeptides (151).

Regardless of the methodological approach selected for protein identification, there is still a gap between protein identification and biomarker discovery. *In silico* approaches have revealed more accurate assignments and identified relevant glycobiomarkers to clinical translation. This strategy encompasses several bioinformatics tools to validate protein identification (SequestHT, Proteome Discover and SwissProt database), glycosylation sites (NetNGlyc and NetOGlyc), biological functions (Panther, STRING, Cytoscape, UniProtKB), and associations to histological data (Oncomine) (67, 154, 155).

In summary, given the large panoply of methodological approaches it is now possible to personalize workflows towards more accurate access to cellular and tissue glycome and glycoproteome, ultimately facilitating clinical translation.

5. Aims and scopes

Preliminary studies carried out in the hosting research group have highlighted that the BC glycoproteome is an important source of clinically relevant biomarkers. Moreover, it has been demonstrated that specific protein short-chain *O*-glycoforms such as the STn antigen are associated to chemoresistance and poor prognosis. However, characterization of the BC membrane glycoproteome remains challenging due to its complex structural nature, posing significant analytical challenges to conventional proteomics approaches. Moreover, both glycome and glycoproteome present dynamic natures, rapidly adapting in response to microenvironmental stimuli. Based on these considerations, this work devotes to systematizing an analytical roadmap to address the BC glycoproteome foreseeing clinical translation. Moreover, it envisages to evaluate the impact of two salient microenvironmental features driving cancer hallmarks: hypoxia and glucose deprivation. We anticipate that this knowledge will be of key importance for guiding future glycoproteomics studies for targetable biomarkers in hypoxic niches.

This thesis comprehends the following specific objectives:

I. Establish a protocol to address the cancer cell membrane glycome and glycoproteome;

II. Provide insights on the BC glycoproteome, highlighting potential clinically relevant glycoproteins;

III. Analyse the influence of hypoxia and/or glucose deprivation in the BC *O*-glycome envisaging the molecular rational for downstream glycoproteomics and functional studies.

These objectives are comprehensively addressed in chapters II and III of this thesis. Accordingly, chapter II aims to respond to objectives I and II, while chapter III focuses on responding to objectives III. The chapters follow a research paper format, including an abstract, a brief introduction, material and methods, results and discussion. Finally, chapter IV provides an integrative overview of the results, along with concluding remarks and future perspectives.

Chapter II | A Bioinformatics-Assisted Workflow to address the Plasma Membrane Glycoproteome: Biomarker Discovery Using Bladder Cancer Cell Models

This chapter is part of a manuscript under the same title by Azevedo R and Relvas-Santos M *et al.*, currently in preparation for submission

Abstract

Changes in the plasma membrane glycoproteome play a key role in cancer development and progression, constituting an important source of targetable cancer biomarkers. Moreover, the identification of particular glycans may translate into more specific cancer signatures of clinical utility. Nevertheless, the non-templated, context-dependent and rather heterogeneous structural nature of glycans has posed a significant analytical difficulty for glycoproteome characterization by conventional proteomics. Therefore, glycoproteomics studies frequently require a prior comprehensive understanding of the glycome. Moreover, the distinct product ion spectra of glycopeptides frequently raises difficulties for tackling mass spectrometry data using conventional fragmentation methods (CID, HCD) and bioinformatics tools for protein spectra annotation. Herein, we devote to propose a bioinformatics-assisted analytical protocol to address these limitations using three widely studied BC cell models. Briefly, we have applied a recently developed Cellular *O*-glycome Reporter/Amplification method for glycomics characterization, which later allowed designing adequate enrichment strategies by lectin affinity chromatography and enabled glycosites identification. All cell lines presented sialylated forms of the T antigen as dominant glycoforms, in agreement with previous studies in bladder tumours. Samples were then enriched for glycoproteins carrying these glycans by Peanut Agglutinin (PNA) Lectin Affinity Chromatography after neuraminidase digestion and subsequently identified by bottom-up nanoLC-CID-MS/MS-based proteomics. Data was curated for glycoproteins of interest based on gene ontology for membrane glycoproteins and the potential presence of *O*-glycosites by NetOGlyc. Approximately, 1300 glycoproteins were identified for the three cell lines, approximately 10% of which were common to the three cell lines. Glycoproteins were then comprehensively integrated with available transcriptomics and immunopathological information using Oncomine and Protein Atlas and integrated with previous BC glycoproteomics data. This generated a library of potentially clinically relevant glycoproteins for future validation. This sets an important roadmap for many laboratories focusing on cancer biomarkers for clinical applications and highlights the potential of exploring web-based bioinformatics tools and databases for more comprehensive and integrated data mining.

Introduction

The plasma membrane provides structural integrity and maintains cellular polarity by anchoring the cytoskeleton and allowing extracellular matrix attachment. Moreover, it endows cell-cell crosstalk through protein interactions (156). While approximately 10% of the proteins encoded by the human genome have been experimentally observed in the plasma membrane, many can be found in intracellular organelles and secreting vesicles at a given stage of its cycle, suggesting a role in a wide array of biological events (157). Particularly, the plasma membrane glycoproteome is mainly composed by proteins mediating cellular response to extracellular stimuli, endocytosis, and cellular adhesion (158).

Cancer-associated genetic and epigenetic instability allied to deregulations in alternative splicing events are amongst a wide array of aspects impacting on plasma membrane protein structure, abundance and functionality. Such alterations frequently aid tumour cells to achieve several hallmarks of cancer by activating oncogenic pathways, while impacting negatively cellular adhesion and immune recognition (159). Moreover, many of these events originate tumour-associated antigens and neoantigens holding great potential for targeted therapeutics, many of which have been already explored in cancer immunotherapy (160). As such, considerable efforts have been devoted to the comprehensive characterization of the plasma membrane proteome envisaging novel cancer biomarkers for more effective therapeutics. Moreover, specific glycosylated moieties may allow narrowing the membrane proteome to clinically relevant glycoforms. Showcasing this aspect, a recent targeted investigation of the BC glycoproteome highlighted that specific MUC16 glycoforms (CA125 antigen) could be used to define subsets of chemoresistant patients, whereas no associations could be found based solely on the presence of the protein (67).

Nevertheless, the high glycosylation frequency and glycosites density presented by membrane glycoproteins poses a significant analytical hurdle to conventional proteomics protocols. Such difficulties are further aggravated by the non-templated and context dependent nature of glycan structures. As such, a prior knowledge of glycan structures is required for increasing the chances of glycoprotein and glycosites identification. Moreover, glycomics studies enable the design of adequate glycoprotein enrichment strategies, which impact positively on protein identification and greatly expands the dynamic range of identified proteins. However, glycosylation raises a major difficulty for protein identification by conventional bottom-up bioinformatics tools used for

protein annotation from tandem mass spectrometry data. In fact, most available bioinformatics tools base their identification protocols on typical peptide fragmentation patterns, greatly penalizing the presence of post-translational modifications. This is particularly critical for glycopeptides that, due to the sugar moiety and depending on the ion fragmentation method, may generate product ion spectra exhibiting molecular information from both glycan-bearing and non-glycan-bearing peptide, making spectral annotation a challenging task. This particular feature leads common proteomics database search engines to scoring glycopeptides with lower identification confidence values, resulting in a general underidentification of glycopeptides. Facing these difficulties, we have recently reported that bioinformatics tools exploring gene ontology and glycosites prediction (NetOGlyc, NetNGlyc) may be used to curate glycoproteomics datasets that include low confidence protein identifications (154). Moreover, glycoproteomics data may be comprehensively integrated with transcriptomics and proteomics web-based databases to highlight clinically relevant and targetable biomarkers. Taking into account the potential of bioinformatics in glycoproteome research, we now aim to systematize a comprehensive bioinformatics-assisted protocol for glycobiomarker discovery using cancer cell models as starting point. Emphasis will be set on BC *O*-glycoproteome (glycosylations of Ser/Thr), which has previously been reported to present significant alterations according to the severity of the lesions (15, 67). We anticipate that this may constitute the basis for panomics integrated workflow for tangible biomarker discovery in cancer.

Material and Methods

Cell Culture

The T24 (grade III), 5637 (grade II) and HT1376 (grade III) BC cell lines were acquired from DSMZ (Düsseldorf, Germany) and recently characterized and authenticated by our group (161). Accordingly, the T24 cell line is representative of the FGFR3/CCND1 oncogenic pathway, presenting *HRAS* mutation and overexpression of *CCND1*. Both 5637 and HT1376 cells represent the E2F3/RB1 pathway with loss of one *RB1* copy and mutation of the remaining copy. Additionally, HT1376 cells exhibit *PTEN* gene deletion and no alterations in *PIK3CA*, which in combination with the inactivation of *p53* translates into a more invasive and metastatic potential. In contrast, the 5637 cell line presents *PIK3CA* gene deletion and no *PTEN* alterations, translating into a less-

invasive phenotype. The cells were cultured in RPMI 1640 + GlutaMAX™ medium (Gibco™, Thermo Fisher Sientific), supplemented with 10% heat-inactivated FBS (Gibco™, Thermo Fisher Sientific) and 1% penicillin-streptomycin (10,000 Units/mL penicillin; 10,000 µg/mL streptomycin; Gibco™, Thermo Fisher Sientific). Cell lines were cultured as a monolayer at 37°C in a 5% CO_2 humidified atmosphere.

O-glycomics

Cellular *O*-glycome patterns were characterized based on the Cellular *O*-glycome Reporter/Amplification method (162). Briefly, benzyl-α-D-GalNAc (benzyl 2-acetamido-2-deoxy-α-D-galactopyranoside) (Sigma-Aldrich) were peracetylated by addition of 450 µl of pyridine and 3 ml of anhydride acetic and incubated for 30 min at 30ºC, followed by chloroform-water extraction. The organic phase containing the acetylated reporter (Benzyl-α-D-GalNAcAc$_3$) was then evaporated to dryness in a vacuum concentrator evaporator, resuspended in 50 µl of DMSO and diluted to 150 µM of culture medium with 10% FBS and 1% penicillin-streptomycin. Confluent adherent cells (approximately 7x10^6 cells) were then incubated with Benzyl-α-D-GalNAcAc$_3$ for 24h. The media was then collected, centrifuged at 1200 rpm for 5 min and filtered in a 10 kDa centrifugal filter (Amicon Ultra-4, Merck Millipore) by centrifugation for 1h at 2500 x g. The flow through was purified in Sep-Pak 3 cc C18 cartridges (Waters) by reversed-phase gravity chromatography. Briefly, the column was pre-conditioned with acetonitrile and then equilibrated with 0.1% TFA aqueous solution prior to sample injection. The column was then washed with 0.1% TFA and Bn-*O*-glycans were eluted with 50% acetonitrile/0.1% TFA aqueous solution, followed by dryness in a vacuum concentrator evaporator. Finally, Bn-*O*-glycans were permethylated. The labelled glycans were first dissolved in a 500 µl DMSO/NaOH slurry for 30 min and permethylated with methyl iodide for 30 min. Permethylated glycans were isolated by liquid-liquid extraction with chloroform and water (1:1) and dried in a vacuum concentrator evaporator.

MALDI-TOF analysis was performed in a Bruker UltrafleXtreme MALDI-TOF/TOF mass spectrometer. Permethylated Bn-*O*-glycans were first resuspended in 25 µl methanol and 1:1 matrix:sample mixes were spotted onto a MTP 384 polished steel target plate, air dried and analysed by MALDI-TOF mass spectrometry in positive ion reflector mode over the mass range 700 to 4000 Da. Laser attenuation was set to 95% and *ca.*5000 shots were accumulated. The matrix used was 2,5-dihydroxibenzoic acid (DHB), 10 mg/ml in 50% methanol, 0.1% TFA in water. Spectra were subjected to external calibration using the peptide calibrant provided by the manufactured. After peak

assignment internal calibration was performed using assigned peak masses. Peak masses-structures assignement followed current knowledge of *O*-glycosylation pathways. Relative glycan expression was calculated in comparison to the sum of all ions corresponding to glycan species. All experiments were done in triplicates.

Glycoprotein enrichment and digestion

Plasma membrane proteins were extracted from whole cells ($20x10^6$) by scrapping with fractionation buffer (20mM HEPES buffer (pH=7.4), 10mM KCl, 2mM $MgCl_2$, 1mM EDTA and 1mM EGTA) on ice. Cell suspension was then passed through a 27G needle and left on ice for 20 min. Samples were then centrifuged at 720 x g for 5 min at 4ºC to remove nuclei, transferred to a fresh tube and recentrifuged at 10.000 x g for 5 min at 4ºC to remove mitochondria. Samples were transferred to polycarbonate centrifuge bottles with cap assemblies and centrifuged for 1h at 100.000g at 4ºC in a Beckman Coulter Optima L-XP series ultracentrifuge. Pellets were resuspended in fractioning buffer and passed through a 25G needle before centrifugation for 45 min at 100.000g at 4ºC. Finally, pellets were resuspended in an appropriate volume of TBS/0.1% SDS. Plasma membrane enriched fractions were then digested with α-neuraminidase [10 U *Clostridium perfringens* neuraminidase Type VI (Sigma)] and enriched for glycoproteins expressing the T antigen by PNA lectin agarose (Vector laboratories) chromatography. The columns were equilibrated and washed after sample injection with TBS/0.05% SDS and glycoproteins-enriched extracts were then eluted with 3% acetic acid. These extracts were dried in a vacuum concentrator evaporator, resuspended in loading buffer and run on an SDS-PAGE gel. Glycoprotein fractions were excised from the gel, then directly reduced with 10 mM DTT (Sigma) for 45 min at 56°C, alkylated with 10 mM iodoacetamide (Sigma) in the dark for 30 min, and digested with 0.1 µg/µL of trypsin (Promega).

nanoLC-MS/MS analysis

A nanoLC system (Dionex, 3000 Ultimate nano-LC) was coupled online to an LTQ-Orbitrap XL mass spectrometer (Thermo Scientific) equipped with a nano-electrospray ion source (Thermo Scientific, EASY-Spray source). Eluent A was aqueous formic acid (0.2%) and eluent B was formic acid (0.2%) in acetonitrile. Samples (20 µl) were injected directly into a trapping column (C18 PepMap 100, 5 µm particle size) and

washed with an isocratic flux of 95% eluent A and 5% eluent B at a flow rate of 30 µl/min. After 3 minutes, the flux was redirected to the analytical column (EASY-Spray C18 PepMap, 100 Å, 150 mm × 75µm ID and 3 µm particle size) at a flow rate of 0.3 µl/min. Column temperature was set at 35°C. Peptide separation occurred using a linear gradient of 5–40% eluent B over 90 min., 50–90% eluent B over 5 min and 5 min with 90% eluent B. The mass spectrometer was operated in the positive ion mode, with a spray voltage of 1.9 kV and a transfer capillary temperature of 250°C. Tube lens voltage was set to 120 V. MS survey scans were acquired at an Orbitrap resolution of 60,000 for an m/z range from 300 to 2000. Tandem MS (MS/MS) data was acquired in the linear ion trap using a data dependent method with dynamic exclusion: The top 6 most intense ions were selected for collision induced dissociation (CID). CID settings were 35% normalized collision energy, 2 Da isolation window 30 ms activation time and an activation Q of 0.250. A window of 90 s was used for dynamic exclusion. Automatic Gain Control (AGC) was enabled and target values were $1.00e^{+6}$ for the Orbitrap and $1.00e^{+4}$ for LTQ MSn analysis. Data were recorded with Xcalibur software version 2.1.

Data was analyzed automatically using the SequestHT search engine with the Percolator algorithm for validation of protein identifications (Proteome Discoverer 1.4, Thermo Scientific). Data were searched against the human proteome obtained from the SwissProt database on 22/11/2018 selecting trypsin as the enzyme and allowing for up to 2 missed cleavage sites and a precursor ion mass tolerance of 10 ppm and 0.6 Da for product ions. Carbamidomethylcysteine was selected as a fixed modification, while oxidation of methionine (+15.9) and modification of serine and threonine with HexNacHex (+365.1) was defined as variable modification. In glycoproteomics studies, due to the high lability of sugar moieties under CID conditions, and the consequent difficulty in identifying modified peptides, Sequest results of low confidence peptides were also considered. Protein grouping filters were thus set to consider PSMs with low confidence and ΔCn better than 0.05. The strict maximum parsimony principle was applied.

Bioinformatics

For curation of plasma membrane proteins from BC *O*-glycoproteomics dataset, protein annotation tables for each cell line were generated using gene ontology (GO) terms for cellular location through the Software Tool for Researching Annotations of Proteins (STRAP) (163). Molecular and biological functions were also explored. The retrieve/ID mapping of UniProtKB (http://www.uniprot.org/) (164) was then used to

reconfirm the topological domain and subcellular location of proteins retrieved by STRAP. Then, membrane proteins were sorted in relation to *O*-glycosylation sites using NetOGlyc version 4.0 (http://www.cbs.dtu.dk/services/NetOGlyc/) (165). To generate the final curated protein list, cell membrane proteins with at least 2 peptides identified with low confidence were validated manually through their spectra using Proteome Discoverer 1.4.

The subset of plasma membrane proteins expressed by all cell lines was analyzed regarding their protein-protein interactions, molecular and biological functions and involved KEGG pathways using the Search Tool for the Retrieval of Interacting Genes/Proteins (STRING) version 10.5 (http://string-db.org/) (166). A network with biological processes considering only significant pathways ($p \leq 0.05$) were constructed for these common proteins using the following parameters: a GO tree interval of min. 4 and max. 10, and a kappa score of 0.64 in ClueGO plugin for Cytoscape (http://www.cytoscape.org/) (167).

All plasma membrane proteins were analyzed using Oncomine™ (https://www.oncomine.org/) (168, 169), according to their overexpression in BC (NMIBC and MIBC) compared to healthy tissues through RNAseq technology. A $p \leq 0.05$ as well as a 2-fold variation of expression were considered. Expression of these proteins in BC patient samples and healthy tissue was also analyzed using The Human Protein Atlas (170, 171).

Results

We elected three aggressive BC cell lines of different histological backgrounds (Grade II and III) and representative of two distinct carcinogenesis pathways. The cell lines were first submitted to glycomics characterization, which helped guiding downstream glycoproteomics protocols and glycoprotein identification. We demonstrate how bioinformatics tools based on gene ontology (GO) of protein cellular location combined with *O*-glycosites prediction may facilitate the curation of glycoproteomics datasets. Finally, we attempt to combine our data with available transcriptomics and proteomics information using web-based tools to pinpoint clinically relevant proteins for downstream validation (Scheme 1).

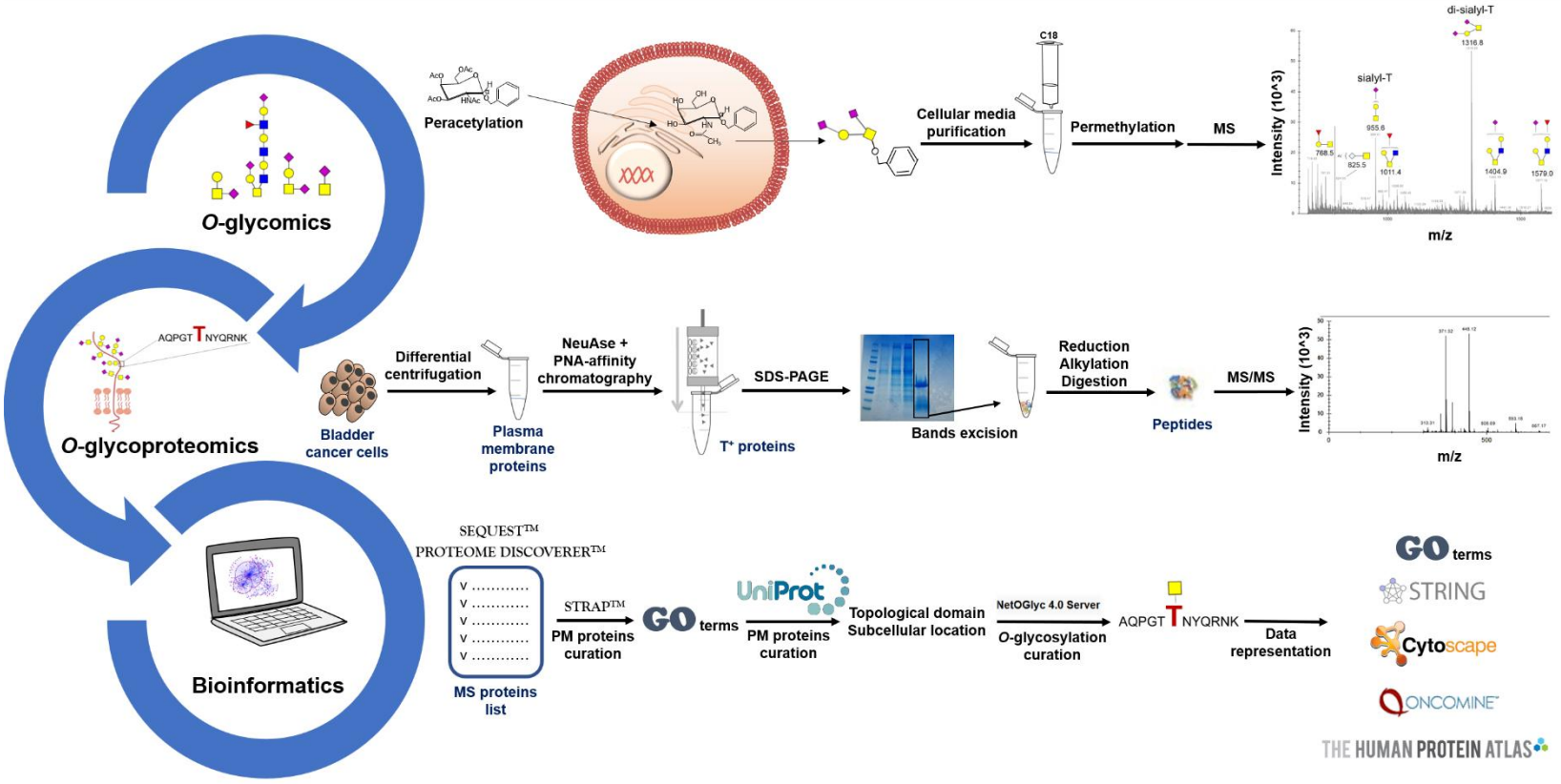

Scheme 1 - Illustration of the bioinformatics-assisted analytical protocol. The high glycosylation frequency and glycosites density presented by membrane glycoproteins poses a significant analytical hurdle to conventional proteomics protocols. Such difficulties are further aggravated by the non-templated and context dependent nature of glycan structures. As such, a prior knowledge of glycan structures is required for increasing the chances of glycoprotein and glycosites identification. Accordingly, *O*-glycoproteome characterization was performed using the Cellular *O*-glycome Reporter/Amplification method. Briefly, a Bn-GalNAc precursor is peracetylated to favor its plasma membrane diffusion, subsequently deacetylated by intracellular deacetylases and further extended by the available glycosylation machinery. Once biosynthesized the extended Bn-GalNAc glycans are secreted back into the extracellular medium. After recovery by reverse phase chromatography, *O*-glycans were permethylated to facilitate ionization and stabilize labile sugars, thus enabling downstream analysis by MALDI-TOF-MS. Taking into account glycomics studies, membrane protein extracts were subsequently digested with sialidase and enriched for glycoproteins expressing the T-antigen by Peanut Agglutinin (PNA) Lectin Affinity Chromatography. Glycoproteins were identified based on a conventional bottom-up proteomics workflow comprehending trypsin digestion and analysis by nanoLC-CID-MS/MS followed by protein annotation using SEQUEST.

Glycomics

O-glycomics analysis was based on a recent molecular reporter technology using a glycan mimetic of the simplest form of *O*-glycosylation (Bn-GalNAc). Briefly, Bn-GalNAc was first peracetylated to render it more hydrophobic to passively diffuse through the plasma membrane. The compound is then rapidly deacetylated by intracellular deacetylases, glycosylated by the available glycosylation machinery and secreted back into the extracellular medium. After recovery by reverse phase chromatography, the glycan mimetic was permethylated to make it more hydrophobic to facilitate ionization and stabilize labile sugars such as fucose and sialic acids, thus enabling downstream analysis by MALDI-TOF-MS (162).

A total of 19 different glycans were identified (Figure 1), the majority of which belonging to T24 (n=18 glycans) and HT1376 (n=14) grade III cell lines, whereas the grade II cell line presented a more homogenous nature at the glycan level (n=5). In fact, the 5637 cell line mainly expressed mono and di-sialylated T and core 2 antigens, while grade III cell lines also presented evidences of more elongated and sialylated core 2 structures. Nevertheless, mono and/or di-sialylated T antigens were predominant glycan species in all cell lines, in agreement with previous observations in bladder tumours by immunohistochemistry (67). Interestingly, the sialyl-T and di-sialyl-T ratio was higher for grade II compared to grade III cell lines, supporting a shift towards oversialylation upon grade increase, as suggested by previous reports (67, 74, 76). Nevertheless, more studies involving more cell lines of different molecular backgrounds and tumour tissues showing distinct clinicopathological features are required to support this hypothesis. In summary, glycomics analysis highlighted sialylated T antigens as preferential *O*-glycoforms presented by BC cell models, supporting enrichment strategies focusing on this glycans before downstream glycoproteomics studies.

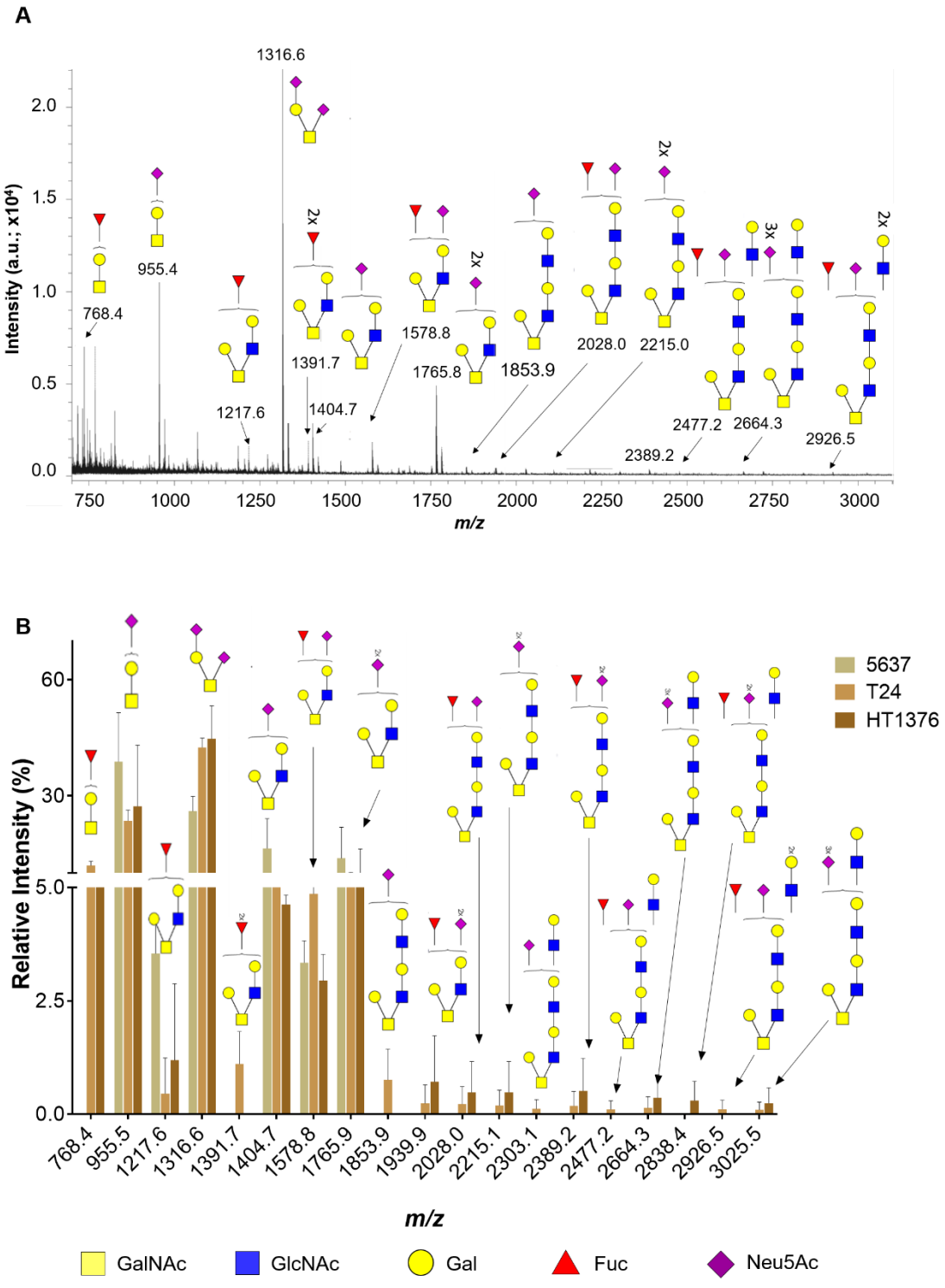

Figure 1. Glycome repertoire for 5637, T24 and HT1376 cell lines in bladder cancer. (**A)** Typical cellular *O*-Glycome Reporter/Amplification MALDI-TOF-MS for T24 cell line. The mass spectra highlights mono and di-sialylated T antigens, at m/z = 955.4 and 1316.6, as dominant glycan species. Less abundant ions include fucosylated T antigens (m/z= 768.4) and fucosylated and/or sialylated short-chain core 2 glycans (m/z= 1391.7, 1578.8, and 1765.8, respectively). Vestigial signals corresponding to more extended glycans were also evident at m/z= 1853.9, 2028.0, 2215.0, 2477.2, 2664.3 and 2926.5. **(B)** Glycome repertoire for bladder cancer cell lines 5637, T24 and HT1376. All cell lines present similar *O*-glycomes, showing mono- and di-sialylated T antigens as the most abundant glycans.

Glycoproteomics and Bioinformatics

Samples were first enriched for plasma membrane proteins by ultracentrifugation of cell protein extracts. Taking into account glycomics studies, membrane protein extracts were subsequently digested with sialidase and enriched for glycoproteins expressing the T-antigen by PNA affinity chromatography. Glycoproteins were identified based on a conventional bottom-up proteomics workflow comprehending trypsin digestion and analysis by nanoLC-CID-MS/MS followed by protein annotation using SEQUEST. On average, we have identified with high confidence less than 100 glycoproteins for each cell lines (26 glycoproteins for 5637; 47 for T24; 84 for HT1376); nevertheless, this was based on less than 5% of the species subjected to MS/MS. Such observations reinforce the notion that conventional proteomics annotation tools fail to accurately identify proteins carrying post-translational modifications, significantly diminishing our view on the proteome, as previously demonstrated (172, 173). To increase protein identification and sequence coverage, we have included the possibility of HexHexNAc as variable modifications of Ser and Thr residues (T antigen). We have also significantly decreased SEQUEST's identification threshold to include low/medium confidence peptides and proteins. This allowed accommodating glycopeptides that under CID fragmentation present very characteristic product ion spectra which are scored with low confidence by the SEQUEST algorithm. The resulting protein list, presenting a significant number of low confidence identifications, was then curated for proteins presenting a plasma membrane location based on gene ontology (GO) and screened for potential *O*-glycosylation sites using NetOGlyc. Sorted proteins were then validated for glycopeptides exhibiting the T antigen as post-translational modification. Overall, we have identified 1037 glycoproteins potentially expressing sialylated T antigens, which significantly contrasted with the identifications relying solely on high scoring glycoproteins. These findings reinforce the importance of a comprehensive assessment of mass spectrometry data backed by bioinformatics tools capable of sorting potentially glycosylated membrane proteins. Nevertheless, our strategy retrieved a higher number of identifications for grade III cell lines in relation to the grade II model (62% in T24 and 76% in HT1376 *vs* 55% in 5637; Figure 3A). Since all cell lines present similar *O*-glycosylation patterns in terms of sialylated T antigens (Figure 1), the higher number of identified proteins in grade III cell lines may be explained by increased glycosite density and/or *de novo* glycosylation accompanying progression, which should also be explored in future studies involving a broader cell line panel and a quantitative evaluation of the proteome. Interestingly, the percentage of proteins shared by the three

cell lines was only 14%, suggesting some degree of similarity at *O*-glycoproteome level. Moreover, the glycoproteome of all cell lines share similar biological and molecular functions, while having similar intracellular distribution (Figure 2). According to a STRING analysis, these glycoproteins show a significant degree of interaction, suggesting a high level of synergism towards common biological functions (Figure 3). Moreover, GO analysis suggests that many of these glycoproteins interact to drive cellular motion (Figures 3 and 4), as previously highlighted by our glycoproteomics studies in BC cell models (74) and tumours (67). Finally, GO term analysis suggests that these glycoproteins may contribute to sort and carry molecular information across different subcellular compartments. This hypothesis is further reinforced by the fact that all the identified glycoproteins may be found in more than one subcellular location, as highlighted by Figure 5. Supporting these observations, many intracellular proteins have been found at the cell membrane in cancer cells, constituting important sources of highly specific cancer biomarkers (174-177). In addition, the main represented functions and processes of these glycoproteins include substrate-specific transport and ion channel activities, suggesting key participation in cellular homeostasis, as well as in cytoskeletal protein binding, denoting a potential role in defining cellular shape. In turn, the main intracellular pathways in which these glycoproteins are prevalent include the ABC transporters network, several players in the regulation of the cytoskeleton, and proteoglycan-mediated signaling pathways (Figure 3). The majority of biological processes highlighted in the cytoscape analysis include cell-cell and cell-extracellular matrix adhesion mainly mediated by Integrin beta-1 (ITGB1), C-terminal focal adhesion targeting (FAT), and vinculin (VCL). Moreover, immunological processes such as Interleukin-2 (IL-2) secretion and activation of $CD8^{+}$αβ T cells are also mediated by hub proteins as Ezrin (EZR) and Major Histocompatibility Complex, Class I (HLA-A), respectively. Importantly, several biological processes concerning protein targeting to the plasma membrane where in place, as well as cytoskeletal anchoring at the plasma membrane with the main contribution of ITGB1. Finally, biological processes concerning growth factor pathways were also activated, namely the platelet-derived growth factor response and PI3K pathway activation with key intervention of feline sarcoma-related (FER) proteins (Figure 4). Based on these insights, ITGB1 seems to be involved in more than one biological process highlighted by cytoscape analysis. Interestingly, treatment failure in metastatic BC is commonly caused by acquisition of resistance to chemotherapy in association with tumour progression. In this context, first-line chemotherapy resistant 5637, T24 and HT1376 cells overexpress integrin β1 which is key to extracellular matrix adhesion, suggesting that the evaluation of integrin β1 as a

potential therapeutic target for BC in vivo might be of value (178). Moreover, loss of β1-integrins was also associated with increased invasive potential of BC cells (179).

In summary, the integrative functional analysis of the identified glycoproteins suggests a common ground related with cellular homeostasis, shape and motility. Future studies should devote to disclosing the functional role of the identified glycoproteins in cancer as well as the role of glycosylation in membrane glycoprotein functions.

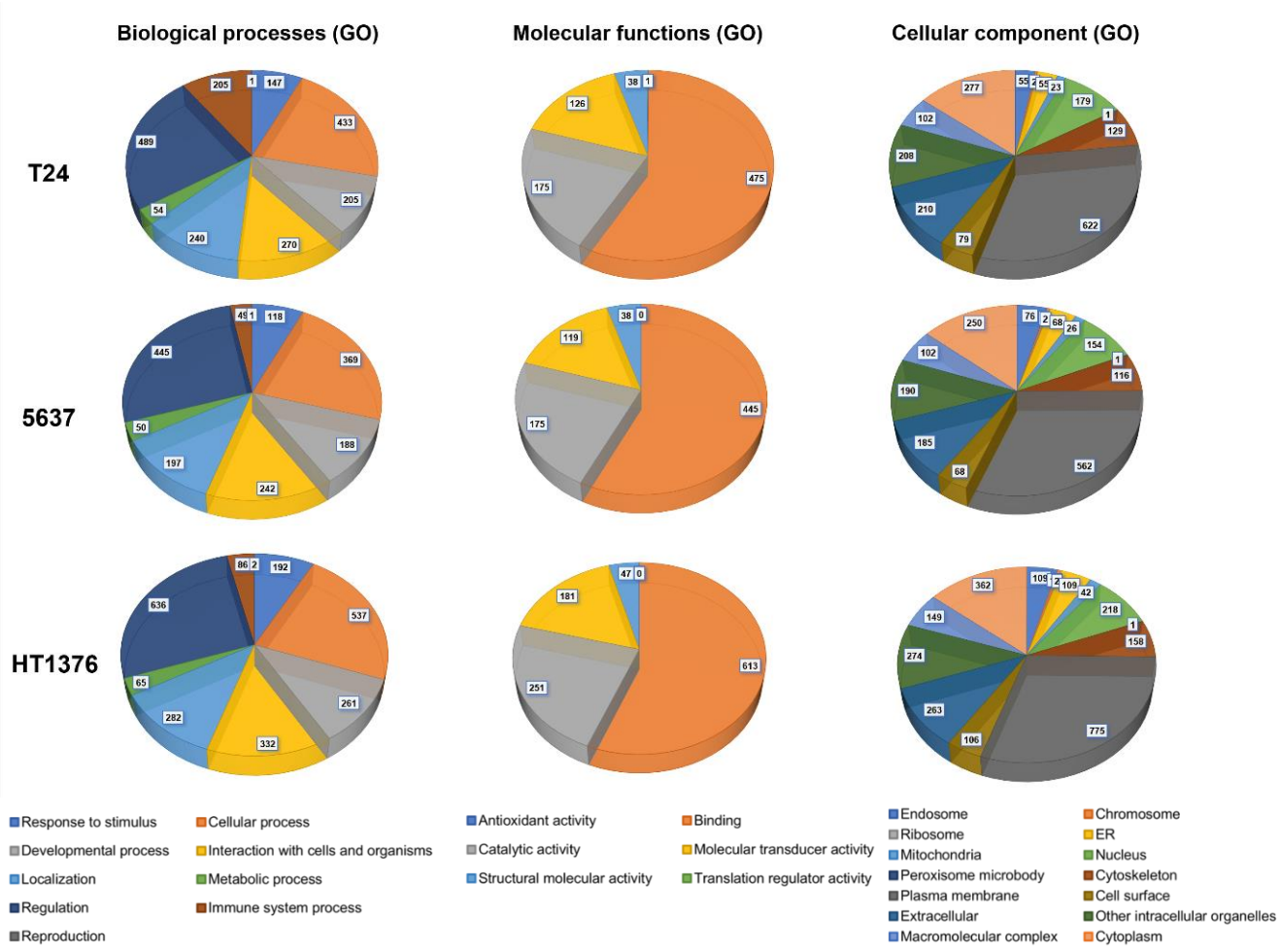

Figure 2 - Characterization of bladder cancer cell lines according to GO terms using STRAP program. The glycoproteome of all cell lines share similar biological and molecular functions, apparently having fairly the same intracellular distribution throughout organelles.

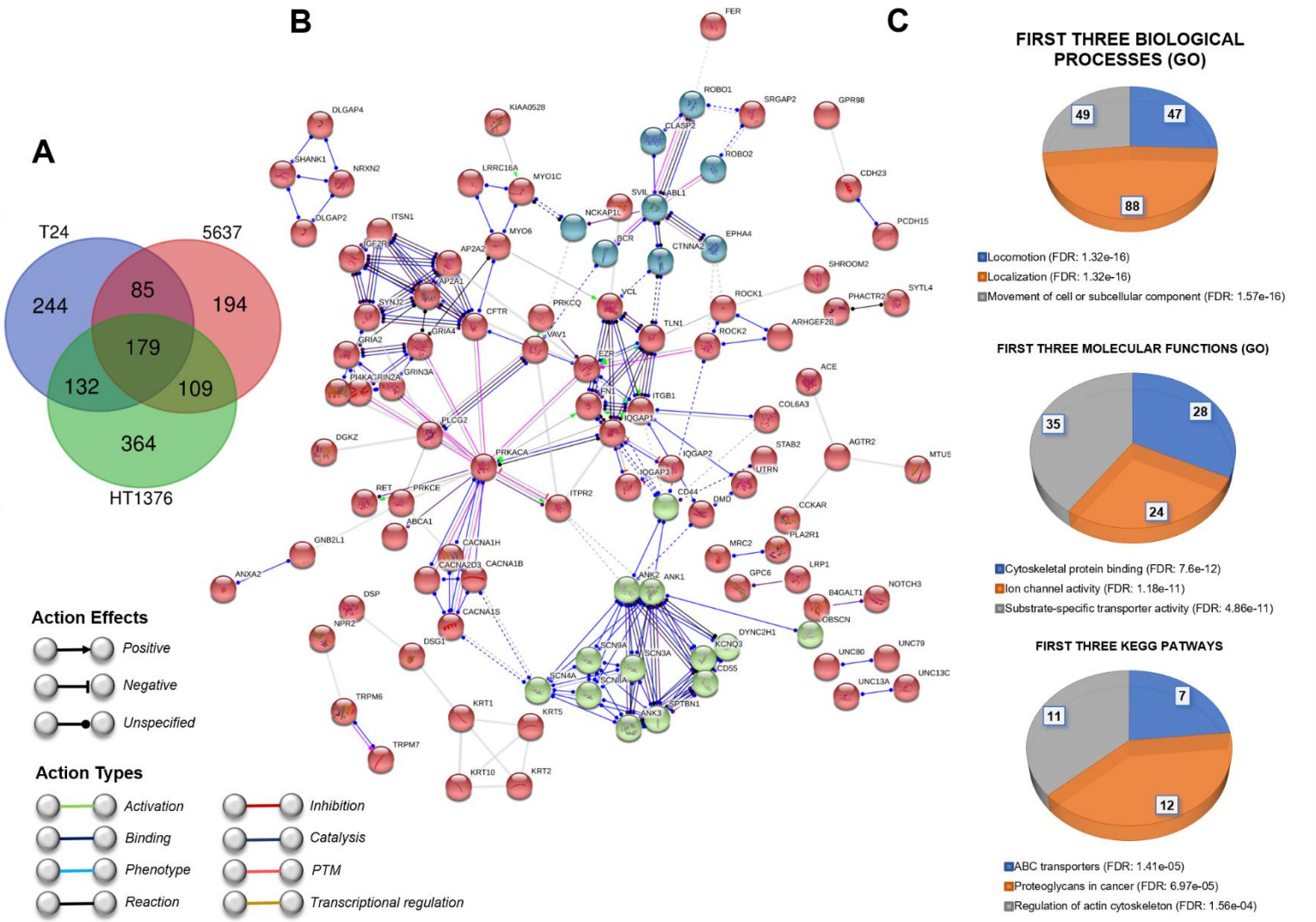

Figure 3 - String map for glycoproteins that are common to all cell lines and main biological processes, cellular functions and KEGG pathways. Common glycoproteins to the three cell lines show a significant degree of interaction, suggesting a high level of synergism. The main represented molecular functions and processes of these glycoproteins include substrate-specific transport and ion channel activities, suggesting key participation in cellular homeostasis, as well as in cytoskeletal protein binding, denoting a potential role in defining cellular shape. The main intracellular pathways in which these glycoproteins are prevalent include the ABC transporters network, several players in the regulation of the cytoskeleton, and proteoglycan-mediated signalling pathways.

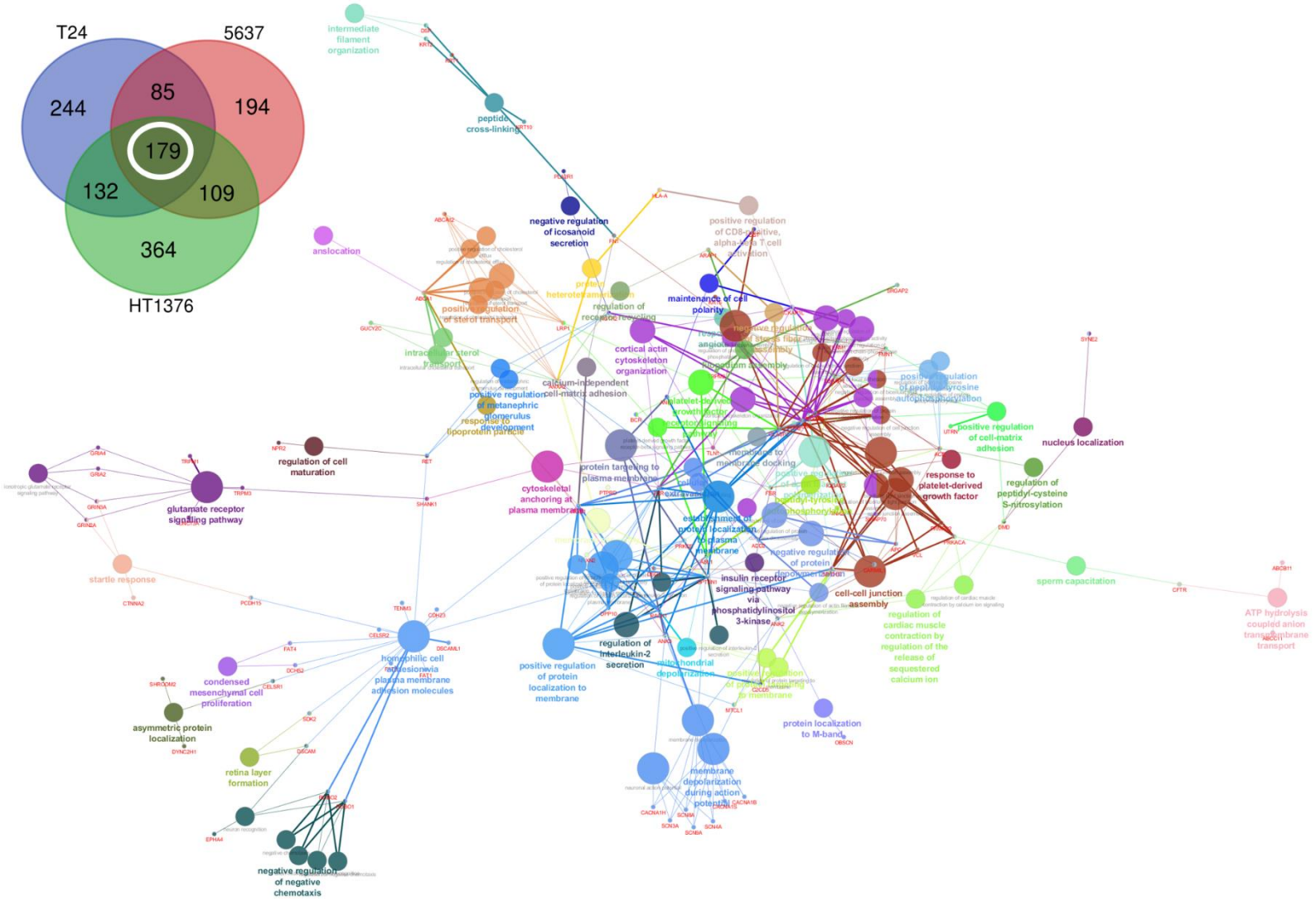

Figure 4. Cytoscape analysis highlighting the major biological processes governed by bladder cancer cell lines plasma membrane proteins. The majority of biological processes highlighted include: i) cell-cell and cell-extracellular matrix adhesion (Integrin beta-1 (ITGB1), C-terminal focal adhesion targeting (FAT), and vinculin (VCL) as hub proteins); ii) positive regulation of Interleukin-2 (IL-2) secretion and CD8+αβ T cells activation (Ezrin (EZR) and MHC-I (HLA-A) as hub proteins); iii) protein targeting to the plasma membrane and cytoskeletal anchoring (ITGB1 as hub protein), and iv) growth factor pathways (PI3K and feline sarcoma-related (FER) as hub proteins).

Figure 5 - Cellular Distribution of identified proteins. The figure highlights that all identified glycoproteins may be found in more than one subcellular location.

Bioinformatics for Identification of Targetable Biomarkers

Identified glycoproteins were then matched against the Oncomine RNAseq cancer database to sort proteins previously reported as overexpressed in bladder tumours in comparison to the healthy urothelium (Figure 6). Emphasis was set in the identification of glycoproteins associated to muscle invasion, which currently lacks effective therapeutics approaches (15). Approximately 19% of them were overexpressed in bladder tumours (253 glycoproteins) being distributed as follows: 103 glycoproteins in NMIBC, 112 in MIBC as well as NMIBC, and 38 in MIBC. We then focused attention on the 150 glycoproteins showing some degree of association with invasive lesions. The RNAseq levels for these glycoproteins were also compared with protein abundance in bladder tumours available on The Human Protein Atlas database, containing immunohistochemistry data. The majority of upregulated genes showed relevant translation at the protein level (81% of the 150 glycoproteins; Figure 6). The high degree of consensus between mRNA and corresponding proteins supports the rationale of using transcriptomics data as a starting point to identify potentially clinically relevant glycoproteins for downstream validation. Moreover, a restricted group of 29 proteins are exclusively overexpressed in MIBC and may play a critical role in advanced disease. This includes the well-studied and widely accepted BC stem cell biomarker CD44 (180, 181) that has been previously reported to be abnormally glycosylated in the malignant urothelium (67). In addition, 22 of the identified glycoproteins had been previously detected by targeted glycoproteomics in bladder tumour samples showing resistance to chemotherapy (identified in red in Figure 6). Moreover, the overexpression of 14 of these glycoproteins (ADAM10, ANX1, ATP1B1, CASP10, CPNE3, DST, ENO1, FAT2, KCNN4, LY75, MUC16, PIK3CA, PTPRF and YWHAH) had been previously associated with decreased survival in BC, according to The Human Protein Atlas. In addition, there is evidence that ADAM10 is overexpressed in BC and regulates malignant cell growth and invasion (182). ANX1 is also overexpressed in BC and its expression correlates with BC differentiation (183), while mutations in PIK3CA are key oncogenic drivers in BC (184). The remaining proteins remain unexplored in the context of BC, except for MUC16, which has been associated with chemoresistance (67). Future studies should devote to validating the expression of these glycoproteins and associated glycosylation in BC cell lines as well as in tumour samples to determine its functional and clinical relevance.

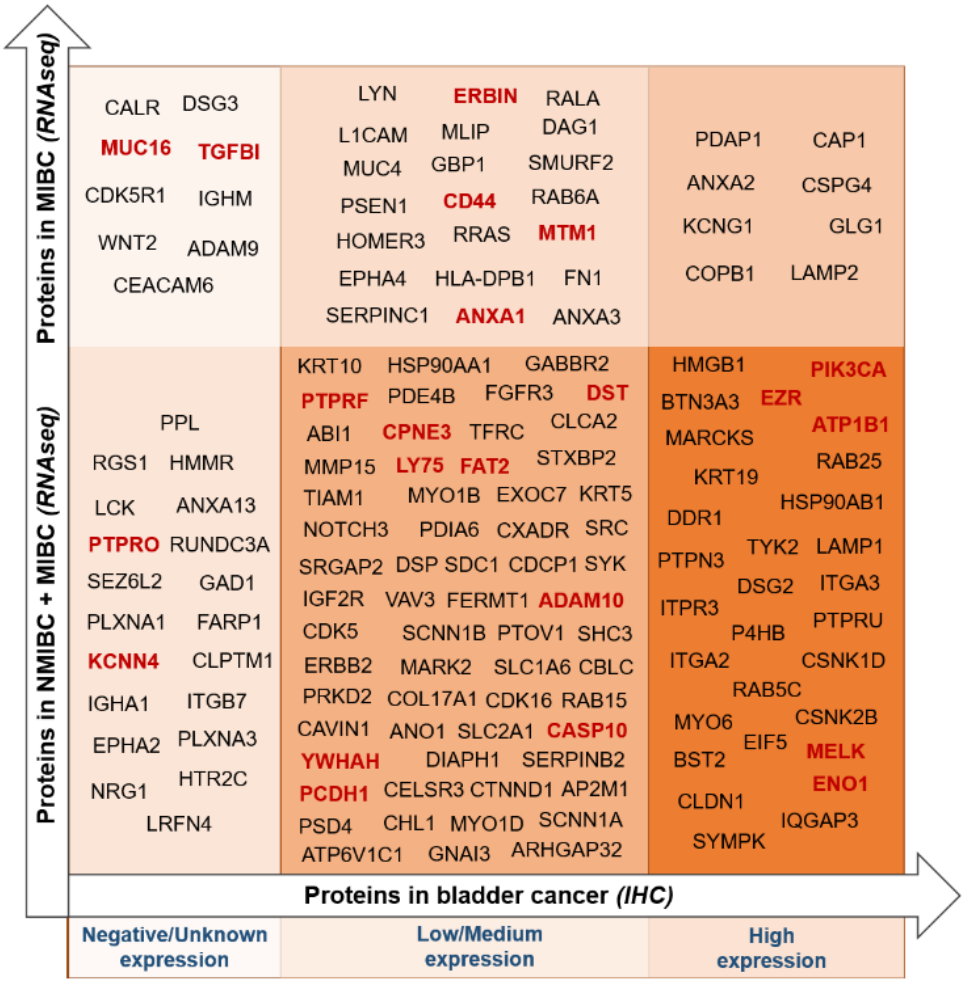

Figure 6 - Oncomine RNAseq cancer database analysis sorting the identified glycoproteins according with its previously reported expression in bladder tumours compared to the healthy urothelium. Approximately 19% of the identified proteins were overexpressed in bladder tumours (253 glycoproteins) being distributed as follows: 103 glycoproteins in NMIBC, 112 in MIBC as well as NMIBC, and 38 in MIBC.

Concluding Remarks

The membrane glycoproteome is a dynamic entity that changes according to the cells physiological context (185). Moreover, alterations in the membrane glycoproteome are frequently associated with cancer and drive key oncogenic features (186). Membrane glycoproteome remodeling has been mainly associated to changes in gene expression and alterations in the cancer glycome (187, 188). The combination of these events often originates cancer-specific molecular signatures holding tremendous potential for clinical intervention. Nevertheless, studying the membrane glycoproteome remains challenging, requiring a customization of conventional proteomics protocols to accommodate the

structural subtleties originated by glycosylation. Moreover, the glycobiology field has not yet started to explore the full potential of web-available molecular data repositories to comprehensively integrate its findings.

This work has addressed these limitations by systematizing a bioinformatics-assisted roadmap for comprehensive interrogation of the cancer glycoproteome regarding molecular function and potentially novel cancer biomarkers. We have focused on BC, which has been previously described by our group to present relevant and disease-stage dependent glycomics and glycoproteomics signatures (15, 67, 74). Exploring three of the most well characterized BC cell models, we used glycomics as a starting point for targeted glycoproteomics. This revealed sialylated T antigens has the most relevant class of *O*-glycans, irrespectively of the molecular nature of the cell line, thus in agreement with previous studies in bladder tumours (67). We further demonstrated that gene ontology sorting combined with glycosites prediction enables the curation of ultra-tolerant SEQUEST database searches for glycoproteins of potential interest. This significantly broadened the number of identified glycoproteins in comparison to non-curated assessment based solely on SEQUEST high scoring glycoproteins.

We have identified a higher number of glycoproteins in grade III cell compared to the grade II cell line but also an array of glycoproteins common to all cell lines. Finally, we used bioinformatics tools to comprehensively tackle the molecular and biological role of the cancer glycoproteome, which may be of key interest for guiding downstream functional studies. In particular, we have demonstrated that all cell lines presented common glycoproteomics signatures that drive cytoskeleton remodeling, cell motility and adhesion. Future studies should be devoted to fully disclose the contribution of individual glycoproteins and glycans to these events.

Finally, we have comprehensively matched our findings with reports available on RNAseq and protein databases, in an attempt to highlight cancer-associated expression patterns of potential clinical relevance. This led to the identification of glycoproteins that had been previously found to carry altered glycosylation in chemoresistant bladder tumours, thus reinforcing the relevance of our analytical approach. Amongst these glycoproteins were MUC16 (189) and the stem-cell biomarker CD44. Interestingly, validation experiments by western blot for CD44 highlighted a novel level of complexity potentially arising from alternative splicing mechanisms, which also warrant future confirmation. This list also includes proteins generally found in subcellular compartments that may at some point of its half-life be targeted to the plasma membrane in cancer cells, as previously reported in many cases (174-176). Future studies should devote to

sorting the clinical relevance of the most promising targets using a well characterized and diversified set of patient samples.

In summary, despite the preliminary nature of these findings facing clinical translation, our bioinformatics-assisted multi-omics platform as demonstrated potential for generating relevant molecular information for guiding future studies.

Chapter III | Bladder cancer *O*-glycome microenvironmental regulation: the role of oxygen and glucose

This chapter is part of a manuscript under the same title by Peixoto A and Relvas-Santos M *et al.*, currently in preparation for submission

Abstract

Invasive bladder tumours overexpress the cell-surface Sialyl-Tn (STn) and sialylated T antigens, which stems from a premature stop in protein *O*-glycosylation. However, the events leading to such deregulation in protein glycosylation are mostly unknown. Since hypoxia and glucose deprivation are salient features of advanced stage tumours, we searched into how it influences BC cells glycophenotype, envisaging future targeted glycoproteomics.

Based on these insights, three BC cell lines with distinct genetic and molecular backgrounds (T24, 5637 and HT1376) were submitted to hypoxia and/or glucose deprivation. At 24h exposure to hypoxia all cell lines overexpressed HIF-1α and increased lactate biosynthesis, denoting a shift toward anaerobic metabolism. Importantly, cell viability was maintained in all experimental conditions, with measurable proliferative decrease under hypoxia and further under glucose deprivation for all cell lines. Glycomics studies highlighted the synergic effect of hypoxia and glucose deprivation, leading to an overall decrease in *O*-glycans abundance, with predominance of sialylated Tn and T antigens. Concomitantly, both fucosylated core 1 and extended structures beyond core 1 were loss or significantly decreased. Accordingly, targeting STn/ST-expressing glycoproteins may offer potential to treat tumour hypoxic niches harbouring more malignant cells.

Introduction

Hypoxia is a salient feature of bladder tumours that has been highly associated to tumour invasion, metastization and resistance to therapy (190, 191), urging the molecular-assisted identification of hypoxic niches and rational design of targeted therapeutics. Alterations in the membrane glycoproteome in response to microenvironmental stimuli, including oxygen and nutrient availability, hold tremendous potential for addressing this problem. Amongst the molecular events driving glycoproteome remodelling are alterations in glycosylation. In fact, it was recently reported that triple negative breast cancer facing hypoxia and serum deprivation change their *O*-GalNAc glycosylation due to the upregulation of fucosyl- and sialyltransferases (192). Moreover, hypoxia-inducible factor 1-alpha (HIF-1α), a transcription factor that accumulates in hypoxic cancer cells, has been found to modulate the expression of fucosyltransferases and sialyltransferases responsible for $SLe^{a/x}$ antigens biosynthesis

in colon and pancreatic tumours (128, 193). These glycan terminal epitopes mediate cancer cell adhesion to E-selectin on epithelial cells and consequently metastasis, supporting a key role for hypoxia in these events. Following these observations, our group has recently demonstrated that hypoxia also induces severe alterations in the *O*-glycosylation of BC cells (74). Studies based on immunoassays showed that hypoxic BC cells overexpressed the short-chain carbohydrate antigen sialyl-Tn (STn), responsible for enhanced cell motility (68), invasion (74) and immune escape (77), while being an independent poor prognostic factor (73, 79). Targeted glycoproteomics focusing on this antigen supported profound alterations in the membrane glycoproteome with emphasis on key mediators of cell adhesion. Amongst the most striking observations was that hypoxic cells expressed a significant number of integrins, protocadherins and cadherins carrying the STn antigen in comparison to non-hypoxic cells. Concomitantly, hypoxic cells experienced cytoskeleton remodelling and acquired a more motile phenotype (67, 74). Such observations strongly suggest that the microenvironment may significantly impact on membrane glycoproteome functionality through altered glycosylation. Moreover, post-translational alterations may originate unique molecular fingerprints at the cell surface for targeting hypoxic niches. However, the impact of the microenvironment in glycosylation is still poorly understood, requiring more in-depth omics approaches. As such, here we envisage to fill that gap focusing on the *O*-glycocode. Emphasis will be devoted to understanding the impact of hypoxia combined with glucose deprivation, which generally occurs in hypoxic niches due defective vasculature. This knowledge will help guiding future glycoproteomics studies towards the understanding of the functional impact of the microenvironment and its clinical relevance in cancer.

Material and Methods

Cell lines

Three representative urothelial BC cell lines (T24, 5637 and HT1376) were used as models for this study (see molecular profile of cell lines in the material and methods section of chapter II) (161). Under basal conditions of normoxia and/or glucose abundance, cells were mantained in RPMI 1640 + GlutaMAX™-I medium (Gibco™, Thermo Fisher Scientific) supplemented with 10% heat-inactivated fetal bovine serum (Gibco™, Thermo Fisher Sientific) and 1% penicillin-streptomycin (10,000 Units/mL

penicillin; 10,000 µg/mL streptomycin, Gibco™, Thermo Fisher Scientific) at 37 ºC in a 5% CO_2 humidified atmosphere. For experimental assays under glucose and/or oxygen shortage, cells were cultured in RPMI Medium 1640 (1x) without D-Glucose (Gibco™, Thermo Fisher Scientific) and maintained in a Galaxy 48R (New Brunswick) hypoxia chamber in a 99.9% N_2 and 0.1% O_2 humidified atmosphere.

Cell viability assay

Cell viability was determined using the Trypan Blue Exclusion Test of Cell Viability and the percentage of viable cells was calculated by dividing the number of viable cells by the number of total cells and multiplying by 100. Cells uptacking trypan blue were considered non-viable.

Cell proliferation assay

Cell proliferation was evaluated using the colorimetric Cell Proliferation ELISA, BrdU (Roche, Sigma-Aldrich), based on the measurement of the incorporation of bromodeoxyuridine (5-bromo-2'-deoxyuridine, a synthetic nucleoside analogue of thymidine) into newly synthesized DNA of proliferative cells. Procedure steps were followed according to the manufacturer instructions and results were monitored at 450 nm using a microplate reader (iMARK™, Bio-Rad). All experiments were performed in triplicates.

L-lactate assay

The L–Lactate colorimetric Assay Kit (Abcam) was used to detect L(+)-Lactate in cultured cells. Procedure steps were followed according to the manufacturer instructions and results were monitored at 450 nm using a microplate reader (iMARK™, Bio-Rad). All experiments were performed in triplicates.

HIF-1α expression

The expression of the hypoxic biomarker HIF-1α was evaluated by quantitative sandwich ELISA method, using the Invitrogen™ HIF-1 Alpha ELISA Kit. Procedure steps were followed according to the manufacturer instructions and results were monitored at 450 nm using a microplate reader (iMARK^{TM}, Bio-Rad). All experiments were performed in duplicates.

Cellular *O*-glycome

The cellular *O*-glycome was accessed as described in Chapter II and analysed by MALDI-TOF-MS. The samples were also analysed by nanoLC-ESI-MS, using the analytical set up described in Chapter II. The nanoLC eluent gradient was adapted: permethylated glycan separation occurred using a linear gradient of 10% eluent B over 10 min, 10-38% eluent B over 10 min, 38-50% eluent B over 35 min, 50-90% eluent B over 10 min and 90% eluent B over 10 min. The mass spectrometer operation conditions were maintained.

Relative glycan abundances result translate the ratio between chromatographic areas of individual glycan species and the sum of chromatographic areas of all identified glycans. The analysis of the *O*-glycome of 5637, T24 and HT1376 cell lines under standard normoxia conditions was performed for three biological replicates. Results reported for the *O*-glycome of hypoxic and/or glucose deprived cells refer to duplicate biological experiments.

Statistics

Statistical analysis was performed using the Student's T-test for unpaired samples. Differences were considered to be significant when $p < 0.05$. The coefficient of variation (CV) was used to measure the dispersion of data points around the mean for glycans under MALDI-TOF-MS and electrospray analysis.

Results and Discussion

Hypoxia and glucose deprivation are salient features of bladder tumours, as a result of uncontrolled proliferation and defective neovasculature. These microenvironmental challenges are expected to impact significantly on the membrane glycoproteome, with emphasis on *O*-glycosylation, as demonstrated by a recent preliminary study (74). Herein, we attempt to provide a comprehensive overview on BC cells *O*-glycode envisaging future targeted glycoproteomics. As such, we elected as models three of the most representative and well-studied urothelial cancer cell lines (5637, T24 and HT1376) (161, 194).

Cellular hypoxia and cell proliferation

To define hypoxia conditions, we first evaluated the hypoxic biomarkers HIF-1α and lactate levels in the three cell lines grown in normoxia (21% O_2) and hypoxia (0.1% O_2). Cells were exposed to hypoxia for 24h, 48h and 72h, which had no significant impact on cell viability. We then evaluated variations in the hypoxia marker HIF-1α levels overtime to identify cellular adaptation to oxygen shortage. According to Figure 1A, HIF-1α levels were higher at 24h and significantly decreased at 48 and 72h. No significant differences were observed for HIF-1α levels between 48h and 72h in all cell lines, suggesting an adaptation to hypoxia after acute exposure, as previously described (74). However, for HT1376 cells, HIF-1α levels peak after 6h of hypoxia exposure, possibly due to its intrinsic deletion of PTEN and inactivation of p53, previously associated to promotion of HIF-1α expression (195). In addition, we observed a striking increase in intracellular lactate in all cell lines after 24h in hypoxia (10 times higher in comparison to normoxia), confirming the metabolic adaptation to low oxygen tensions (Figure 1B). Moreover, 24h of exposure to low oxygen significantly decreased proliferation in all cell lines, also in agreement with previous observations (Figure 2) (74, 196). These viable and not proliferative cells are of particular interest, since they may be representative of chemotherapy-resistant hypoxic niches in solid tumours. Based on these results, subsequent studies involving hypoxia were performed at 24h, including with HT1376 cells, since 6h seem to be a too short period of time to observe functional adaptation to the hypoxic stress, as previously described (74).

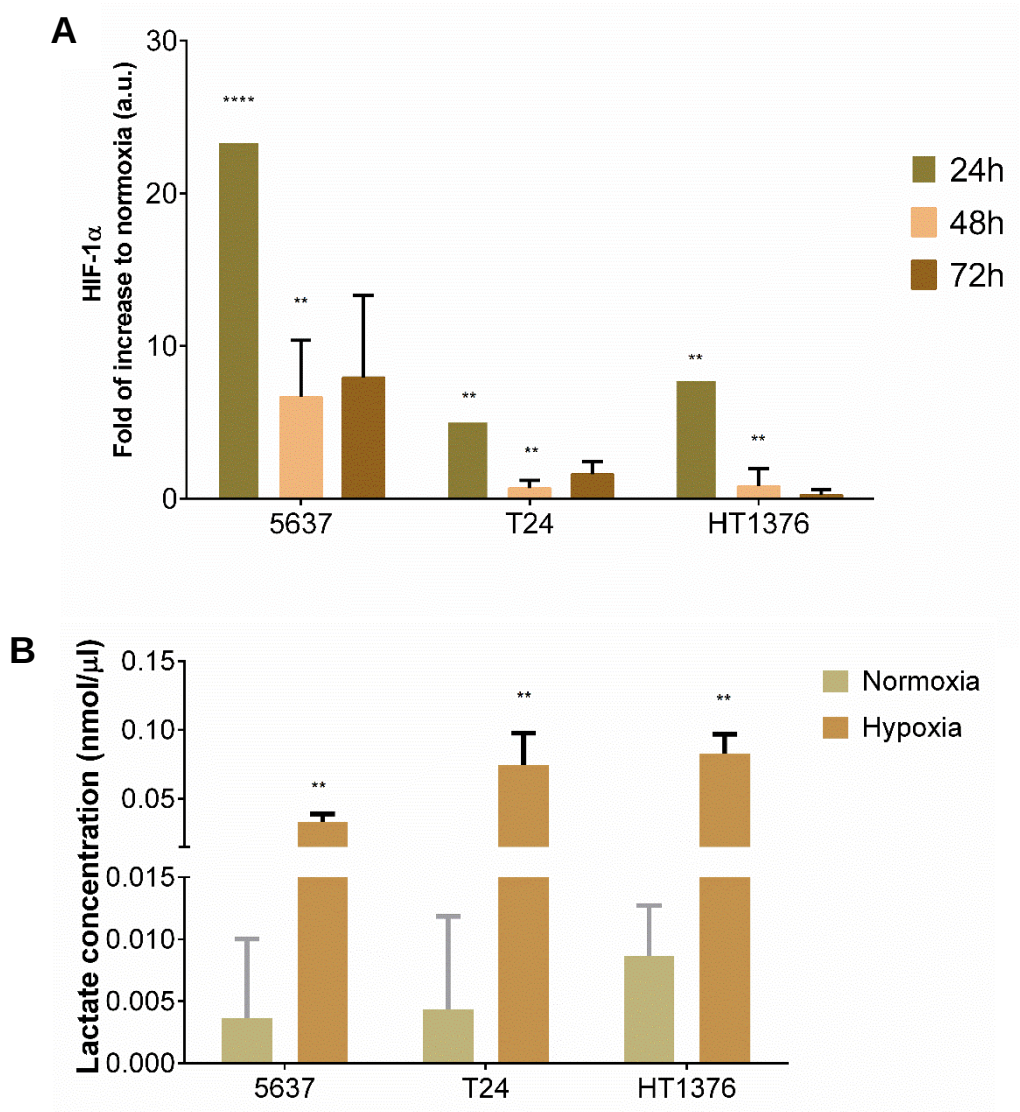

Figure 1 –. **(A)** Bladder cancer cell lines expression of HIF-1α hypoxia biomarker over-time **(B)** Lactate production in bladder cancer cell lines under normoxic and hypoxic conditions. **p < 0.01; **** p < 0,0001 (Students T-test)

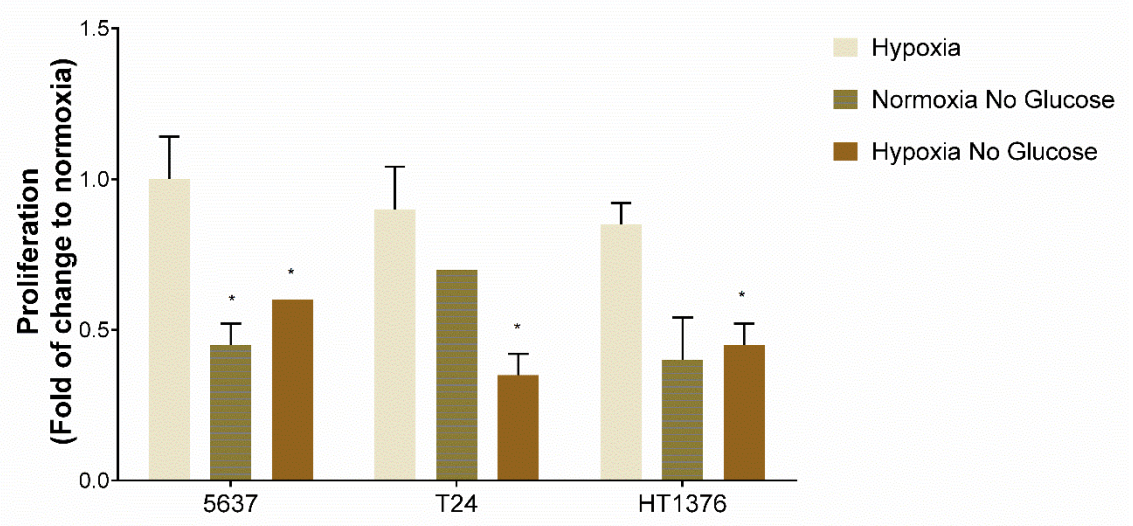

Figure 2 – Impact of hypoxia, glucose deprivation and both factors in cell proliferation. *p < 0.05; (Student's T-test).

O-glycomics analysis by MALDI-TOF-MS and nanoLC-ESI-MS

In chapter II we have addressed the glycan repertoire of BC cells by cellular *O*-Glycome Reporter/Amplification (CORA) and MALDI-TOF-MS (143). Accordingly, despite markedly different molecular backgrounds, all cell lines presented similar glycosylation patterns. In this chapter, we have reanalysed the samples by nanoLC-ESI-MS to provide a more quantitative assessment of the glycans. The ions identified by both methods have been summarized in Table S2 and confirmed mono and di-sialylated T antigens (*m/z* = 933.5 and *m/z* = 1294.7) as major species in all cell lines. nanoLC-ESI-MS analysis also revealed significant amounts of fucosylated core 1 (*m/z* = 746.4) in all cell lines, which was not detected by MALDI for the 5637 cell line. Differences in matrix composition, sugars concentrations and its possible influence in matrix crystallization are common features of MALDI-based analysis that may account for these differences. In addition, nanoLC-ESI-MS highlighted the presence of the STn antigen and several fucosylated and/or sialylated core 2 glycans (*m/z* = 729.4, *m/z* = 991.5, *m/z* = 1178.6, respectively; Table S2) in all models, which was also not evident by MALDI. Contrastingly, MALDI-TOF-MS analysis identified a higher number of vestigial high molecular weight species, whereas electrospray analysis revealed a higher number of less extended *O*-glycans. This may be explained by the fact that electrospray analysis was conducted for a mass range window bellow 2000 Da and permethylated *O*-glycans preferentially ionize as mono-charged species. However, both methods demonstrate that *O*-glycans extension beyond core 1 is a rare event (bellow 5% of expressed species), irrespectively of the cell line. Finally, the higher variability presented by MALDI-TOF-MS in comparison to electrospray for paired analysis of independent samples supports the use of nanoLC-ESI-MS for semi-quantitative proposes (Table S1).

Hypoxia and Glucose regulation of glycosylation

Cells were then grown in normoxia and hypoxia with or without suppression of glucose to disclose individual contributions as well as the synergistic impact of these conditions on the glycome. Noteworthy, neither glucose suppression nor its combination with hypoxia impacted in cell viability of grade III cells, denoting these cells high capacity to adapt to these microenvironmental changes. Notwithstanding, the grade II cell line 5637 demonstrated a mild decrease in viability, suggesting that more differentiated cells might be more susceptible to these environmental challenges, which warrants future

confirmation. As depicted in Figure 3-5, hypoxia presented limited impact on the *O*-glycome, including total amount of *O*-glycans, glycan chain extension beyond core 1, sialylation and fucosylation, irrespectively of the cell line. On the other hand, the removal of glucose from the culture media induced a massive reduction in *O*-glycans biosynthesis and completely abolished its extension, irrespectively of the cell line. Moreover, it decreased the fucosylation/sialylation ratio by inducing both a decrease in fucosylation and an increase in sialylation. The combination of glucose suppression with oxygen shortage further reinforced this phenotype. Moreover, the increase in sialylation associated to glucose and ultimately hypoxia is mostly driven by an increase in STn, especially for T24 and HT1376 cell lines, and sialyl-T antigens expression (*m/z* = 933.5; Table S2), while reducing core 1 fucosylation (*m/z* = 746.4, Table S2) (Figure 5). More detailed structural studies by tandem mass spectrometry and nuclear magnetic resonance are required to fully elucidate the nature of core 1 fucosylation and sialylation. In particular, focusylated core 1 is being described for the first time in bladder cancer and, to our knowledge, its biosynthesis has not yet been described. As such, a comprehensive understanding of the glycosyltransferases repertoire and its regulation by oxygen and glucose deprivation will also be critical for glycocode elucidation. Ultimately, it may help elucidating the biological and biochemical mechanisms driving the shift from fucosylation to sialylation. Nevertheless, previous studies have provided key insights that may also help guiding our understanding on bladder cancer glycobiology and ultimately foreseen the translation of these results. While sialylated T antigens have been widely observed in the healthy urothelium as well as in bladder tumours, irrespectively of their histological origin (67), the nature of the sialylation is still poorly understood. However, *ST3GAL1* overexpression, the main enzyme responsible by *O*-3 sialylation of the T antigen (originating sialyl-3-T, S3T) has been considered part of the initial oncogenic transformation of the bladder and is associated with cancer progression and recurrence (71). On the other hand, our group has recently reported that both *O*-3 and *O*-6 sialylated forms of the T antigen co-exist and are significantly increased in more advanced tumours, known to be highly hypoxic (67). Therefore, future studies should also devote to understanding the nature of core 1 sialylation *in vivo* and its spatio-temporal evolution through the course of disease, including response to the microenvironment. Furthermore, T24 and HT1376 MIBC cell models present a clear increase in STn under O_2 and glucose deprivation, potentially mimicking the glycosylation of hypoxic tumour areas. Similar observations were made for muscle invasive bladder tumours, where the STn antigen co-localized with hypoxic tumour areas of high nuclear HIF-1α expression (74). Likewise, the STn antigen has been observed in

non-proliferative tumour areas (68), further reinforcing a glycophenotype associated to hypoxia and cell quiescence. It has been well described that hypoxic niches promote cell quiescence and ultimately the development of cancer stem-cell characteristics (197). A possible association between STn antigen expression and such phenotypes has been previously suggested for different models (198, 199) and, according to this study, it may be triggered by microenvironmental factors, which warrants future confirmation.

In summary, we have demonstrated that glucose deprivation is a major driver of *O*-glycome remodelling in BC cells and that these effects are enhanced by hypoxia. Overall, under O_2 and glucose suppression, cancer cells significantly decreased their *O*-glycosylation levels and glycan chains length, most likely in response to metabolic reprogramming towards lower energy consumption (128, 136) and in response to decreased biosynthesis of sugars donors necessary to feed glycosylation pathways (117). Moreover, cancer cells acquire a more sialylated short-chain phenotype whose functional implications are yet to be fully understood. Nevertheless, we have also previously reported that STn antigen overexpression is part of an array of mechanisms that enable cancer cells to evade immune response (77) Also, C2GnT-expressing bladder tumour cells express heavily core 2 O-glycosylated MUC1 which interacts with galectin-3 to attenuate the interaction of tumor cells with NK cells, allowing tumour cells to survive longer in host blood circulation and potentially metastasize (78). Moreover, hypersialylation of tumor ligands for NKG2D receptors, expressed by NK cells, NK1.1+ T cells, γδ T cells, activated CD8+αβ T cells and macrophages, is thought to repulse their interaction with NKG2D receptors via highly negative charge repulsions; thereby hampering immune response (200). Tumor-derived sialoglycans also inhibit CD8+ T cell cytotoxicity by interfering with lytic granule trafficking and exocytosis in response to TCR engagement (201). Therefore, it is possible that oversialylation may allow cells to escape undetected immune recognition, further reinforcing the adaptive capacity of cancer cells to hypoxic niches. Despite the preliminary status of these findings, data is supported by the common patterns presented by all three cell lines, reinforcing its value; however, it requires future structural validation *in vivo* and *ex vivo*. Efforts should also be set on understanding the impact of the microenvironment on glycogenes expression, glycosyltransferases and glycosidases activity and regulation of glycan-associated biosynthesis pathways. Finally, it is critical to disclose the biological impact resulting from a massive reduction of *O*-glycans biosynthesis as a result of glucose suppression and hypoxia.

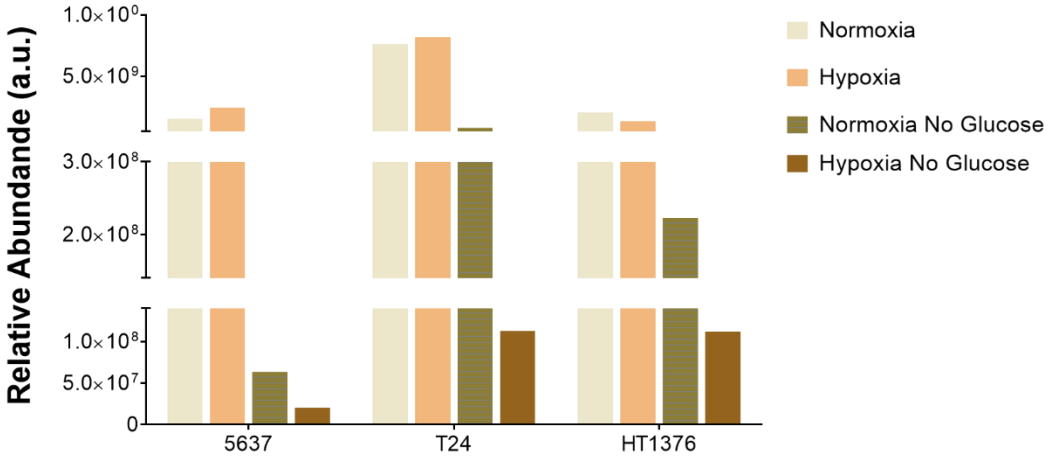

Figure 3 – Relative abundance of *O*-glycans facing different microenvironmental challenges.

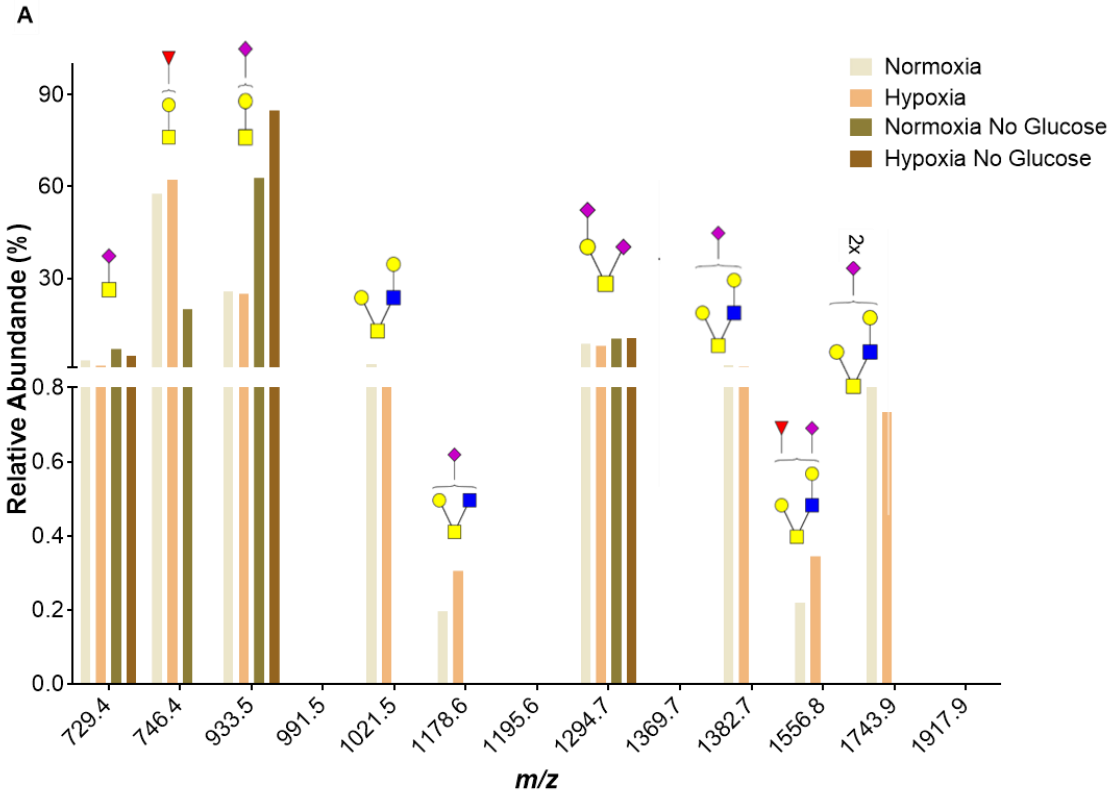

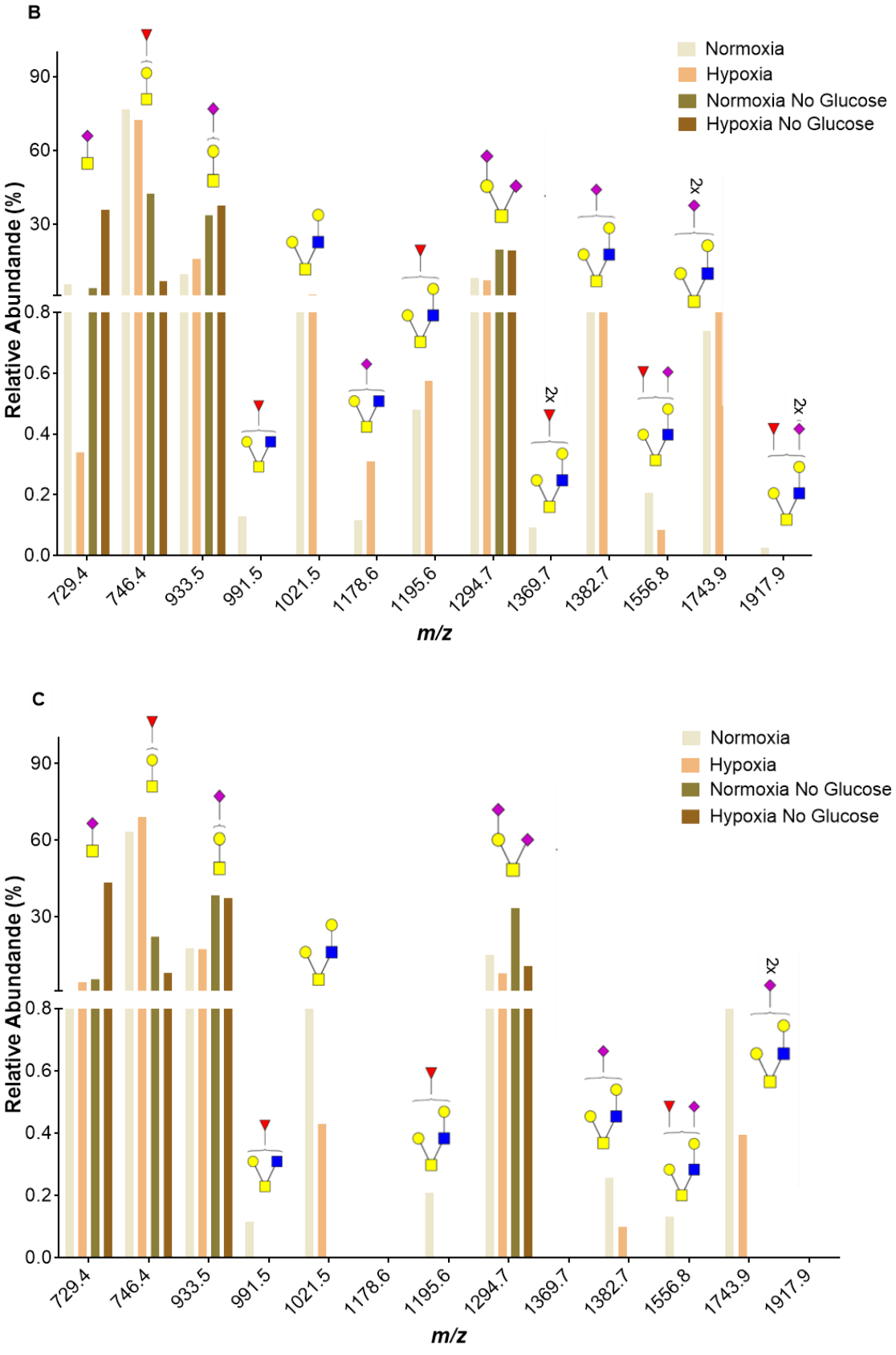

Figure 4 – Graphical representation of relative abundance of each *O*-GalNAc structure under Normoxia, Hypoxia, Normoxia No Glucose and Hypoxia No Glucose for each bladder cancer cell model **(A)** 5637, **(B)** T24, **(C)** HT1376.

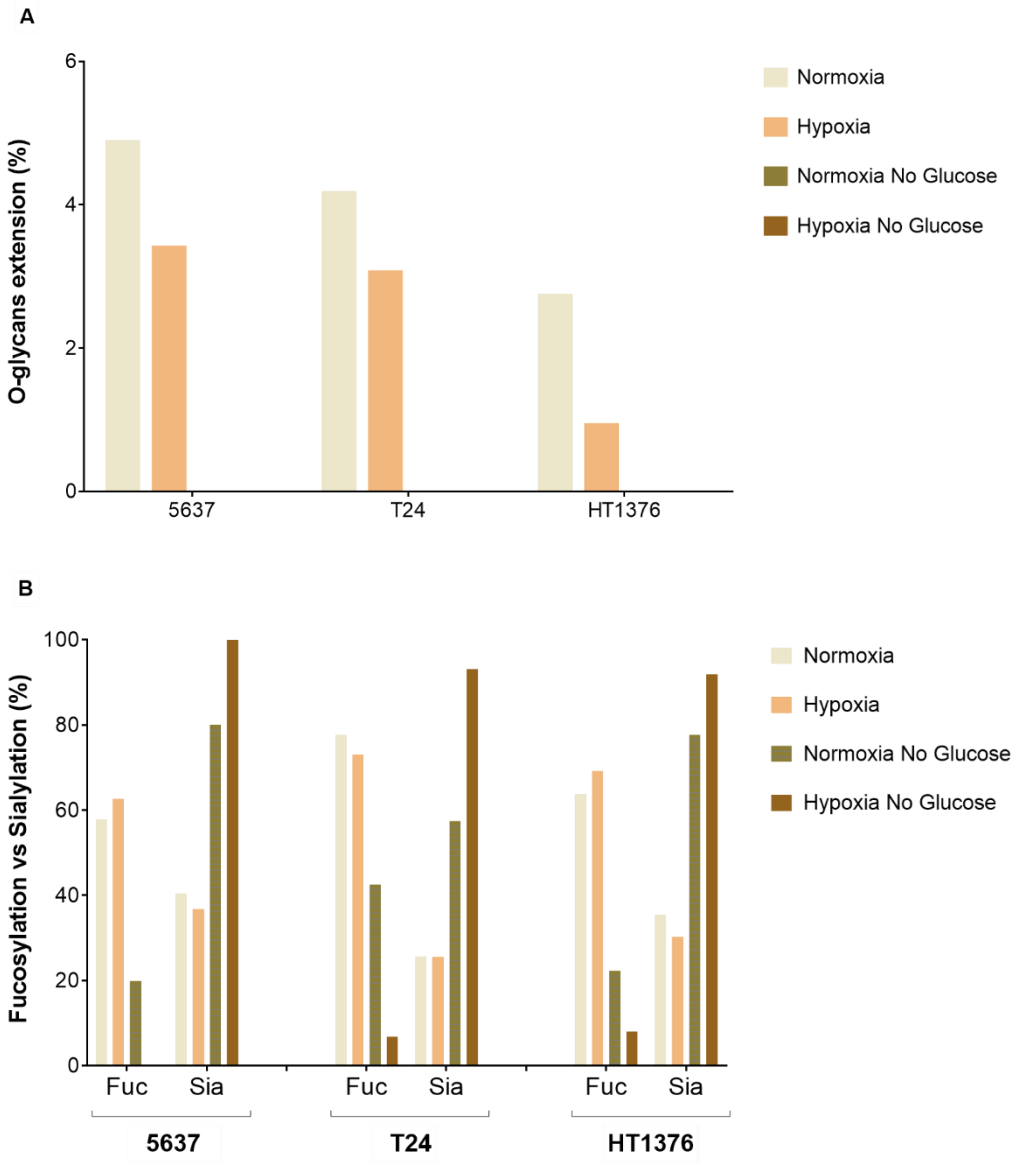

Figure 5 – **Comparative relative abundance of *O*-GalNAc structures in bladder cancer cell lines. (A)** Comparison between short-chain and extended (core 2- related structures) *O*-glycans; **(B)** Comparison between fucosylated and sialylated structures

Concluding remarks

Herein we present a preliminary and exploratory application of the systematized cellular *O*-glycomic workflow presented on chapter II, highlighting the use of nanoLC-ESI-MS for semi-quantitative proposes. In summary, it is described that glucose is a key driver of glycome remodelling and that the synergic effect of hypoxia and glucose deprivation leads to a drastic decrease in *O*-glycans abundance, with predominance of sialylated Tn and T antigens. Concomitantly, both fucosylated core 1 and extended

structures beyond core 1 were loss or significantly decreased. While the functional implications of these observations are yet unknown, previous reports support direct implications in cell motility and immune escape (74, 202) that should be comprehensively evaluated. This workflow now allows a broad vision on the microenvironmental regulation of the entire *O*-glycome, opening an avenue to disclose glycosylation changes driving tumour cells adaptation envisaging new targeted approaches to these more aggressive clones. These findings may ultimately guide future studies focusing on disclosing the role of glycosylation in hypoxic niches and its contribution to cancer progression and dissemination. In addition, relevant glycomics information has been generated to guide future understanding about the hypoxic cells glycoproteome. This will foster functional studies as well as the identification of cancer-specific biomarkers against hypoxic cells, generally endowed with more aggressive phenotypes.

Chapter IV | Concluding remarks

It has been long known that advanced bladder tumours present aberrant glycosylation, associated to worst prognosis and disease progression. Moreover, *O*-glycosylation constitutes a main post-translational modification of cell surface proteins and is responsible by altered biological role of several glycoproteins, towards a more aggressive phenotype and tumour dissemination. A comprehensive understanding of BC *O*-glycome and glycoproteome, as well as the main events underlying its regulation may pave the way for targeted intervention. However, the glycome and glycoproteome of bladder tumours and relevant cell models to aid functional and clinical studies is still poorly understood. Moreover, to study the glycoproteome remains challenging, requiring more accurate workflows to accommodate glycosylation-related information.

Focusing on BC, widely studied by our group, we implemented a systematized bioinformatic-assisted roadmap for comprehensively address the glycome and glycoproteome of three of the most widely studied BC cell models. Glycomics analysis highlighted mono- and di-sialylated T antigens as major *O*-glycoforms in these cells, in accordance with previous reports of our research group (67) This information allowed designing targeted glycoproteomics and facilitated downstream glycoprotein identification by mass spectrometry. Finally, we bring together several advances in bioinformatics based on GO terms and glycosites prediction tools for tackling ultra-tolerant proteomics datasets for potential glycoproteins. We have further demonstrated that this procedure significantly increases the number of identifications in relation to bottom-up proteomics protocols for protein annotation, which rely on product ion spectra fitting conventional peptide fragmentation patterns. Accordingly, our protocol identified over 1000 potential glycoproteins carrying sialyl-T antigens, 14% of which were detected in all cell models, irrespectively of its significantly different genetic background. Amongst these glycoproteins, many of them show a high degree of interaction, suggesting common biological functions, namely in cytoskeleton remodelling, adhesion and cellular motility. Interestingly, further analysis suggests that many glycoproteins may sort and carry molecular information across cellular organelles, which is supported by the fact that all these glycoproteins can be found at least in more than one subcellular localization. Finally, bioinformatics analysis combining transcriptomics and protein analysis data enabled the identification of glycoproteins potentially overexpressed in bladder tumours in relation to the healthy urothelium. While the majority of glycoproteins is overexpressed in NMIBC and MIBC, a restrict group of 29 overexpressed glycoproteins, including bladder cancer-stem cell biomarker CD44, were exclusive of MIBC. Interestingly, 22 of the identified glycoproteins have also been previously reported in chemoresistant tumours, and 19 glycoproteins were associated with decreased survival in BC. As such,

our bioinformatics-assisted multi-omics platform provided relevant molecular information for guiding future studies, including a library of glycoproteins holding potential for cancer detection and targeted therapeutics. Future studies will involve its validation in cancer cell models, large series of bladder tumours representative of different stages of the disease as well as healthy human tissues. Efforts should also be set on disclosing the functional impact of the most promising targets aiming towards the necessary rationale for clinical intervention. Another relevant aspect relies on disclosing the functional implications of altered glycosylation in these proteins, as well as its contribution to disease. Moreover, our analytical approach may now be implemented to evaluate the impact of critical cancer microenvironmental features in the glycome and glycoproteome, amongst other events.

The second part of this work has devoted to a comprehensive interrogation of the BC *O*-glycome of cells facing oxygen and glucose deprivation, a frequent event in highly proliferative and more aggressive tumours as a result of deficient vasculature. We observed that BC cell models under these microenvironmental conditions significantly decreased proliferation, while maintaining viability, in agreement with observations in bladder tumours (74). While hypoxia had little effect on the *O*-glycome, sugar deprivation and the combination of both factors promoted a massive decrease in *O*-glycosylation in all cell lines, suggesting the expression of “naked proteins” at the cell surface. This event is accompanied by an evident remodelling of the *O*-glycome that includes a stop in *O*-glycan extension beyond core 1, the replacement of fucosylated by sialylated core 1 glycans and, to less extent, the overexpression of the STn antigen. While the functional implications associated to most of these alterations at the cell membrane remain unknown, many studies support that the STn plays a key role in disease progression and dissemination in BC. In particular, the STn antigen has been implicated in increased cell motility and invasion capacity, repression of immune responses against cancer cells and may be implicated in metastasis, since it is frequently observed in circulating tumour cells, lymph nodes and the metastasis (75, 76). Moreover, the STn antigen has been mostly localized in non-proliferative and hypoxic tumour areas of proliferative tumours, thus in agreement with our studies *in vitro*. Moreover, hypersialylation has been linked to tumour growth, apoptosis, metastasis, immunotolerance, and resistance to therapy, ultimately driving more aggressive phenotypes (77). These findings provide the first comprehensive vision on the BC *O*-glycome facing hypoxia-associated features. Despite the exploratory nature of the present study, the data is supported by common patterns presented by all cell lines. Therefore, it casts the necessary rational for future understanding of the glycoproteome and ultimately clinical intervention. It also provides

key insights to guide studies directed to understanding the microenvironmental regulation of glycosylation pathways. Future studies should focus on validating these findings, including a broader range of cell models and understanding the functional and clinical implications of these findings.

In summary, we have provided a strategy to comprehensively interrogate the glycome and glycoproteome, setting the necessary analytical basis for biomarker discovery in BC. Finally, we have provided evidences that glucose levels drive profound *O*-glycome remodelling that is further intensified by oxygen shortage, whose functional implications are yet to be disclosed. Nevertheless, the necessary rationale has been created to proceed with glycoproteomics studies envisaging highly tumour specific epitopes for targeted therapeutics, namely of more aggressive clones.

References

1. Ferlay J, Soerjomataram I, Dikshit R, Eser S, Mathers C, Rebelo M, et al. Cancer incidence and mortality worldwide: sources, methods and major patterns in GLOBOCAN 2012. Int J Cancer. 2015;136(5):E359-86.
2. Babjuk M, Bohle A, Burger M, Capoun O, Cohen D, Comperat EM, et al. EAU Guidelines on Non-Muscle-invasive Urothelial Carcinoma of the Bladder: Update 2016. Eur Urol. 2017;71(3):447-61.
3. Siegel RL, Miller KD, Jemal A. Cancer statistics, 2015. CA Cancer J Clin. 2015;65(1):5-29.
4. Burger M, Catto JW, Dalbagni G, Grossman HB, Herr H, Karakiewicz P, et al. Epidemiology and risk factors of urothelial bladder cancer. Eur Urol. 2013;63(2):234-41.
5. Miyazaki J, Nishiyama H. Epidemiology of urothelial carcinoma. Int J Urol. 2017;24(10):730-4.
6. Wong MCS, Fung FDH, Leung C, Cheung WWL, Goggins WB, Ng CF. The global epidemiology of bladder cancer: a joinpoint regression analysis of its incidence and mortality trends and projection. Sci Rep. 2018;8(1):1129.
7. Wu W, Tong Y, Zhao Q, Yu G, Wei X, Lu Q. Coffee consumption and bladder cancer: a meta-analysis of observational studies. Sci Rep. 2015;5:9051.
8. Solomon JP, Hansel DE. The Emerging Molecular Landscape of Urothelial Carcinoma. Surg Pathol Clin. 2016;9(3):391-404.
9. Yousef PG, Gabril MY. An update on the molecular pathology of urinary bladder tumors. Pathol Res Pract. 2018;214(1):1-6.
10. Dovedi SJ, Davies BR. Emerging targeted therapies for bladder cancer: a disease waiting for a drug. Cancer Metastasis Rev. 2009;28(3-4):355-67.
11. Dinney CP, McConkey DJ, Millikan RE, Wu X, Bar-Eli M, Adam L, et al. Focus on bladder cancer. Cancer Cell. 2004;6(2):111-6.
12. Amin MB. Histological variants of urothelial carcinoma: diagnostic, therapeutic and prognostic implications. Mod Pathol. 2009;22 Suppl 2:S96-S118.
13. Mendiratta P, Grivas P. Emerging biomarkers and targeted therapies in urothelial carcinoma. Ann Transl Med. 2018;6(12):250.
14. Alfred Witjes J, Lebret T, Comperat EM, Cowan NC, De Santis M, Bruins HM, et al. Updated 2016 EAU Guidelines on Muscle-invasive and Metastatic Bladder Cancer. Eur Urol. 2017;71(3):462-75.

15. Azevedo R, Peixoto A, Gaiteiro C, Fernandes E, Neves M, Lima L, et al. Over forty years of bladder cancer glycobiology: Where do glycans stand facing precision oncology? Oncotarget. 2017;8(53):91734-64.
16. Zlotta AR, Fleshner NE, Jewett MA. The management of BCG failure in non-muscle-invasive bladder cancer: an update. Can Urol Assoc J. 2009;3(6 Suppl 4):S199-205.
17. Pinto-Leite R, Arantes-Rodrigues R, Ferreira R, Palmeira C, Colaco A, Moreira da Silva V, et al. Temsirolimus improves cytotoxic efficacy of cisplatin and gemcitabine against urinary bladder cancer cell lines. Urol Oncol. 2014;32(1):41 e11-22.
18. Svatek RS, Hollenbeck BK, Holmang S, Lee R, Kim SP, Stenzl A, et al. The economics of bladder cancer: costs and considerations of caring for this disease. Eur Urol. 2014;66(2):253-62.
19. Silva J, Arantes-Rodrigues R, Pinto-Leite R, Faustino-Rocha AI, Fidalgo-Goncalves L, Santos L, et al. Synergistic Effect of Carboplatin and Piroxicam on Two Bladder Cancer Cell Lines. Anticancer Res. 2017;37(4):1737-45.
20. Massari F, Ciccarese C, Santoni M, Brunelli M, Conti A, Modena A, et al. The route to personalized medicine in bladder cancer: where do we stand? Target Oncol. 2015;10(3):325-36.
21. Carneiro BA, Meeks JJ, Kuzel TM, Scaranti M, Abdulkadir SA, Giles FJ. Emerging therapeutic targets in bladder cancer. Cancer Treat Rev. 2015;41(2):170-8.
22. Azevedo R, Ferreira JA, Peixoto A, Neves M, Sousa N, Lima A, et al. Emerging antibody-based therapeutic strategies for bladder cancer: A systematic review. J Control Release. 2015;214:40-61.
23. Pulido M, Roubaud G, Cazeau AL, Mahammedi H, Vedrine L, Joly F, et al. Safety and efficacy of temsirolimus as second line treatment for patients with recurrent bladder cancer. BMC Cancer. 2018;18(1):194.
24. Tsujita Y, Horiguchi A, Tasaki S, Isono M, Asano T, Ito K, et al. STAT3 inhibition by WP1066 suppresses the growth and invasiveness of bladder cancer cells. Oncol Rep. 2017;38(4):2197-204.
25. Choi W, Porten S, Kim S, Willis D, Plimack ER, Hoffman-Censits J, et al. Identification of distinct basal and luminal subtypes of muscle-invasive bladder cancer with different sensitivities to frontline chemotherapy. Cancer Cell. 2014;25(2):152-65.
26. Van den Steen P, Rudd PM, Dwek RA, Opdenakker G. Concepts and principles of O-linked glycosylation. Crit Rev Biochem Mol Biol. 1998;33(3):151-208.
27. Helenius A, Aebi M. Intracellular functions of N-linked glycans. Science. 2001;291(5512):2364-9.

28. Kannagi R, Izawa M, Koike T, Miyazaki K, Kimura N. Carbohydrate-mediated cell adhesion in cancer metastasis and angiogenesis. Cancer Sci. 2004;95(5):377-84.
29. Rodrigues JG, Balmana M, Macedo JA, Pocas J, Fernandes A, de-Freitas-Junior JCM, et al. Glycosylation in cancer: Selected roles in tumour progression, immune modulation and metastasis. Cell Immunol. 2018.
30. Trombetta ES. The contribution of N-glycans and their processing in the endoplasmic reticulum to glycoprotein biosynthesis. Glycobiology. 2003;13(9):77R-91R.
31. Holemann A, Seeberger PH. Carbohydrate diversity: synthesis of glycoconjugates and complex carbohydrates. Curr Opin Biotechnol. 2004;15(6):615-22.
32. Shrimal S, Cherepanova NA, Gilmore R. Cotranslational and posttranslocational N-glycosylation of proteins in the endoplasmic reticulum. Semin Cell Dev Biol. 2015;41:71-8.
33. Burda P, Aebi M. The dolichol pathway of N-linked glycosylation. Biochim Biophys Acta. 1999;1426(2):239-57.
34. Zhao Y, Nakagawa T, Itoh S, Inamori K, Isaji T, Kariya Y, et al. N-acetylglucosaminyltransferase III antagonizes the effect of N-acetylglucosaminyltransferase V on alpha3beta1 integrin-mediated cell migration. J Biol Chem. 2006;281(43):32122-30.
35. Zhao YY, Takahashi M, Gu JG, Miyoshi E, Matsumoto A, Kitazume S, et al. Functional roles of N-glycans in cell signaling and cell adhesion in cancer. Cancer Sci. 2008;99(7):1304-10.
36. Kornfeld R, Kornfeld S. Assembly of asparagine-linked oligosaccharides. Annu Rev Biochem. 1985;54:631-64.
37. Spiro RG. Protein glycosylation: nature, distribution, enzymatic formation, and disease implications of glycopeptide bonds. Glycobiology. 2002;12(4):43R-56R.
38. Ju T, Aryal RP, Kudelka MR, Wang Y, Cummings RD. The Cosmc connection to the Tn antigen in cancer. Cancer Biomark. 2014;14(1):63-81.
39. Brockhausen I, Stanley P. O-GalNAc Glycans. In: rd, Varki A, Cummings RD, Esko JD, Stanley P, Hart GW, et al., editors. Essentials of Glycobiology. Cold Spring Harbor (NY)2015. p. 113-23.
40. Marcos NT, Pinho S, Grandela C, Cruz A, Samyn-Petit B, Harduin-Lepers A, et al. Role of the human ST6GalNAc-I and ST6GalNAc-II in the synthesis of the cancer-associated sialyl-Tn antigen. Cancer Res. 2004;64(19):7050-7.
41. Brockhausen I. Biosynthesis of Complex Mucin-Type O-Glycans. In: Mander L, Liu H-W, editors. Comprehensive Natural Products II Chemistry and Biology. Elsevier Science2010. p. 315-50.

42. Loureiro LR, Sousa DP, Ferreira D, Chai W, Lima L, Pereira C, et al. Novel monoclonal antibody L2A5 specifically targeting sialyl-Tn and short glycans terminated by alpha-2-6 sialic acids. Sci Rep. 2018;8(1):12196.
43. Gill DJ, Clausen H, Bard F. Location, location, location: new insights into O-GalNAc protein glycosylation. Trends Cell Biol. 2011;21(3):149-58.
44. Zachara N, Akimoto Y, Hart GW. The O-GlcNAc Modification. In: rd, Varki A, Cummings RD, Esko JD, Stanley P, Hart GW, et al., editors. Essentials of Glycobiology. Cold Spring Harbor (NY)2015. p. 239-51.
45. Fisi V, Miseta A, Nagy T. The Role of Stress-Induced O-GlcNAc Protein Modification in the Regulation of Membrane Transport. Oxid Med Cell Longev. 2017;2017:1308692.
46. Yang X, Qian K. Protein O-GlcNAcylation: emerging mechanisms and functions. Nat Rev Mol Cell Biol. 2017;18(7):452-65.
47. Wells L, Vosseller K, Hart GW. Glycosylation of nucleocytoplasmic proteins: signal transduction and O-GlcNAc. Science. 2001;291(5512):2376-8.
48. Nagel AK, Ball LE. Intracellular protein O-GlcNAc modification integrates nutrient status with transcriptional and metabolic regulation. Adv Cancer Res. 2015;126:137-66.
49. Liu C, Li J. O-GlcNAc: A Sweetheart of the Cell Cycle and DNA Damage Response. Front Endocrinol (Lausanne). 2018;9:415.
50. Ong Q, Han W, Yang X. O-GlcNAc as an Integrator of Signaling Pathways. Front Endocrinol (Lausanne). 2018;9:599.
51. Yang G, Tan Z, Lu W, Guo J, Yu H, Yu J, et al. Quantitative glycome analysis of N-glycan patterns in bladder cancer vs normal bladder cells using an integrated strategy. J Proteome Res. 2015;14(2):639-53.
52. Guo JM, Zhang XY, Chen HL, Wang GM, Zhang YK. Structural alterations of sugar chains in urine fibronectin from bladder cancer patients and its enzymatic mechanism. J Cancer Res Clin Oncol. 2001;127(8):512-9.
53. Ishimura H, Takahashi T, Nakagawa H, Nishimura S, Arai Y, Horikawa Y, et al. N-acetylglucosaminyltransferase V and beta1-6 branching N-linked oligosaccharides are associated with good prognosis of patients with bladder cancer. Clin Cancer Res. 2006;12(8):2506-11.
54. Sheinfeld J, Reuter VE, Fair WR, Cordon-Cardo C. Expression of blood group antigens in bladder cancer: current concepts. Semin Surg Oncol. 1992;8(5):308-15.
55. Orntoft TF, Wolf H, Watkins WM. Activity of the human blood group ABO, Se, H, Le, and X gene-encoded glycosyltransferases in normal and malignant bladder urothelium. Cancer Res. 1988;48(15):4427-33.

56. Thorpe SJ, Abel P, Slavin G, Feizi T. Blood group antigens in the normal and neoplastic bladder epithelium. J Clin Pathol. 1983;36(8):873-82.

57. Bergman S, Javadpour N. The cell surface antigen A, B or O(H) as an indicator of malignant potential in stage A bladder carcinoma: preliminary report. J Urol. 1978;119(1):49-51.

58. Cordon-Cardo C, Reuter VE, Lloyd KO, Sheinfeld J, Fair WR, Old LJ, et al. Blood group-related antigens in human urothelium: enhanced expression of precursor, LeX, and LeY determinants in urothelial carcinoma. Cancer Res. 1988;48(14):4113-20.

59. Limas C, Lange PH. Lewis antigens in normal and neoplastic urothelium. Am J Pathol. 1985;121(1):176-83.

60. St Hill CA. Interactions between endothelial selectins and cancer cells regulate metastasis. Front Biosci (Landmark Ed). 2011;16:3233-51.

61. Numahata K, Satoh M, Handa K, Saito S, Ohyama C, Ito A, et al. Sialosyl-Le(x) expression defines invasive and metastatic properties of bladder carcinoma. Cancer. 2002;94(3):673-85.

62. Hegele A, Mecklenburg V, Varga Z, Olbert P, Hofmann R, Barth P. CA19.9 and CEA in transitional cell carcinoma of the bladder: serological and immunohistochemical findings. Anticancer Res. 2010;30(12):5195-200.

63. Kajiwara H, Yasuda M, Kumaki N, Shibayama T, Osamura Y. Expression of carbohydrate antigens (SSEA-1, sialyl-Lewis X, DU-PAN-2 and CA19-9) and E-selectin in urothelial carcinoma of the renal pelvis, ureter, and urinary bladder. Tokai J Exp Clin Med. 2005;30(3):177-82.

64. Lu YC, Chen CN, Chu CY, Lu J, Wang BJ, Chen CH, et al. Calreticulin activates beta1 integrin via fucosylation by fucosyltransferase 1 in J82 human bladder cancer cells. Biochem J. 2014;460(1):69-78.

65. Ju T, Lanneau GS, Gautam T, Wang Y, Xia B, Stowell SR, et al. Human tumor antigens Tn and sialyl Tn arise from mutations in Cosmc. Cancer Res. 2008;68(6):1636-46.

66. Reis CA, Osorio H, Silva L, Gomes C, David L. Alterations in glycosylation as biomarkers for cancer detection. J Clin Pathol. 2010;63(4):322-9.

67. Cotton S, Azevedo R, Gaiteiro C, Ferreira D, Lima L, Peixoto A, et al. Targeted O-glycoproteomics explored increased sialylation and identified MUC16 as a poor prognosis biomarker in advanced-stage bladder tumours. Mol Oncol. 2017;11(8):895-912.

68. Ferreira JA, Videira PA, Lima L, Pereira S, Silva M, Carrascal M, et al. Overexpression of tumour-associated carbohydrate antigen sialyl-Tn in advanced bladder tumours. Mol Oncol. 2013;7(3):719-31.

69. Yokoyama M, Ohoka H, Oda H, Oda T, Utsumi S, Takeuchi M. Thomsen-Friedenreich antigen in bladder cancer tissues detected by monoclonal antibody. Hinyokika Kiyo. 1988;34(2):255-8.

70. Limas C, Lange P. T-antigen in normal and neoplastic urothelium. Cancer. 1986;58(6):1236-45.

71. Videira PA, Correia M, Malagolini N, Crespo HJ, Ligeiro D, Calais FM, et al. ST3Gal.I sialyltransferase relevance in bladder cancer tissues and cell lines. BMC Cancer. 2009;9:357.

72. Santos SN, Junqueira MS, Francisco G, Vilanova M, Magalhaes A, Dias Baruffi M, et al. O-glycan sialylation alters galectin-3 subcellular localization and decreases chemotherapy sensitivity in gastric cancer. Oncotarget. 2016;7(50):83570-87.

73. Costa C, Pereira S, Lima L, Peixoto A, Fernandes E, Neves D, et al. Abnormal Protein Glycosylation and Activated PI3K/Akt/mTOR Pathway: Role in Bladder Cancer Prognosis and Targeted Therapeutics. PLoS One. 2015;10(11):e0141253.

74. Peixoto A, Fernandes E, Gaiteiro C, Lima L, Azevedo R, Soares J, et al. Hypoxia enhances the malignant nature of bladder cancer cells and concomitantly antagonizes protein O-glycosylation extension. Oncotarget. 2016;7(39):63138-57.

75. Neves M, Azevedo R, Lima L, Oliveira MI, Peixoto A, Ferreira D, et al. Exploring sialyl-Tn expression in microfluidic-isolated circulating tumour cells: A novel biomarker and an analytical tool for precision oncology applications. N Biotechnol. 2018.

76. Lima L, Neves M, Oliveira MI, Dieguez L, Freitas R, Azevedo R, et al. Sialyl-Tn identifies muscle-invasive bladder cancer basal and luminal subtypes facing decreased survival, being expressed by circulating tumor cells and metastases. Urol Oncol. 2017;35(12):675 e1- e8.

77. Carrascal MA, Severino PF, Guadalupe Cabral M, Silva M, Ferreira JA, Calais F, et al. Sialyl Tn-expressing bladder cancer cells induce a tolerogenic phenotype in innate and adaptive immune cells. Mol Oncol. 2014;8(3):753-65.

78. Suzuki Y, Sutoh M, Hatakeyama S, Mori K, Yamamoto H, Koie T, et al. MUC1 carrying core 2 O-glycans functions as a molecular shield against NK cell attack, promoting bladder tumor metastasis. Int J Oncol. 2012;40(6):1831-8.

79. Lima L, Severino PF, Silva M, Miranda A, Tavares A, Pereira S, et al. Response of high-risk of recurrence/progression bladder tumours expressing sialyl-Tn and sialyl-6-T to BCG immunotherapy. Br J Cancer. 2013;109(8):2106-14.

80. Bertout JA, Patel SA, Simon MC. The impact of O2 availability on human cancer. Nat Rev Cancer. 2008;8(12):967-75.
81. Harris AL. Hypoxia--a key regulatory factor in tumour growth. Nat Rev Cancer. 2002;2(1):38-47.
82. Bristow RG, Hill RP. Hypoxia and metabolism. Hypoxia, DNA repair and genetic instability. Nat Rev Cancer. 2008;8(3):180-92.
83. Semenza GL. HIF-1: mediator of physiological and pathophysiological responses to hypoxia. J Appl Physiol (1985). 2000;88(4):1474-80.
84. Loboda A, Jozkowicz A, Dulak J. HIF-1 and HIF-2 transcription factors--similar but not identical. Mol Cells. 2010;29(5):435-42.
85. Zagorska A, Dulak J. HIF-1: the knowns and unknowns of hypoxia sensing. Acta Biochim Pol. 2004;51(3):563-85.
86. Marin-Hernandez A, Gallardo-Perez JC, Ralph SJ, Rodriguez-Enriquez S, Moreno-Sanchez R. HIF-1alpha modulates energy metabolism in cancer cells by inducing over-expression of specific glycolytic isoforms. Mini Rev Med Chem. 2009;9(9):1084-101.
87. Makino Y, Cao R, Svensson K, Bertilsson G, Asman M, Tanaka H, et al. Inhibitory PAS domain protein is a negative regulator of hypoxia-inducible gene expression. Nature. 2001;414(6863):550-4.
88. Xia X, Lemieux ME, Li W, Carroll JS, Brown M, Liu XS, et al. Integrative analysis of HIF binding and transactivation reveals its role in maintaining histone methylation homeostasis. Proc Natl Acad Sci U S A. 2009;106(11):4260-5.
89. Mole DR, Blancher C, Copley RR, Pollard PJ, Gleadle JM, Ragoussis J, et al. Genome-wide association of hypoxia-inducible factor (HIF)-1alpha and HIF-2alpha DNA binding with expression profiling of hypoxia-inducible transcripts. J Biol Chem. 2009;284(25):16767-75.
90. Mucaj V, Shay JE, Simon MC. Effects of hypoxia and HIFs on cancer metabolism. Int J Hematol. 2012;95(5):464-70.
91. Semenza GL. Hypoxia-inducible factor 1 (HIF-1) pathway. Sci STKE. 2007;2007(407):cm8.
92. Dengler VL, Galbraith M, Espinosa JM. Transcriptional regulation by hypoxia inducible factors. Crit Rev Biochem Mol Biol. 2014;49(1):1-15.
93. Petrova V, Annicchiarico-Petruzzelli M, Melino G, Amelio I. The hypoxic tumour microenvironment. Oncogenesis. 2018;7(1):10.

94. Flamant L, Notte A, Ninane N, Raes M, Michiels C. Anti-apoptotic role of HIF-1 and AP-1 in paclitaxel exposed breast cancer cells under hypoxia. Mol Cancer. 2010;9:191.

95. Wong BW, Marsch E, Treps L, Baes M, Carmeliet P. Endothelial cell metabolism in health and disease: impact of hypoxia. EMBO J. 2017;36(15):2187-203.

96. Graeber TG, Osmanian C, Jacks T, Housman DE, Koch CJ, Lowe SW, et al. Hypoxia-mediated selection of cells with diminished apoptotic potential in solid tumours. Nature. 1996;379(6560):88-91.

97. Luoto KR, Kumareswaran R, Bristow RG. Tumor hypoxia as a driving force in genetic instability. Genome Integr. 2013;4(1):5.

98. Ramlee MK, Wang J, Toh WX, Li S. Transcription Regulation of the Human Telomerase Reverse Transcriptase (hTERT) Gene. Genes (Basel). 2016;7(8).

99. Krock BL, Skuli N, Simon MC. Hypoxia-induced angiogenesis: good and evil. Genes Cancer. 2011;2(12):1117-33.

100. Shao C, Yang F, Miao S, Liu W, Wang C, Shu Y, et al. Role of hypoxia-induced exosomes in tumor biology. Mol Cancer. 2018;17(1):120.

101. Cramer T, Yamanishi Y, Clausen BE, Forster I, Pawlinski R, Mackman N, et al. HIF-1alpha is essential for myeloid cell-mediated inflammation. Cell. 2003;112(5):645-57.

102. Vander Heiden MG, Cantley LC, Thompson CB. Understanding the Warburg effect: the metabolic requirements of cell proliferation. Science. 2009;324(5930):1029-33.

103. Amoedo ND, Valencia JP, Rodrigues MF, Galina A, Rumjanek FD. How does the metabolism of tumour cells differ from that of normal cells. Biosci Rep. 2013;33(6).

104. Muz B, de la Puente P, Azab F, Luderer M, Azab AK. Hypoxia promotes stem cell-like phenotype in multiple myeloma cells. Blood Cancer J. 2014;4:e262.

105. Denko NC. Hypoxia, HIF1 and glucose metabolism in the solid tumour. Nat Rev Cancer. 2008;8(9):705-13.

106. Younes M, Brown RW, Stephenson M, Gondo M, Cagle PT. Overexpression of Glut1 and Glut3 in stage I nonsmall cell lung carcinoma is associated with poor survival. Cancer. 1997;80(6):1046-51.

107. Younes M, Juarez D, Lechago LV, Lerner SP. Glut 1 expression in transitional cell carcinoma of the urinary bladder is associated with poor patient survival. Anticancer Res. 2001;21(1B):575-8.

108. Baer S, Casaubon L, Schwartz MR, Marcogliese A, Younes M. Glut3 expression in biopsy specimens of laryngeal carcinoma is associated with poor survival. Laryngoscope. 2002;112(2):393-6.

109. Pedersen PL, Mathupala S, Rempel A, Geschwind JF, Ko YH. Mitochondrial bound type II hexokinase: a key player in the growth and survival of many cancers and an ideal prospect for therapeutic intervention. Biochim Biophys Acta. 2002;1555(1-3):14-20.

110. Semenza GL. HIF-1: upstream and downstream of cancer metabolism. Curr Opin Genet Dev. 2010;20(1):51-6.

111. Ullah MS, Davies AJ, Halestrap AP. The plasma membrane lactate transporter MCT4, but not MCT1, is up-regulated by hypoxia through a HIF-1alpha-dependent mechanism. J Biol Chem. 2006;281(14):9030-7.

112. Kim JW, Tchernyshyov I, Semenza GL, Dang CV. HIF-1-mediated expression of pyruvate dehydrogenase kinase: a metabolic switch required for cellular adaptation to hypoxia. Cell Metab. 2006;3(3):177-85.

113. Zhang H, Gao P, Fukuda R, Kumar G, Krishnamachary B, Zeller KI, et al. HIF-1 inhibits mitochondrial biogenesis and cellular respiration in VHL-deficient renal cell carcinoma by repression of C-MYC activity. Cancer Cell. 2007;11(5):407-20.

114. Chen Z, Li Y, Zhang H, Huang P, Luthra R. Hypoxia-regulated microRNA-210 modulates mitochondrial function and decreases ISCU and COX10 expression. Oncogene. 2010;29(30):4362-8.

115. Fukuda R, Zhang H, Kim JW, Shimoda L, Dang CV, Semenza GL. HIF-1 regulates cytochrome oxidase subunits to optimize efficiency of respiration in hypoxic cells. Cell. 2007;129(1):111-22.

116. Manzari B, Kudlow JE, Fardin P, Merello E, Ottaviano C, Puppo M, et al. Induction of macrophage glutamine: fructose-6-phosphate amidotransferase expression by hypoxia and by picolinic acid. Int J Immunopathol Pharmacol. 2007;20(1):47-58.

117. Shirato K, Nakajima K, Korekane H, Takamatsu S, Gao C, Angata T, et al. Hypoxic regulation of glycosylation via the N-acetylglucosamine cycle. J Clin Biochem Nutr. 2011;48(1):20-5.

118. Hisanaga K, Onodera H, Kogure K. Changes in levels of purine and pyrimidine nucleotides during acute hypoxia and recovery in neonatal rat brain. J Neurochem. 1986;47(5):1344-50.

119. Keppler OT, Hinderlich S, Langner J, Schwartz-Albiez R, Reutter W, Pawlita M. UDP-GlcNAc 2-epimerase: a regulator of cell surface sialylation. Science. 1999;284(5418):1372-6.

120. Kathagen-Buhmann A, Schulte A, Weller J, Holz M, Herold-Mende C, Glass R, et al. Glycolysis and the pentose phosphate pathway are differentially associated with the dichotomous regulation of glioblastoma cell migration versus proliferation. Neuro Oncol. 2016;18(9):1219-29.
121. Rao X, Duan X, Mao W, Li X, Li Z, Li Q, et al. O-GlcNAcylation of G6PD promotes the pentose phosphate pathway and tumor growth. Nat Commun. 2015;6:8468.
122. Ma Z, Vosseller K. Cancer metabolism and elevated O-GlcNAc in oncogenic signaling. J Biol Chem. 2014;289(50):34457-65.
123. Sodi VL, Khaku S, Krutilina R, Schwab LP, Vocadlo DJ, Seagroves TN, et al. mTOR/MYC Axis Regulates O-GlcNAc Transferase Expression and O-GlcNAcylation in Breast Cancer. Mol Cancer Res. 2015;13(5):923-33.
124. Ferrer CM, Lynch TP, Sodi VL, Falcone JN, Schwab LP, Peacock DL, et al. O-GlcNAcylation regulates cancer metabolism and survival stress signaling via regulation of the HIF-1 pathway. Mol Cell. 2014;54(5):820-31.
125. Pescador N, Villar D, Cifuentes D, Garcia-Rocha M, Ortiz-Barahona A, Vazquez S, et al. Hypoxia promotes glycogen accumulation through hypoxia inducible factor (HIF)-mediated induction of glycogen synthase 1. PLoS One. 2010;5(3):e9644.
126. Pelletier J, Bellot G, Gounon P, Lacas-Gervais S, Pouyssegur J, Mazure NM. Glycogen Synthesis is Induced in Hypoxia by the Hypoxia-Inducible Factor and Promotes Cancer Cell Survival. Front Oncol. 2012;2:18.
127. Silva-Filho AF, Sena WLB, Lima LRA, Carvalho LVN, Pereira MC, Santos LGS, et al. Glycobiology Modifications in Intratumoral Hypoxia: The Breathless Side of Glycans Interaction. Cell Physiol Biochem. 2017;41(5):1801-29.
128. Koike T, Kimura N, Miyazaki K, Yabuta T, Kumamoto K, Takenoshita S, et al. Hypoxia induces adhesion molecules on cancer cells: A missing link between Warburg effect and induction of selectin-ligand carbohydrates. Proc Natl Acad Sci U S A. 2004;101(21):8132-7.
129. Alisson-Silva F, Freire-de-Lima L, Donadio JL, Lucena MC, Penha L, Sa-Diniz JN, et al. Increase of O-glycosylated oncofetal fibronectin in high glucose-induced epithelial-mesenchymal transition of cultured human epithelial cells. PLoS One. 2013;8(4):e60471.
130. Nakajima K, Kitazume S, Angata T, Fujinawa R, Ohtsubo K, Miyoshi E, et al. Simultaneous determination of nucleotide sugars with ion-pair reversed-phase HPLC. Glycobiology. 2010;20(7):865-71.

131. Vasconcelos-Dos-Santos A, Loponte HF, Mantuano NR, Oliveira IA, de Paula IF, Teixeira LK, et al. Hyperglycemia exacerbates colon cancer malignancy through hexosamine biosynthetic pathway. Oncogenesis. 2017;6(3):e306.

132. Abdel Rahman AM, Ryczko M, Pawling J, Dennis JW. Probing the hexosamine biosynthetic pathway in human tumor cells by multitargeted tandem mass spectrometry. ACS Chem Biol. 2013;8(9):2053-62.

133. Chiaradonna F, Ricciardiello F, Palorini R. The Nutrient-Sensing Hexosamine Biosynthetic Pathway as the Hub of Cancer Metabolic Rewiring. Cells. 2018;7(6).

134. Weihofen WA, Berger M, Chen H, Saenger W, Hinderlich S. Structures of human N-Acetylglucosamine kinase in two complexes with N-Acetylglucosamine and with ADP/glucose: insights into substrate specificity and regulation. J Mol Biol. 2006;364(3):388-99.

135. Palorini R, Votta G, Pirola Y, De Vitto H, De Palma S, Airoldi C, et al. Protein Kinase A Activation Promotes Cancer Cell Resistance to Glucose Starvation and Anoikis. PLoS Genet. 2016;12(3):e1005931.

136. Palorini R, Cammarata FP, Balestrieri C, Monestiroli A, Vasso M, Gelfi C, et al. Glucose starvation induces cell death in K-ras-transformed cells by interfering with the hexosamine biosynthesis pathway and activating the unfolded protein response. Cell Death Dis. 2013;4:e732.

137. Freeze HH, Hart GW, Schnaar RL. Glycosylation Precursors. In: rd, Varki A, Cummings RD, Esko JD, Stanley P, Hart GW, et al., editors. Essentials of Glycobiology. Cold Spring Harbor (NY)2015. p. 51-63.

138. Zhou S, Huang Y, Dong X, Peng W, Veillon L, Kitagawa DAS, et al. Isomeric Separation of Permethylated Glycans by Porous Graphitic Carbon (PGC)-LC-MS/MS at High Temperatures. Anal Chem. 2017;89(12):6590-7.

139. Jensen PH, Karlsson NG, Kolarich D, Packer NH. Structural analysis of N- and O-glycans released from glycoproteins. Nat Protoc. 2012;7(7):1299-310.

140. Veillon L, Huang Y, Peng W, Dong X, Cho BG, Mechref Y. Characterization of isomeric glycan structures by LC-MS/MS. Electrophoresis. 2017;38(17):2100-14.

141. Harvey DJ. Derivatization of carbohydrates for analysis by chromatography; electrophoresis and mass spectrometry. J Chromatogr B Analyt Technol Biomed Life Sci. 2011;879(17-18):1196-225.

142. Kudelka MR, Nairn AV, Sardar MY, Sun X, Chaikof EL, Ju T, et al. Isotopic labeling with cellular O-glycome reporter/amplification (ICORA) for comparative O-glycomics of cultured cells. Glycobiology. 2018;28(4):214-22.

143. Kudelka MR, Antonopoulos A, Wang Y, Duong DM, Song X, Seyfried NT, et al. Cellular O-Glycome Reporter/Amplification to explore O-glycans of living cells. Nat Methods. 2016;13(1):81-6.

144. Frantzi M, Latosinska A, Fluhe L, Hupe MC, Critselis E, Kramer MW, et al. Developing proteomic biomarkers for bladder cancer: towards clinical application. Nat Rev Urol. 2015;12(6):317-30.

145. Zhang Y, Fonslow BR, Shan B, Baek MC, Yates JR, 3rd. Protein analysis by shotgun/bottom-up proteomics. Chem Rev. 2013;113(4):2343-94.

146. Thelen JJ, Miernyk JA. The proteomic future: where mass spectrometry should be taking us. Biochem J. 2012;444(2):169-81.

147. Yates JR, Ruse CI, Nakorchevsky A. Proteomics by mass spectrometry: approaches, advances, and applications. Annu Rev Biomed Eng. 2009;11:49-79.

148. Capri J, Whitelegge JP. Full Membrane Protein Coverage Digestion and Quantitative Bottom-Up Mass Spectrometry Proteomics. Methods Mol Biol. 2017;1550:61-7.

149. Young NL, DiMaggio PA, Plazas-Mayorca MD, Baliban RC, Floudas CA, Garcia BA. High throughput characterization of combinatorial histone codes. Mol Cell Proteomics. 2009;8(10):2266-84.

150. Ge Y, Lawhorn BG, ElNaggar M, Strauss E, Park JH, Begley TP, et al. Top down characterization of larger proteins (45 kDa) by electron capture dissociation mass spectrometry. J Am Chem Soc. 2002;124(4):672-8.

151. Silva AMN, Vitorino R, Domingues MRM, Spickett CM, Domingues P. Post-translational modifications and mass spectrometry detection. Free Radic Biol Med. 2013;65:925-41.

152. Gingras AC, Gstaiger M, Raught B, Aebersold R. Analysis of protein complexes using mass spectrometry. Nat Rev Mol Cell Biol. 2007;8(8):645-54.

153. Ball LE, Berkaw MN, Buse MG. Identification of the major site of O-linked beta-N-acetylglucosamine modification in the C terminus of insulin receptor substrate-1. Mol Cell Proteomics. 2006;5(2):313-23.

154. Azevedo R, Silva AMN, Reis CA, Santos LL, Ferreira JA. In silico approaches for unveiling novel glycobiomarkers in cancer. J Proteomics. 2018;171:95-106.

155. Azevedo R, Soares J, Gaiteiro C, Peixoto A, Lima L, Ferreira D, et al. Glycan affinity magnetic nanoplatforms for urinary glycobiomarkers discovery in bladder cancer. Talanta. 2018;184:347-55.

156. Orlando K, Guo W. Membrane organization and dynamics in cell polarity. Cold Spring Harb Perspect Biol. 2009;1(5):a001321.

157. Cooper G. Cell Membranes. The Cell: A Molecular Approach 2nd edition Sunderland (MA): Sinauer Associates2000.
158. Keren K. Cell motility: the integrating role of the plasma membrane. Eur Biophys J. 2011;40(9):1013-27.
159. Fouad YA, Aanei C. Revisiting the hallmarks of cancer. Am J Cancer Res. 2017;7(5):1016-36.
160. Vigneron N. Human Tumor Antigens and Cancer Immunotherapy. Biomed Res Int. 2015;2015:948501.
161. Pinto-Leite R, Carreira I, Melo J, Ferreira SI, Ribeiro I, Ferreira J, et al. Genomic characterization of three urinary bladder cancer cell lines: understanding genomic types of urinary bladder cancer. Tumour Biol. 2014;35(5):4599-617.
162. Kudelka MR, Antonopoulos A, Wang Y, Duong DM, Song X, Seyfried NT, et al. Cellular O-Glycome Reporter/Amplification to explore O-glycans of living cells. Nature Methods. 2015;13:81.
163. Bhatia VN, Perlman DH, Costello CE, McComb ME. Software tool for researching annotations of proteins: open-source protein annotation software with data visualization. Anal Chem. 2009;81(23):9819-23.
164. The UniProt C. UniProt: the universal protein knowledgebase. Nucleic Acids Res. 2017;45(D1):D158-D69.
165. Steentoft C, Vakhrushev SY, Joshi HJ, Kong Y, Vester-Christensen MB, Schjoldager KT, et al. Precision mapping of the human O-GalNAc glycoproteome through SimpleCell technology. EMBO J. 2013;32(10):1478-88.
166. Szklarczyk D, Morris JH, Cook H, Kuhn M, Wyder S, Simonovic M, et al. The STRING database in 2017: quality-controlled protein-protein association networks, made broadly accessible. Nucleic Acids Res. 2017;45(D1):D362-D8.
167. Bindea G, Mlecnik B, Hackl H, Charoentong P, Tosolini M, Kirilovsky A, et al. ClueGO: a Cytoscape plug-in to decipher functionally grouped gene ontology and pathway annotation networks. Bioinformatics. 2009;25(8):1091-3.
168. Williams HL, Walsh K, Diamond A, Oniscu A, Deans ZC. Validation of the Oncomine() focus panel for next-generation sequencing of clinical tumour samples. Virchows Arch. 2018;473(4):489-503.
169. Rhodes DR, Yu J, Shanker K, Deshpande N, Varambally R, Ghosh D, et al. ONCOMINE: a cancer microarray database and integrated data-mining platform. Neoplasia. 2004;6(1):1-6.

170. Uhlen M, Fagerberg L, Hallstrom BM, Lindskog C, Oksvold P, Mardinoglu A, et al. Proteomics. Tissue-based map of the human proteome. Science. 2015;347(6220):1260419.

171. Uhlen M, Zhang C, Lee S, Sjostedt E, Fagerberg L, Bidkhori G, et al. A pathology atlas of the human cancer transcriptome. Science. 2017;357(6352).

172. Bogdanow B, Zauber H, Selbach M. Systematic Errors in Peptide and Protein Identification and Quantification by Modified Peptides. Mol Cell Proteomics. 2016;15(8):2791-801.

173. Chick JM, Kolippakkam D, Nusinow DP, Zhai B, Rad R, Huttlin EL, et al. A mass-tolerant database search identifies a large proportion of unassigned spectra in shotgun proteomics as modified peptides. Nat Biotechnol. 2015;33(7):743-9.

174. Hovanessian AG, Soundaramourty C, El Khoury D, Nondier I, Svab J, Krust B. Surface expressed nucleolin is constantly induced in tumor cells to mediate calcium-dependent ligand internalization. PLoS One. 2010;5(12):e15787.

175. Wang H, Yan H, Fu A, Han M, Hallahan D, Han Z. TIP-1 translocation onto the cell plasma membrane is a molecular biomarker of tumor response to ionizing radiation. PLoS One. 2010;5(8):e12051.

176. Wang C, Cui T, Feng W, Li H, Hu L. Role of Numb expression and nuclear translocation in endometrial cancer. Oncol Lett. 2015;9(4):1531-6.

177. van Putten JPM, Strijbis K. Transmembrane Mucins: Signaling Receptors at the Intersection of Inflammation and Cancer. J Innate Immun. 2017;9(3):281-99.

178. Vallo S, Rutz J, Kautsch M, Winkelmann R, Michaelis M, Wezel F, et al. Blocking integrin beta1 decreases adhesion in chemoresistant urothelial cancer cell lines. Oncol Lett. 2017;14(5):5513-8.

179. Liebert M, Washington R, Stein J, Wedemeyer G, Grossman HB. Expression of the VLA beta 1 integrin family in bladder cancer. Am J Pathol. 1994;144(5):1016-22.

180. Liu G, Cheng K, Lo CY, Li J, Qu J, Neelamegham S. A Comprehensive, Open-source Platform for Mass Spectrometry-based Glycoproteomics Data Analysis. Mol Cell Proteomics. 2017;16(11):2032-47.

181. Hofner T, Macher-Goeppinger S, Klein C, Schillert A, Eisen C, Wagner S, et al. Expression and prognostic significance of cancer stem cell markers CD24 and CD44 in urothelial bladder cancer xenografts and patients undergoing radical cystectomy. Urol Oncol. 2014;32(5):678-86.

182. Fu L, Liu N, Han Y, Xie C, Li Q, Wang E. ADAM10 regulates proliferation, invasion, and chemoresistance of bladder cancer cells. Tumour Biol. 2014;35(9):9263-8.

183. Kang WY, Chen WT, Huang YC, Su YC, Chai CY. Overexpression of annexin 1 in the development and differentiation of urothelial carcinoma. Kaohsiung J Med Sci. 2012;28(3):145-50.

184. Ross RL, McPherson HR, Kettlewell L, Shnyder SD, Hurst CD, Alder O, et al. PIK3CA dependence and sensitivity to therapeutic targeting in urothelial carcinoma. BMC Cancer. 2016;16:553.

185. Rudd P, Karlsson NG, Khoo KH, Packer NH. Glycomics and Glycoproteomics. In: rd, Varki A, Cummings RD, Esko JD, Stanley P, Hart GW, et al., editors. Essentials of Glycobiology. Cold Spring Harbor (NY)2015. p. 653-66.

186. Vajaria BN, Patel PS. Glycosylation: a hallmark of cancer? Glycoconj J. 2017;34(2):147-56.

187. Sheta R, Woo CM, Roux-Dalvai F, Fournier F, Bourassa S, Droit A, et al. A metabolic labeling approach for glycoproteomic analysis reveals altered glycoprotein expression upon GALNT3 knockdown in ovarian cancer cells. J Proteomics. 2016;145:91-102.

188. Glavey SV, Huynh D, Reagan MR, Manier S, Moschetta M, Kawano Y, et al. The cancer glycome: carbohydrates as mediators of metastasis. Blood Rev. 2015;29(4):269-79.

189. Lakshmanan I, Salfity S, Seshacharyulu P, Rachagani S, Thomas A, Das S, et al. MUC16 Regulates TSPYL5 for Lung Cancer Cell Growth and Chemoresistance by Suppressing p53. Clin Cancer Res. 2017;23(14):3906-17.

190. Yang X, Yin H, Zhang Y, Li X, Tong H, Zeng Y, et al. Hypoxia-induced autophagy promotes gemcitabine resistance in human bladder cancer cells through hypoxia-inducible factor 1alpha activation. Int J Oncol. 2018;53(1):215-24.

191. Xue M, Chen W, Xiang A, Wang R, Chen H, Pan J, et al. Hypoxic exosomes facilitate bladder tumor growth and development through transferring long non-coding RNA-UCA1. Mol Cancer. 2017;16(1):143.

192. Albuquerque APB, Balmana M, Mereiter S, Pinto F, Reis CA, Beltrao EIC. Hypoxia and serum deprivation induces glycan alterations in triple negative breast cancer cells. Biol Chem. 2018;399(7):661-72.

193. Belo AI, van Vliet SJ, Maus A, Laan LC, Nauta TD, Koolwijk P, et al. Hypoxia inducible factor 1alpha down regulates cell surface expression of alpha1,2-fucosylated glycans in human pancreatic adenocarcinoma cells. FEBS Lett. 2015;589(18):2359-66.

194. Lima L, Gaiteiro C, Peixoto A, Soares J, Neves M, Santos LL, et al. Reference Genes for Addressing Gene Expression of Bladder Cancer Cell Models under Hypoxia: A Step Towards Transcriptomic Studies. PLoS One. 2016;11(11):e0166120.

195. Zundel W, Schindler C, Haas-Kogan D, Koong A, Kaper F, Chen E, et al. Loss of PTEN facilitates HIF-1-mediated gene expression. Genes Dev. 2000;14(4):391-6.
196. Cosse JP, Michiels C. Tumour hypoxia affects the responsiveness of cancer cells to chemotherapy and promotes cancer progression. Anticancer Agents Med Chem. 2008;8(7):790-7.
197. Lin Q, Yun Z. Impact of the hypoxic tumor microenvironment on the regulation of cancer stem cell characteristics. Cancer Biol Ther. 2010;9(12):949-56.
198. Starbuck K, Al-Alem L, Eavarone DA, Hernandez SF, Bellio C, Prendergast JM, et al. Treatment of ovarian cancer by targeting the tumor stem cell-associated carbohydrate antigen, Sialyl-Thomsen-nouveau. Oncotarget. 2018;9(33):23289-305.
199. Ogawa T, Hirohashi Y, Murai A, Nishidate T, Okita K, Wang L, et al. ST6GALNAC1 plays important roles in enhancing cancer stem phenotypes of colorectal cancer via the Akt pathway. Oncotarget. 2017;8(68):112550-64.
200. Nardy AF, Freire-de-Lima L, Freire-de-Lima CG, Morrot A. The Sweet Side of Immune Evasion: Role of Glycans in the Mechanisms of Cancer Progression. Front Oncol. 2016;6:54.
201. Lee HC, Wondimu A, Liu Y, Ma JS, Radoja S, Ladisch S. Ganglioside inhibition of CD8+ T cell cytotoxicity: interference with lytic granule trafficking and exocytosis. J Immunol. 2012;189(7):3521-7.
202. Santos J, Fernandes E, Ferreira JA, Lima L, Tavares A, Peixoto A, et al. P53 and cancer-associated sialylated glycans are surrogate markers of cancerization of the bladder associated with Schistosoma haematobium infection. PLoS Negl Trop Dis. 2014;8(12):e3329.

Appendix

Table S1 – Paired analysis of independent samples comparing MALDI-TOF-MS and nanoLC-ESI-MS.

MALDI-TOF/TOF												
	5637				T24				HT1376			
m/z	Rel. Abundance	SD	n	CV(%)	Rel. Abundance	SD	n	CV(%)	Rel. Abundance	SD	n	CV(%)
768.4	0	0	3	0	12	1	3	9	6	1	3	20
955.5	39	9	3	22	24	3	3	11	27	4	3	14
1217.6	4	1	3	22	0	0	3	41	1	2	3	141
1316.6	26	4	3	15	42	6	3	15	45	5	3	10
1391.7	0	0	3	0	1	1	3	65	0	0	3	0
1404.7	16	4	3	23	6	0	3	7	5	0	3	4
1578.8	3	0	3	14	5	1	3	25	3	1	3	20
1765.9	14	3	3	22	9	1	3	8	10	2	3	16
1853.9	0	0	3	0	1	1	3	89	0	0	3	0
1939.9	0	0	3	0	0	0	3	173	1	1	3	141
2028.0	0	0	3	0	0	0	3	173	0	1	3	141
2215.1	0	0	3	0	0	0	3	173	0	1	3	141
2303.1	0	0	3	0	0	0	3	173	0	0	3	0
2389.2	0	0	3	0	0	0	3	173	1	1	3	141
2477.2	0	0	3	0	0	0	3	173	0	0	3	0
2664.3	0	0	3	0	0	0	3	173	0	1	3	141
2838.4	0	0	3	0	0	0	3	0	0	0	3	141
2926.5	0	0	3	0	0	0	3	173	0	0	3	0
3025.5	0	0	3	0	0	0	3	173	0	0	3	141

nanoLC-ESI-MS												
	5637				T24				HT1376			
m/z	Rel. Abundance	SD	n	CV(%)	Rel. Abundance	SD	n	CV(%)	Rel. Abundance	SD	n	CV(%)
729.4	6	0	3	0	2	0	3	4	1	1	3	70
746.4	77	1	3	1	58	6	3	11	63	2	3	4
933.5	10	0	3	5	26	4	3	15	18	1	3	6
991.5	0	0	3	62	0	0	3	0	0	0	3	173
1021.5	2	1	3	50	2	1	3	70	1	0	3	21
1178.6	0	0	3	173	0	0	3	173	0	0	3	0
1195.6	1	0	3	69	0	0	3	0	0	0	3	173
1294.7	8	0	3	5	12	1	3	9	15	1	3	7
1369.7	0	0	3	173	0	0	3	0	0	0	3	0
1382.7	2	1	3	36	2	1	3	57	0	0	3	15
1556.8	0	0	3	5	0	0	3	90	0	0	3	105
1743.9	1	0	3	41	1	1	3	89	1	1	3	104
1917.9	0	0	3	173	0	0	3	0	0	0	3	0

Table S2 – *O*-glycan structures determined by MALDI-TOF-MS and/or nanoLC-ESI-MS.[1]

				Glycans composition				Cell lines					
								MALDI-TOF-MS			nanoLC-ESI-MS		
Glycan #	Permethylated O-glycans Monoisotopic Mass $[M+Na]^+$ Da	Permethylated O-glycans Monoisotopic Mass $[M+H]^+$ Da	Structure	HexNAc	Hex	Fuc	NeuAc	5637	T24	HT1376	5637	T24	HT1376
1	751.3630	729.3810		1			1				x	x	x
2	768.3783	746.3963		1	1	1			x	x	x	x	x
3	955.4628	933.4808		1	1		1	x	x	x	x	x	x
4	1013.5046	991.5226		2	1	1						x	x
5	1043.5152	1021.5332		2	2						x	x	x
6	1200.5891	1178.6071		2	1		1				x	x	
7	1217.6044	1195.6224		2	2	1		x	x	x		x	x
8	1316.6365	1294.6545		1	1		2	x	x	x	x	x	x
9	1391.6936	1369.7116		2	2	2			x			x	
10	1404.6889	1382.7069		2	2		1	x	x	x	x	x	x
11	1578.7781	1556.7961		2	2	1	1	x	x	x	x	x	x
12	1765.8626	1743.8806		2	2		2	x	x	x	x	x	x
13	1853.9150	1831.9330		3	3		1		x				
14	1939.9518	1917.9698		2	2	1	2		x	x		x	
15	2028.0042	2006.0222		3	3	1	1		x	x			
16	2215.0887	2193.1067		3	3		2		x	x			
17	2303.1411	2281.1591		4	4		1		x				
18	2389.1779	2367.1959		3	3	1	2		x	x			
19	2477.2303	2455.2483		4	4	1	1		x				
20	2664.3148	2642.3328		4	4		2		x	x			
21	2838.4040	2816.422		4	4	1	2			x			
22	2926.4764	2904.4744		5	5	1	1		x				
23	3025.4885	3003.5065		4	4		3		x	x			

[1] Sodiated ions $[M+Na]^+$ Da, in MALDI-TOF-MS; Protonated ions $[M+H]^+$ Da, in nanoLC-ESI-MS